Cross-talk Analysis of Limited Wavelength Interchanging Cross-Connects (L-WIXC) in a WDM Network

by

Punab Chandra Kundu

MASTER OF SCIENCE
In
Electrical and Electronic Engineering

Department of Electrical and Electrical Engineering
BANGLADESH UNIVERSITY OF ENGINEERING AND TECHNOLOGY (BUET)
Dhaka-1000, Bangladesh

June 2011

APPROVAL CERTIFICATE

This thesis titled "CROSSTALK ANALYSIS OF LIMITED-WAVELENGTH-INTERCHANGING CROSSCONNECTS (L-WIXC) IN A WDM NETWORK" submitted by Punab Chandra Kundu, Roll No.- 100606221P has been accepted as satisfactory in partial fulfillment of the requirements for the Degree of **Master of Science in Electrical and Electronic Engineering** June, 2011

BOARD OF EXAMINERS

1. _____
Dr. Satya Prasad Majumder
Professor — Chairman
Department of Electrical and Electronic Engineering (EEE)
Bangladesh University of Engineering and Technology (BUET)
Dhaka-1000, Bangladesh

2. _____
Dr. Md. Saifur Rahman
Professor and Head — Member (Ex-Officio)
Department of Electrical and Electronic Engineering (EEE)
Bangladesh University of Engineering and Technology (BUET)
Dhaka-1000, Bangladesh

3. _____
Dr. Md. Shah Alam
Associate Professor — Member
Department of Electrical and Electronic Engineering (EEE)
Bangladesh University of Engineering and Technology (BUET)
Dhaka-1000, Bangladesh

4. _____
Wg Cdr Dr. Md. Hossam-E-Haider
Instructor — Member (External)
Department of Electrical, Electronic and Computer Engineering (EECE)
MIST, Mirpur Cantonment, Dhaka, Bangladesh.

DECLARATION

It is hereby declared that this thesis or any part of it has not been submitted elsewhere for the award of any degree or diploma.

Punab Chandra Kundu
Roll No.-100606221P

Counter Signed by

Dr. Satya Prasad Majumder
The Supervisor

Dedicated to

My beloved parents

And

Honorable teachers,

Who brought me to this enlightened stage of life

ACKNOWLEDGEMENTS

First and foremost, all praises and gratitude to all mighty God, who created this mysterious universe and led us in the quest for knowledge.

I would like to express my heartful gratitude and profound respect to my supervisor, Dr. Satya Prasad Majumder, Professor, Department of Electrical and Electronic Engineering, Bangladesh University of Engineering and Technology, Dhaka, Bangladesh, for his continuous guidance, support and invaluable advice throughout the progress of my research work for the last two years.

I also express my thanks to my colleagues and superiors who gave me the opportunity to finish this thesis work. I also acknowledge the valuable support provided by my cordial friend Md. Asaduzzaman Khan and my younger brother in this regard.

Last, but not the least, I would like to convey my deepest to my parents, whose contributions are inherent in every word of this work.

ABSTRACT

Limited Wavelength interchanging crossconnect (L-WIXC) is an essential element in a WDM optical network which not only selects the route to be followed but also selects the wavelength to be used along the selected route and improves blocking performance of the network. It is superior to the OXC having full wavelength conversion capability in terms of cost and complexity. Propagation through the switching elements that are the part of OXC results in signal degradation and induces crosstalk both due to device intrinsic losses and their imperfect operation. In this thesis work various types of crosstalk mechanism and their sources for limited wavelength interchanging OXC for various architectures have been identified and analytical formulations for the crosstalk have been carried out for all architectures. The analytical formulations are used to find Bit error rate (BER), power penalty and the effect of number of wavelength converters on a system. A Comparative picture of the system performance has been depicted for all architectures of limited wavelength interchanging OXC which will help the system designer to choose the effective one.

TABLE OF CONTENTS

INDEX

LIST OF FIGURES

LIST OF TABLES

LIST OF ABBREVIATIONS

BER	Bit error rate
DCS	Delivery and coupling switch
DMUX	Demultiplexer
EDFA	Erbium-drop fiber amplifier
E/O	Electrical to optical
IM/DD	Intensity modulation-direct detection
LD	Laser diode
L-WIXC	Limited wavelength interchanging cross-connect
MUX	Multiplexer
MWSF	Multi-wavelength selective filter
O/E	Optical to electrical
OEO	Optical electrical optical
O-O	Optical to optical
OPXC	Optical cross-connect
PP	Power penalty
SDM	Space division multiplexing
SOA	Semiconductor optical amplifier
SSM	Space switch matrix
TDM	Time division multiplexing
UHF	Ultra high frequency
VWP	Virtual wavelength path
WC	Wavelength converter
WDM	Wavelength division multiplexing
WP	Wavelength path
WIXC	Wavelength interchanging cross-connect

Chapter-1

INTRODUCTION

1.1 Introduction to WDM networks

With the advancement of human civilization human being are producing and delivering more and more information. Because information works only when it is to the right place, in the right time and in the right form. So we need to increase information carrying capacity. We have already attained digital technology for the high reliability and high quality signal transmission. However, this technology carries a price: the need for higher information carrying capacity.

Modern communication technology has always tried to use high-frequency signal carriers. The shift from radio frequency to microwave allowed engineers to increase a given system's information carrying capacity tenfold. This success inspired researchers to seek a solution to the problem of reliable communications by continuing to increase microwave frequency. But at a frequency of more than 100 GHz, where microwaves overlap the infrared zone, microwave attenuation in the air reaches such a high level that transmission distance becomes unacceptably short.

The solution appeared to be clear: use a waveguide structure to transmit ultrahigh frequency electromagnetic waves. These waveguides, in the form of steel tubes rectangular in cross section with opening at each end, have now been in use in the years in radar and other UHF systems for delivering and distributing microwaves over very short distances.

In the late 1960s and clearly 1970s, scientists and engineers at Bell Laboratories achieved significant progress in designing waveguides for long distance systems. These waveguides boasted a very impressive characteristic: 238,000 voice channel per unit. But they are extremely insufficient from cost, installation and other practical standpoints which results all these efforts were proving fruitless. Then they tried to increase the carrier frequency even higher than microwave frequency that covers light but guiding light over a significant distance is a multifaceted problem.

In 1953 Narinder Kapany, working at the Imperial College of science and Technology in London, developed a fiber with cladding, thus giving the birth to the structure used in today's optical fiber which is based on total internal reflection. In 1966 Chinese-born British scientist, Charles Kao, delivered a landmark paper "Dielectric Fiber Surface Waveguides for Optical Frequency", which was the key unlocking the door to fiber optic technology. Kao's experiment resulted in an attenuation of more than 1000 db/Km, an unacceptably high loss under any circumstances. In 1970 Robert Maurer, Donald Keck & Peter Schultz of Corning Glass Corporation reported the first

optical fiber with attenuation less than 20 db/Km .At that time they developed an optical fiber manufacturing process that has become the industry's most widely used method. After more than 15 years of extensive work, manufacturer came out with an incredibly low-loss optical fiber with attenuation less than 0.3 db/Km [1].

Early communication system used multimode Optical fiber for signal transmission. But they have to have regenerators every few kilometers, which were expensive to regenerate the signal due to intermodal dispersion. Using single mode fiber effectively eliminates intermodal dispersion and enabled a dramatic increase in the bit rate and distance possible between regenerators.

The introduction of EDFA spurred the development of a completely new generation of systems. A major advantage of EDFA is that they are capable of amplifying signals at many wavelength simultaneously which provide another way of increasing the system capacity: rather than increasing the bit rate, keep the bit rate the same and use more than one wavelength, that is, use wavelength division multiplexing. The use of WDM and EDFAs dramatically brought down the cost of long-haul transmission systems and increased the system capacity [2].

1.2 Wavelength Division Multiplexing (WDM)

Wavelength division Multiplexing (WDM) involves the transmission of a number of different peak wavelength optical signals in parallel on a single optical fiber. Although in spectral terms optical WDM is analogous to electrical frequency division multiplexing, it has the distinction that each channel effectively has access to the entire intensity modulation fiber bandwidth which with current technology is of the order of several gigahertz. This multiplexing strategy overcomes certain power budgetary restrictions associated with electrical time division multiplexing (TDM). In TDM when the transmission rate over a particular optical fiber link is double, a further 3 to 6 db optical power is generally required at the receiver. In case of WDM, however, additional loss is also incurred from the incorporation of wavelength multiplexers and demultiplexers. The potential utilization of the separate wavelength channels to provide dedicated communication services to individual subscriber terminals is an attractive concept within telecommunications [1].

1.3 Merits of WDM

The introduction of WDM techniques in all-optical transport network has the following advantages on the network planning and operation

- To perform simple routing functions in a cost effective manners, through the efficient use of both space and wavelength domains.
- To introduce a certain degree of transparency, leading to easier transport of information coming from different preexisting infrastructures and telecommunication standards without major modifications, to a less hierarchical network by allowing simultaneous transport of different bit rates and exiting digital modulation standards (PDH, SDH, ATM) and finally a high tolerance to future change of the traffic demand and telecommunication standards.
- To devote cost effective facilities to dynamic and flexible rerouting and path protection which is all the more important that the total and link by link traffic load of the network increases.
- To facilitate network scalability; in particular, more wave-lengths can be added at low incremental cost.
- To increase smoothly the transmission capacity of existing fiber links .without reaching the physical limits imposed by current optical technologies. [3].

1.4 Why WDM network

The historical trends have been to increase capacity in the network and at the same time drive down the cost per bit of bandwidth. Service providers generally look for at least a fourfold increase in capacity when planning their network. As a rule of thumb, they expect to get this fourfold increase in capacity at about 2-2.5 times the cost of the current equipments.

There are fundamentally three ways of increasing transmission capacity

1. The first approach is to light up additional fibers or to deploy additional fibers as needed. This is called space division multiplexing (SDM) in which keep the bit rate same but use more fiber.
2. Multiplexing more than one signal on time slot basis that is called Time division multiplexing (TDM).
3. Adding additional wavelengths over the same which is called Wavelength division multiplexing (WDM).

SDM is straightforward upgrade alternative. It is expensive and time consuming. It becomes difficult if fiber has to be deployed in dense metropolitan area.

TDM is useful for grooming traffic at the lower bit rate where optics is not cost effective. At the higher bit rate we have to deal with more transmission impairments over the fiber, specifically chromatic dispersion, polarization- mode dispersion and fiber nonlinearity. In standard single-mode fiber the chromatic dispersion limit is about 60 Km at 10 Gb/s and about 1000 Km at 2.5 Gb/s assuming transmission around 1550 nm. With practical transmitters the distances are even smaller. The 10 Gb/s limit may be further reduced in the presence of self-phase modulation. Beyond these distance the signal must be electronically regenerated or some form of chromatic dispersion compensation must be employed. Finally, nonlinearity effects such as self phase modulation limit the maximum transmission power per channel, resulting in a need for closer amplifier spacing which leads somewhat higher cost. It is also difficult to be implemented since it needs ultra-short optical pulse sources and ultra high speed synchronization systems.

WDM allows to maintain a modest transmission bit rate and have multiple wavelengths over a single fiber .Keeping bit rate low makes the system less vulnerable to chromatic dispersion, polarization-mode dispersion and some types of nonlinearities such as self-phase modulation. On the other hand it is not suitable for deployment over dispersion-shifted fiber because of limitation imposed by four-wave mixing.

WDM systems can be designed to be transparent system. It allows different wavelengths to carry data at different bit rates and protocol formats which can be a major advantage in some cases.

Finally WDM provide flexibility in building networks. It is more cost effective where a small fraction of traffic is to be added or dropped by using add/drop element [2].

1.5 Optical Cross-connect (OXC)

An optical cross-connect (OXC) is a device used by telecommunications carriers to switch high speed optical signals in a fiber optic network.

There are several ways to realize an OXC. One can implement an OXC in the electronic domain: all the input optical signals are converted into electronic signals after they are de-multiplexed by de-multiplexers. The electronic signals are then switched by an electronic switch module. Finally the switched electronic signals are converted back into optical signals by using them to modulate lasers and then the resulting optical signals are multiplexed by optical multiplexers onto outlet optical fibers. This is known as an "O-E-O" (Optical-Electrical-Optical) design. Cross-connects based on an O-E-O switching process generally has a key limitation: the electronic circuits limit the maximum bandwidth of the signal. Such architecture prevents an OXC from performing with same speed as an all-optical cross-connect, and is not transparent to the network protocols used. On the other hand, it is easy to monitor signal quality in an O-E-O device, since everything is converted back to the electronic format at the switch node. An additional advantage is that the optical signals are re-generated, so they leave the node free of dispersion and attenuation. An electronic OXC is also called an opaque OXC.

Switching optical signals in an all-optical device is the second approach to realize an OXC. Such a switch is often called a transparent OXC photonic cross-connect (PXC). Specifically, optical signals de-multiplexed, and then the de-multiplexed wavelengths are switched by optical switch modules. After switching, the optical signals are multiplexed onto output fibers by optical multiplexers. Such switch architecture keeps the features of data rate and protocol transparency. However, because the signals are kept in the optical format, the transparent OXC architecture does not allow easy optical signal quality monitoring.

As a compromise between opaque and transparent OXC's, there is a type of OXC called a translucent OXC. In such switch architecture, there is a switch stage which consists of an optical switch module and an electronic switch module. Optical signals passing through the switch stage can be switched either by the optical switch module or the electronic switch module. In most cases, the optical switch module is preferred for purpose of transparency.

When the optical switch modules switching interfaces are all busy or an optical signal needs signal regeneration through an O-E-O conversion process, the electronic module is used. Translucent OXC nodes provide a compromise of full optical signal transparency and comprehensive optical signal monitoring. It also provides the possibility of signal re-generation at each node [4-9].

1.6 Motivation of the thesis

Previously we have mention that Wavelength Division multiplexing network are attracting more and more attention because of their ability to provide increased capacity, flexibility and possibility of upgrading the existing optical fiber networks to WDM networks. It is not only a promising technique to utilize the enormous band-width of optical fiber but also being regarded as an attractive solution to the increasing demand of bandwidth in future telecommunication system. In this technique multiple wavelength division channels can be operated on a single fiber simultaneously following the fundamental constrains of fiber optic communication is that these channels operate at different wavelengths. In wavelength routed all-optical networks connections are routed by intermediate nodes in optical domain without electronic conversion and this wavelength sensitive routing function is done by Optical cross connect. The optical cross-connect (OXC) controls the lightpaths in a large network in an automated manner, without having to restore to performing manual patch panel connections [10-12]. It is an essential network element enabling reconfigurable optical network, where lightpaths can be set up and taken down as needed [10-12].It offers routing scalability ,bit rate and protocol independence, power saving and increased transport capacity to WDM network.[7,13].

An OXC with wavelength conversion capability is required at the intermediate node to support Non-wavelength Continuous light path. In this case OXC not only selects the route to be followed but also selects the wavelength to be used along the selected route and improves the blocking performance. In [7] it has been found that improvement of call blocking performance saturates when the number of converters in an OXC is greater than a threshold. . So instead of wave length interchanging cross connect having full conversion capability limited wavelength- interchanging cross-connect (L-WIXC) having optimum

number of wavelength converters may be used through sharing due to the cost and complexity of wavelength converters[10].

The key components required to implement an OXC node are passive multiplexers, demultiplexers, splitters, combiners and switches. Propagation through the switching elements that are part of the OXC results in signal degradation both due to device intrinsic losses and their imperfect operation and induces crosstalk. Imperfect switching gives a leakage signal, the wavelength of which can be equal to or different from the signal wavelength. It can be also caused by the imperfection of other devices such as multiplexers, demultiplexers, filters etc. The build up of crosstalk noise on a certain optical channel due to interference with other signals while propagating through the different element of the WDM network could result in serious problems. Crosstalk due to optical cross connect is one of the basic criteria that characterizes the performance of the WDM network [12-15].]. Since optical crosstalk is a major limiting factor, the commercial use of an all optical OXC is so far prevented in WDM networks.

Practical implementation of the OXCs often employs multi-stage structures to achieve the required size with less complexity. To utilize the wavelength converters more efficiently and optimally a number of architectures have been proposed. The architectures of the optical cross-connects have a significant impact on how the unwanted light leaking from the components mix with the actual signal to become crosstalk. In [11] a systematic analysis of such crosstalk has been reported for OXC without wavelength converter, in [12] for OXC with wavelength converter and in [17] for Limited wavelength-interchanging cross-connect only for two architectures but till today, no such analysis for all architectures of OXC with limited wavelength converter has been reported in the literature. Systematic analysis of crosstalk is a useful tool for characterizing the crosstalk performance of optical crossconnect architectures and enables them to compare base on some key performance indicators. Also, by the analysis it will be possible to relate the overall crosstalk to the specifications of individual optical components and, hence, enable system architects to specify certain component specifications for achieving a desired crosstalk performance for the chosen OXC architecture. In this thesis work a systematic analysis of signal distortion crosstalk and their impact on the desired signal will be

considered for various architecture based on space-switching matrices, delivery and coupling switches, and combination of couplers and filters.

1.7 Review of previous Research Works

A lot of research works have been done on Optical cross-connect, their architectures, different type of crosstalk involved while propagating a signal through it and their type and impact. Some are given bellow.

Jingyu Zhou, Roberto Cadeddu, Emillio Casaccia,Carlo Cavazzoni and Michael J. O'Mahony, " Crosstalk in Multiwavelength Optical Cross-Connect Networks." J. Lightwave Technol.,vol. 14,pp. 1423-1435,No.6 May1996 identifies two type of crosstalk mechanisms, their sources, impact and method of reduction crosstalk.

Yunfeng shoe, Kejie Lu and Wanyi Gu, "Coherent and Incoherent Crosstalk in WDM Networks." , J. Lightwave Technol.,vol. 17,pp. 759-764,No.5 May1999 shows the impact of coherent and incoherent crosstalk on an optical signal passing through the optical cross-connect nodes networks.

Tim gyselings, Greet Morthier, and Roel Baets, "Crosstalk Analysis of Multiwavelength Optical Cross-connects" , J. Lightwave Technol.,vol. 17,pp.1273-1283, No.8, August 1999 presents the results of a crosstalk analysis of four optical WDM cross-connect topologies and a optimal set of parameters has been determined to reduced the total crosstalk.

Satoru Okamoto, Atsushi Watanabe and Ken-Ichi Sato, " Optical Path Cross-Connect Node Architectures for Photonic Transport Network.", J. Light wave Technol.,vol. 14,pp.1410-1422, June 1996. explores various Optical path cross-connect nodes architectures, functional conditions required to construct OPXC nodes for WP and VWP networks, the efficiency of network failure restoration etc.

Shoji Kakehashi, Hiroshi Hesegawa, " Optical Cross-connect switch Architectures for Hierarchical Optical Path Networks ." IEICE TRANS.COMMUN., vol.E91-B, No.10 Oct 2008, proposes new switch architectures for hierarchical optical path cross-connect systems which allow incremental expansion of system in terms of the number of input/output fiber ports, wavebands and optical paths per waveband.

Eugenio Iannone , Roberto Sabella , " Optical Path Technologies : A Comparison Among Different Cross-Connect Architectures." J. Lightwave Technol., vol. 14, No. 10, pp.2184-2195, October 1996 in which different optical cross-connect architectures based on either space division or wavelength division switching are analyzed and a comparative investigation is accomplished considering three issue of primary importance: cross-connect modularity, complexity and transmission performance. It also evaluated the transmission performance of a generic path.

M.S. Islam, S.P.Majumder, Ngee Thiam Sim "Performance Limitation of optical cross connect without wavelength converter due to crosstalk , J. opt.Commun.29(2008),71-75 in which an analytical approach for modeling crosstalk have been developed and the impact of different factors of OXC on the performance of a WDM transmission link has been investigated without wavelength converter.

M.S. Islam & S.P. Majumder, " Bit error rate & cross talk performance in optical cross connect with wavelength converter," Journal of Optical Networking, vol.6,No.3, pp. 295-303,March 2007, in which an analytical approach for modeling crosstalk is presented and the impact of different factors of OXC on the performance of a WDM transmission link is also investigated with wavelength converter.

Teck Yoong Chai, Tee Hiang Cheng, Gangxiang shen, Sanjay K. Bose, Chao Lu, " Design and performance of optical cross connect architectures with converter sharing", Optical Networks Magazine July/August 2002 pp.73-83, which addresses the architectures that may be used to provide wavelength conversion in an optical cross-connect node using space switching matrices, delivery –and-coupling switches or various combinations of coupler and filters where the converter is shared and compares the architectures in terms of various features like complexity, expandability, upgradeability, degree of wavelength converter sharing and blocking probability performance under different traffic loading.

Tech Yoong chai and Tee Hiang Cheng , " In band crosstalk analysis of optical cross-connect Architectures" Journal of Lightwave Technology, vol. 23, No. 2, pp. 688-701, February 2005, which presents inband crosstalk in several important classes of optical cross-connect (OXC) architectures and derives the expression for the power penalty imposed by crosstalk to compare the architectures in a systematic way.

Tech Yoong chai,Tee Hiang Cheng, Sanjay K. Bose, Chao Lu and Gangiang Shen "Crosstalk Analysis for Limited-wavelength-Interchanging Cross connects" IEEE Photonics Technology Letters, vol. 14, No. 5, pp. 696-698, May 2002, presents crosstalk analysis for Limited-wavelength-Interchanging Cross connects only for two types of architectures.

1.8 Objectives of the thesis:

The main objectives of the research work are:

a) To carry out analysis for the crosstalk due to space switch, mux/demux, optical filters etc in a Limited Wavelength Interchanging Optical Cross Connect (L-WIXC) for a WDM network.
b) To carry out the analysis to find the expression of the coherent and incoherent crosstalk considering different architectures of wavelength interchanging cross-connects (WIXC) with and without limited wavelength conversion facilities.
c) To find the expression of signal to crosstalk ratio at the output of Optical cross connects (OXC) and to find the bit error rate (BER) expression for IM/DD system.
d) To evaluate the BER performance results based on the analysis for different architectures and system parameters like number of input fibers, input power per channel and number of channels per fiber and to determine the optimum system design parameters for a given BER.

1.9 Organization of this thesis

This thesis has been organized as follows

Chapter-1 depicts the history of WDM optical network, its advantages over others multiplexing technique and a brief introduction of OXC.

Chapter-2 depicts the various limited wavelength interchanging OXC architectures and their comparison in terms of hardware requirement.

Crosstalk definition and analytical formulations for various types of crosstalk in limited wavelength interchanging OXC for various architectures are presented in chapter-3.

Chapter-4 depicts result and discussion.

Chapter-5 provides the conclusion and the scope of future works.

Chapter-2
ARCHITECUTRES OF LIMITED WAVELENGTH INTERCHANGING OPTICAL CROSS-CONNECTS (L-WIXCs)

2.1 Introduction

The increase in traffic demand associate with new applications triggering a dramatic growth in capacity requirement for medium and long haul transport networks. Most network providers are tuning to WDM to solve the capacity problem. WDM offers the potential of an enormous increase in transmission throughput by using large bandwidth of optical fibers. Therefore WDM is one of the election techniques for upgrading the capacity of exiting transmission links in a cost effective ways, opening the door to new and potentially efficient all-optical routing scheme, replacing what is nowadays performed by complex.

To avoid an explosion in the cost of routing function, it is essential to introduce a new all-optical layer that can handle large bit rate signals to provide provision for restoration and wavelength switching that allow routing at the wavelength level. All-optical WDM functionality may provide the requirements of the transport network at the transmission path layers level and may also pave the way to less hierarchical network structure.

Archiving the goal of a multichannel path, reconfigurable all-optical network requires the employment of several enabling technologies. OXC is one of them. Several OXC architectures have been proposed depending on number of element requirement (cross-point, tunable filter, etc) Flexibility and blocking probability etc. The placement of wavelength converters is also an issue upon which degree of sharing depends. In this chapter several optical OXC architectures with limited number of wavelength converters will be discussed.

2.2 Basic Elements in L-WIXC

A basic element of an OXC is the space switch used to implement the space-switching matrix (SSM). There are number of technologies available for space switching in the

optical domain, e.g. electro-optic material, interferometer, acousto-optic interaction, thermo capillary effect and micro-electromechanical system (MEMS) etc and large switching matrix can be constructed using basic 2 × 2 elements.

It is also possible to obtain the space-switching function using a Delivery and coupling switching. The DCS is based on star couplers and 1 × 2 switching elements arranged in an array. This could be a very flexible switch allowing, for example, multiplexing of multiple input signals to a single output.

The other important element in an L-WIXC is a wavelength converter to change from one input wavelength to a different output wavelength. It is possible to do this with an Opto-electronic Wavelength converter, which detects the optical signal and then retransmits it at a different wavelength. This has the advantage of doing signal regeneration and will allow considerable flexibility in network control and management. This method may not be preferred in high-speed networks, which would probably like to do all-optical switching for high bandwidth operations. One way of doing this would be through an Optical Gating Wavelength Converter employing an optical device that changes its characteristics depending on the intensity of the input signal. This change causes a continuous wave signal (called a "probe") to be modulated with the information in the input signal. This category includes optical cross-gain and cross-phase modulators. Wave mixing wavelength Converters provide another way of achieving all-optical wavelength conversion. This utilizes the nonlinear interactions between optical signals in a nonlinear optical material to generate a signal at a different wavelength. This includes four-wave mixing based on third-order optical nonlinearities and difference frequency generation based on second-order nonlinearities [9].

2.3 Issues Arise from Multi-stage L-WIXC

In an L-WIXC, the degree of converter sharing will be an issue of concern, as the OXC will have only a limited number of converters. It would obviously be desirable to have an architecture where any converter may be used for any light path through the OXC regardless of its input and output links. In a practical scenario, this may not however be feasible and different architectures would allow different degrees of converter sharing.

Using standard switching terminology, the degree of sharing may be described as being (a) partial sharing, (b) simple full sharing, (c) rearrange able full sharing, or (d) strict full sharing. An OXC supports partial sharing if each converter can be accessed by only a subset of the entire possible light paths that may connect through the OXC. On the other hand, simple full sharing allows any light path to access any converter when the OXC does not have any established light path connections. If there are established light path connections, the existing light paths may prevent a new light path to access a wavelength converter even though the converter is not being used. With rearrange able full sharing, the arriving request can be assigned a wavelength converter by rearranging the existing connections. Strict full sharing gives the greatest freedom in converter access as it allows any free converter to be accessed by a new light path connection independent of the state of the OXC.

Upgradeability and expandability of the OXC designs would also be an issue of major concern when looking at different L-WIXC architectures. As traffic demands increase, the number of converters required will also tend to increase. An expandable OXC architecture would be then more desirable as it would allow the flexibility of adding more converters to the switch with very few structural changes. Further growth in traffic demand may also eventually require the L-WIXC to be upgraded to a WIXC, i.e. an OXC with full conversion [9].

2.4 Architectures of Limited-Wavelength-Interchanging Cross-Connects

Next various OXC architectures based on space-switching matrices, delivery and coupling switches and combinations of couplers and filters has been presented.

2.4.1 L-WIXCs based on space switching matrix (SSM)

Architecture-1 (Share Per Node)

This is one of the basic L-WIXCs. This L-WIXC with the share-per-node architecture will be referred to as SSM-1 and has been shown in Fig. 2.1. In SSM-1, the incoming channels

are separated by the demultiplexers (DMUX). They are then routed by the SSM directly to the proper output (for wavelength continuous light path) or to the wavelength converters and then to the proper output (for non-wavelength continuous light paths) by a second SSM. A star coupler is used instead of multiplexer because the wavelength of the output from the second SSM is not known a priori. The first stage switching is M, (N × N+1) SSM and the second SSM is of dimension M × V, giving a total of N^2M + MN+MV cross-points. In addition, there are a total of N 1 × M DMUXs, N (M +V)× 1 star couplers. The degree of wavelength converter sharing is strictly full and SSM-1 represents an ideal share-per-node architecture [9].

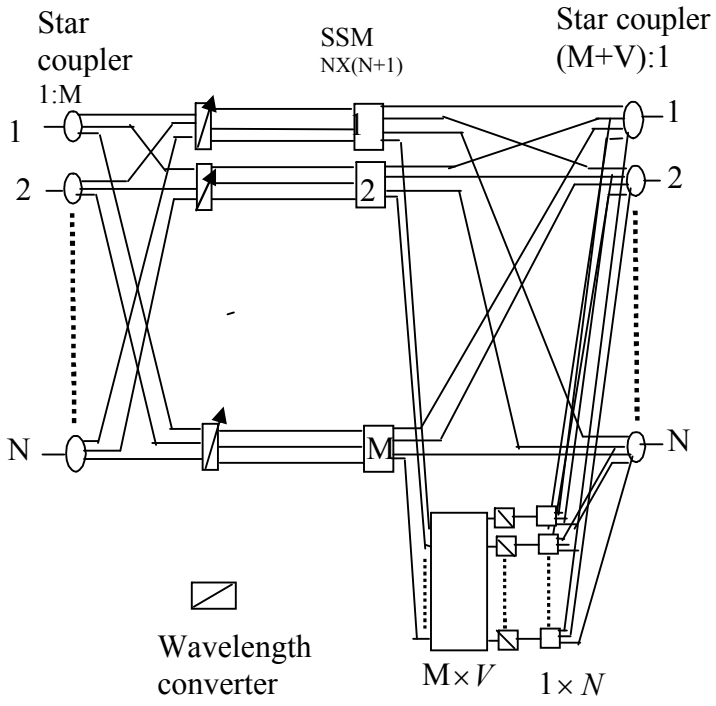

Fig. **2.1** Share Per Node Architecture.

Architecture-2 (Share Per Link)

This is the other basic L-WIXCs which is called SSM -2.The SSM-2 represents an ideal share-per-link architecture. Each input link has a dedicated set of converters that can be accessed by any channel from the input link. It only allows partial sharing of wavelength

converters. This has N^2M cross point, N DMUXs and N star coupler. In SSM-2, the incoming channels are separated by the demultiplexers (DMUX) and then after filtering they go through the wavelength conversion process for non-wavelength continuous light paths .Each link has V_n number of wavelength converters as a whole total V converters. For wavelength continuous light path they need not go through the wavelength conversion process. They are then routed by the SSM directly to the proper output [9].

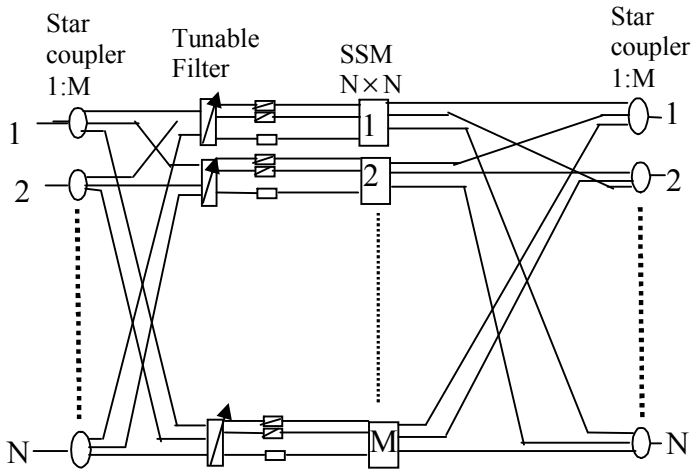

Fig. **2.2** Share Per Link Architecture

2.4.2 L-WIXCs based on delivery and coupling switches (DCS)

The DCS is a very flexible switch allowing, for example, the presence at its outputs of WDM signal obtained by multiplexing the input signal during the switch operation. Thus DCS allows different OXC architectures to be designed. Due to combined effect of wavelength conversion and the adoption of DCS's, tunable filters at the OXC input are not needed and signal demultiplexing can be achieved by a static demultiplexer thus simplifying the input stage structure.

DCS-1

DCS-1 supports strict full converter sharing. Those light paths from an input link that need conversion can be multiplexed to the $(N + 1)^{th}$ output of the corresponding DCS. The SSM

located before tunable filter selects one of the outputs from the star couplers and feeds it into tunable filter to single out a particular wavelength. In DCS-1, the incoming channels are separated by the demultiplexers (DMUX). They are then routed by the DCS directly to the proper output (for wavelength continuous light path) or to a SSM located before the tunable filter and then to the proper output (for non-wavelength continuous light paths) through wavelength conversion process. A star coupler is used instead of multiplexer because the wavelength of the output from the second SSM is not known a priori. DCS-1 comprises N $M \times (N + 1)$ DCSs, V $N \times 1$ and V $1 \times N$ SSMs, N DMUXs, N star couplers and V tunable filters [9].

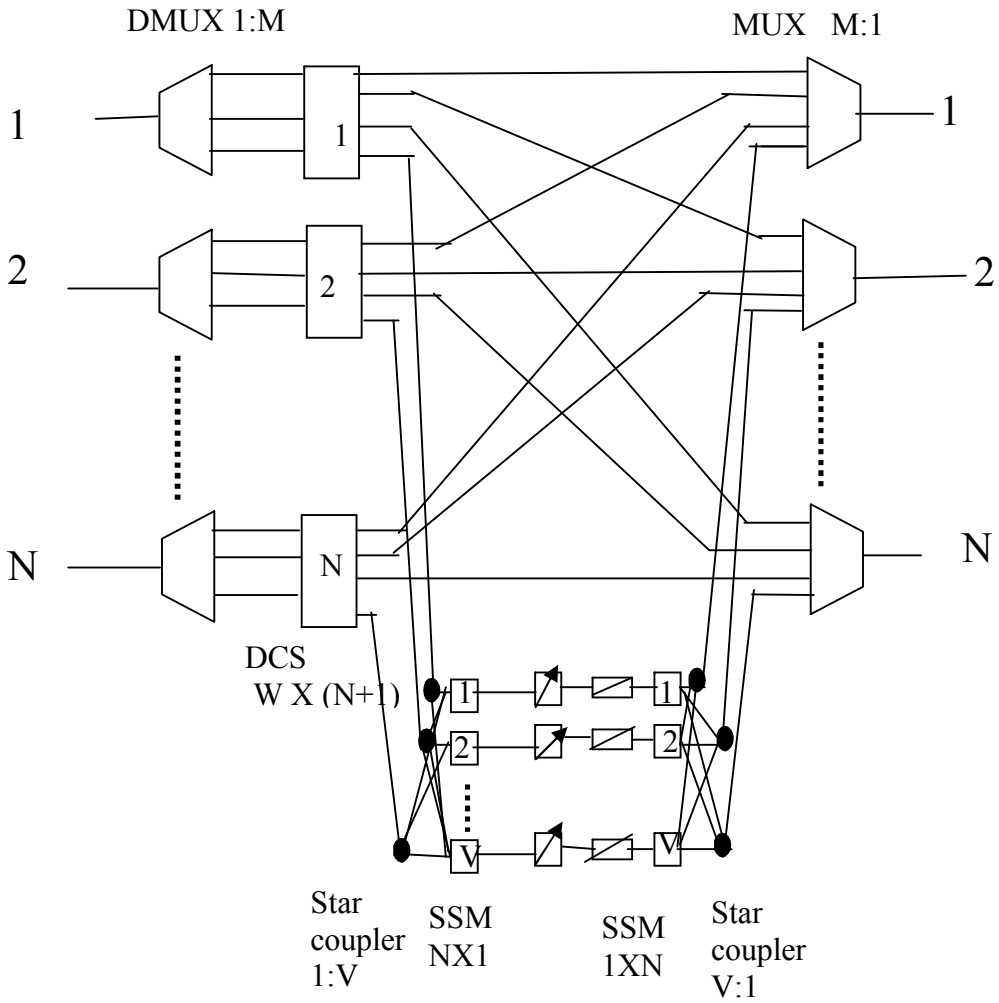

Fig. **2.3** : DCS-1 architecture

DCS-2

This is the second type of DCS-based OXC. It has the capability of connecting multiple inputs to one output, *M* DCSs are sufficient to avoid blocking of the unconverted light paths. Furthermore, if a wavelength converter is available in this architecture, then any converted light path can find its route through the OXC without the link mismatch problem. Wasteful occupancy can be minimized if routing unconverted light paths through the wavelength converters is avoided whenever possible. DCS-2 comprises *M* *N*× *N* DCSs, *N* *1*× M input star couplers, *N* *M*× 1 output star couplers, NM tunable filter and NV_n wavelength converters. In this architecture the incoming channels are separated by the combination of input star couplers and tunable filters. Then they go through the wavelength conversion process for non-wavelength continuous light paths . For wavelength continuous light path they need not go through the wavelength conversion process. They are then routed by the DCS directly to the proper output [9].

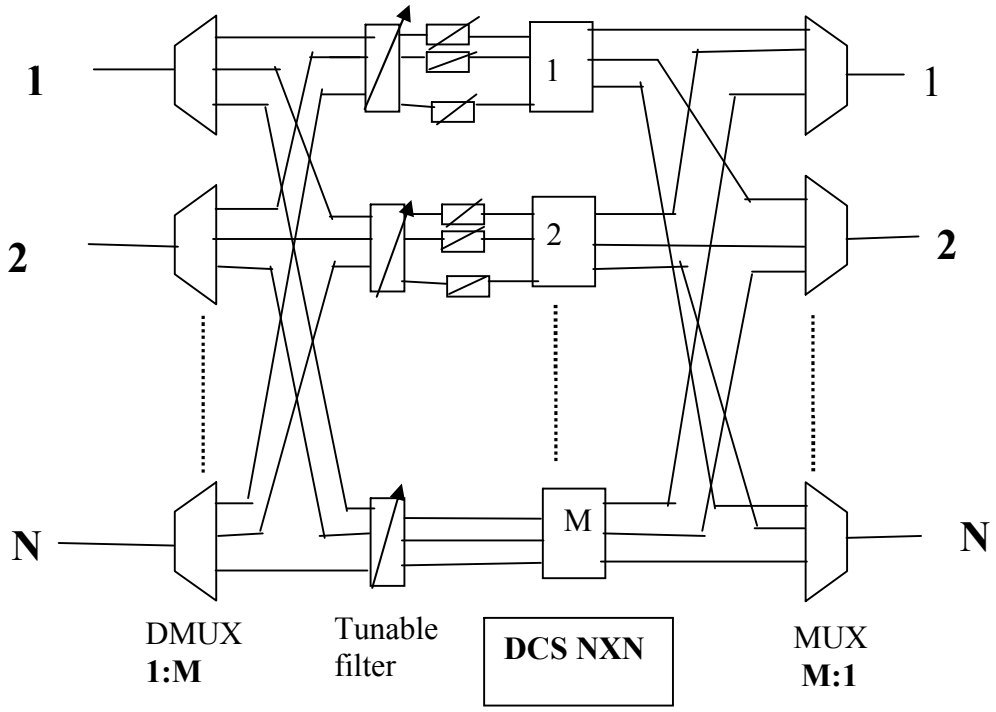

Fig. **2.4** : DCS-2 architecture

2.4.3 L-WIXCs based on couplers and filters

MWSF OXC Architecture

A combination of star couplers and tunable filters may also be used as a switching element. This architecture also called CF-1 architecture is composed of multi-wavelength selective filters and star couplers. A MWSF can select any combination of wavelengths using acousto-optic interaction. The MWSFs will be configured such that signals of the same wavelength are never led to the same star coupler. This limitation makes CF-1 architecture that only allows simple full sharing of wavelength converters. There are *N* identical intermediate modules. In each of this module, only *V* tunable filters followed by wavelength converters. In CF-1 architecture the incoming channels are separated by the combination of input star couplers and MWSF. Then they go through the intermediate modules where the wavelength conversion process for non-wavelength continuous light paths takes place. For wavelength continuous light path they need not go through the wavelength conversion process. They are then combined at the output star couplers. This architecture suffers from high loss due to the splitting of WDM signals. However, they offer superior expandability and upgradeability compared to the other architectures of the same kind [9].

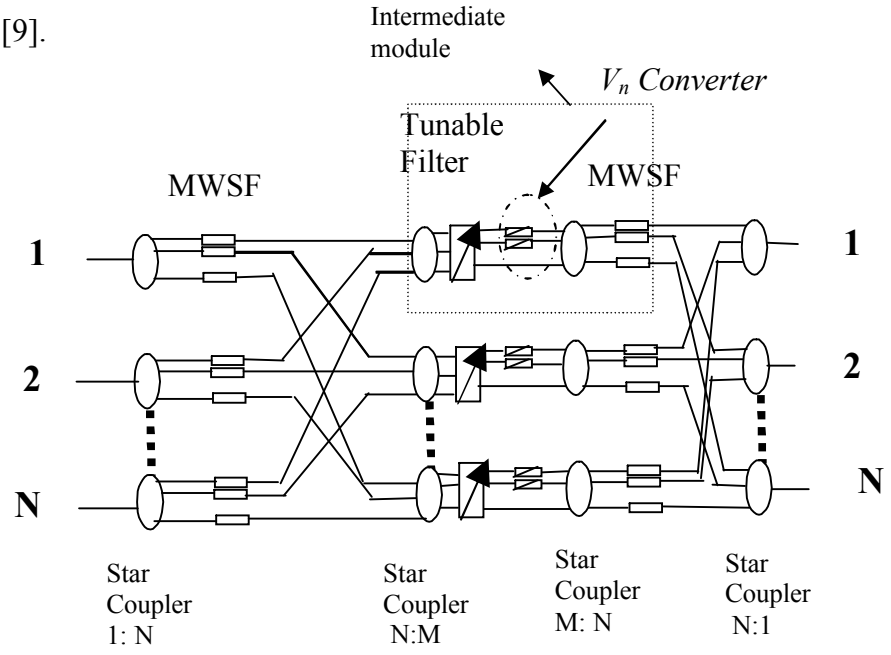

Fig. **2.5** : Multi-wavelength Selective Filters (MWSF) OXC architecture

Wavelength Switch OXC architecture

This is also called CF-2 in which the WDM comb from any of the *N* input links is delivered to every one of the $N \times 1$ SSMs. Each SSM inhibits all but one input comb. The tunable filter at the output of the SSM will then select a channel from the comb. This architecture allows strict full sharing of wavelength converters. This architecture applies a routing scheme that searches first for routes without wavelength converters when routing unconverted light paths will minimize wasteful occupancy. This architecture also suffers from high loss due to the splitting of WDM signals and offer superior expandability and upgradeability like MWSF OXC Architecture [9].

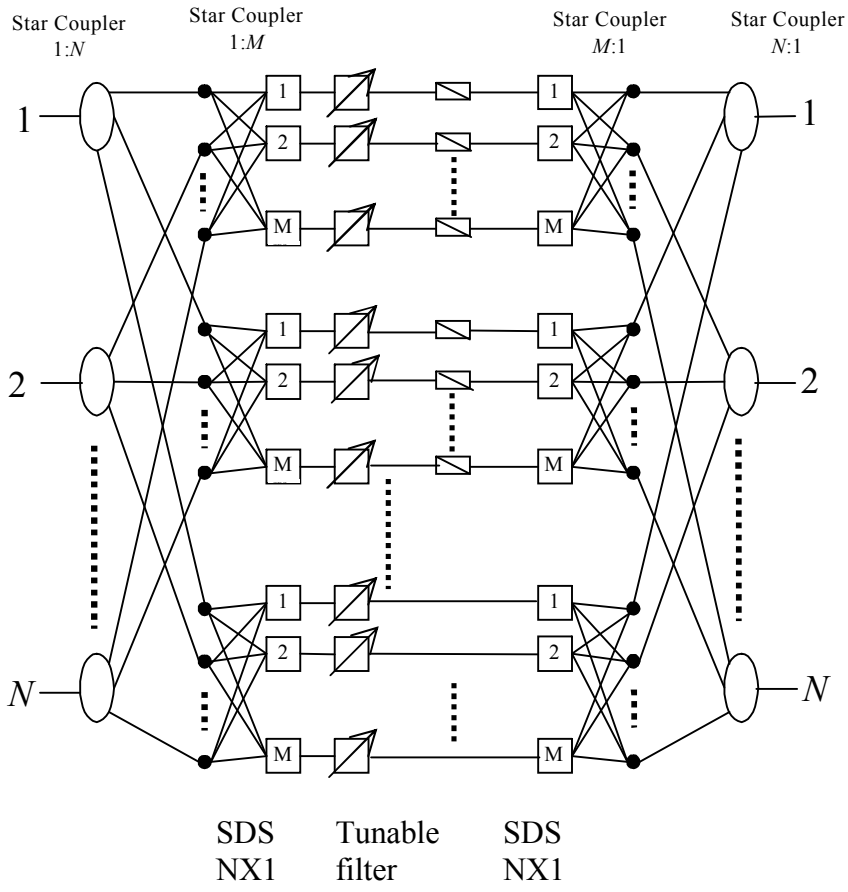

Fig. **2.6** Wavelength switch OXC architecture

2.5 Comparison of Various L-WIXC Architectures

The hardware complexity of different wavelength architectures may be listed as per their requirements of the basic hardware components, e.g. cross-points in the switches, tunable filters, star-couplers, de-multiplexers and multiplexers. We have listed these requirements in Table 1. Given the actual values of N and W, this table may be used to make a comparative study of the relative hardware requirements of each of the L-WIXC architectures discussed earlier. Table 2 gives a summary of some of

Table 1: Complexity comparison of OXC architectures.

Designation	Cross-point	Tunable filter	Star coupler	DMUX	MUX
SSM-1	$NM(N+1) + NV+MV$	-	N	N	-
SSM-2	MN^2	-	N	N	-
DCS-1	$NW(N + 1) + 2NV$	V	$3N$	N	N
DCS-2	MN^2	NM	-	N	N
CF-1	-	NM ($2N^2$ MWSF)	$4N$	-	-
CF-2	$2MN^2$	NM	$2N(N + 1)$	-	-

Table 2: Comparison of OXC architectures.

Designation	Degree of sharing	Wasteful occupancy	Expandability
SSM-1	Strict full	No	Poor
SSM-2	Partial	No	Poor
DCS-1	Strict full	No	Poor
DCS-2	Partial	Yes	Good
CF-1	Simple full	Yes	Good
CF-2	Strict full	Yes	Good

the key features of the respective architectures in terms of degree of sharing that they allows, whether wasteful occupancy is incurred or not and their relative expandability. The SSM-based and DCS-based share-per-node architectures generally require more complex switching than the WIXC. The multi-stage share-per-link architectures, on the other hand, appear very similar to the multi-stage WIXC architectures except that they have fewer converters. This also makes the share-per-link architectures easily upgradeable to WIXC, as stated in Table 2. The share-per-node L-WIXCs using couplers and filters require no additional complexity and are generally easily expandable. However, extensive use of couplers imposes a high splitting loss [9].

Chapter-3

ANALYSIS OF CROSSTALK IN LIMITED WAVELENGTH INTERCHANGING CROSS-CONNECTS (L-WIXC)

3.1 Introduction

As optical crosstalk originating from different sources is responsible for signal degradation, it is a major limiting factor in using OXC. While propagating various type of crosstalks mix with the main signal and overwhelm the signal detection process. Crosstalk also imposes limit on number of channel and transmission distance. For effective signal transmission we have to limit the amount of crosstalk. So it is necessary to have knowledge about the maximum amount of crosstalk that may be encountered with the signal transmission. In this chapter analytical method will be presented to quantify the crosstalk for each architecture of limited wavelength interchanging optical cross-connect (L-WIXC). The various type of crosstalk will be modeled as a Gaussian random process. This approximation is appropriate when there are a large number of crosstalk sources, by virtue of central limit theorem.

3.2 Crosstalk

Crosstalk is the general term given to the effect of other signals on the desired signal. Almost every component in a WDM system introduces crosstalk of some form or another. The components include filters, wavelength multiplexers/demultiplexers, switch, semiconductor opticl amplifiers and the fiber itself. It is the major limitation of all optical WDM system because it degrades the system performance seriously. Two kinds of crosstalks, Interchannel or interband crosstalk and intrachannel or intraband crosstalk. Interchannel or interband crosstalk is the crosstalk which has different wavelength from that of signal wavelength. This is not so sever because this can be removed with narrow-band filters and it produces no beating during detection. It is also called heterodyne crosstalk and during optical detection, it acts as a random factor reducing the signal

extinction ratio thus affecting the accuracy of clock recovery. It is not sensitive to polarization matching between the signal and crosstalk field.

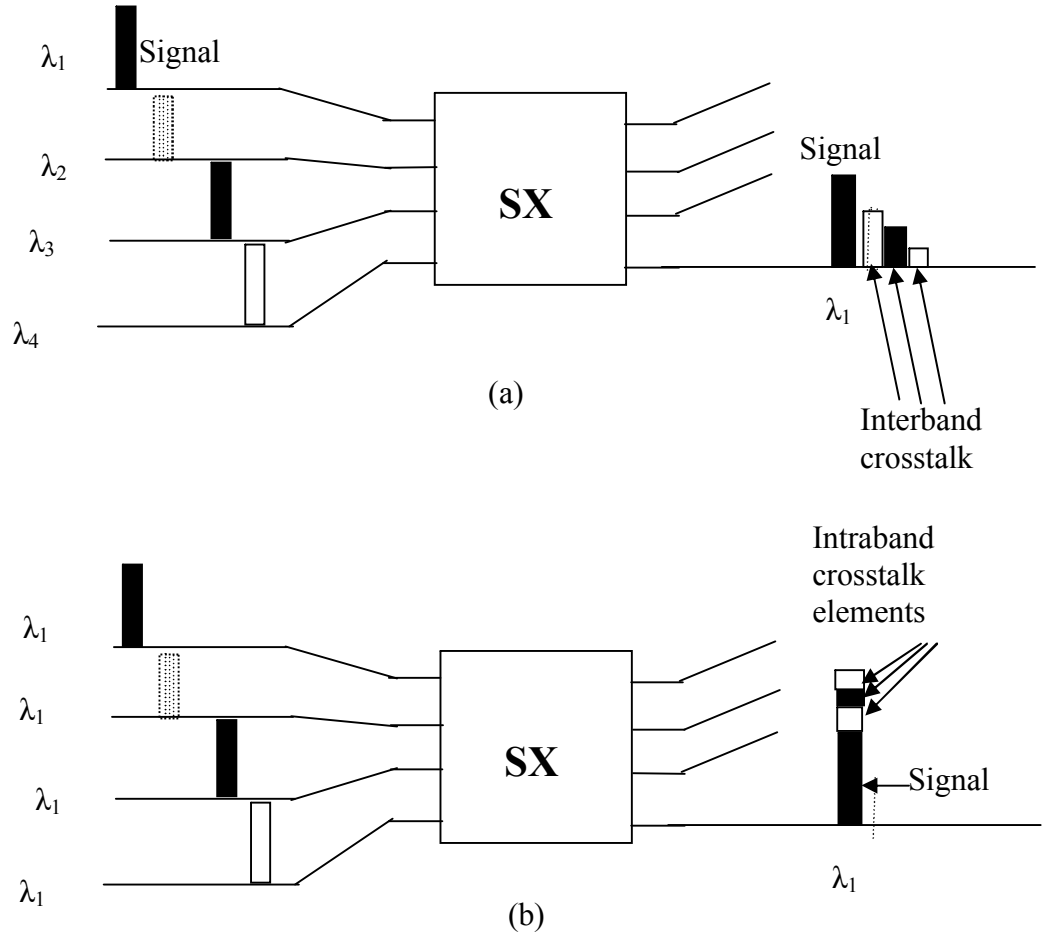

Fig. **3.1** (a) Interband and (b) Intraband crosstalk

Crosstalk which has the same wavelength as the original signal is called intrachannel crosstalk and as it cannot be removed by an optical filter, it accumulates through the network. It is also called homodyne crosstalk. It generates noise power as well as fluctuates the signal power and penalty is highest when the state of polarization is same as that of desired signal. Intraband crosstalk can be divided into two. One is coherent crosstalk and other is incoherent crosstalk. Coherent crosstalk whose phase is correlated with the signal and that of whose phase is not correlated with the signal is called incoherent crosstalk. Incase of coherent crosstalk the total crosstalk is dominated by the beat and causes

fluctuation of the signal. On the other hand incase of incoherent crosstalk the beat term is very small compared with the total crosstalk [10-16]. .

3.3 Assumption in Crosstalk Modeling

Crosstalk model is based on the following assumption:

i) Laser phase noise has uniform distribution;
ii) Phase noise originated from different lasers are independent to each other;
iii) Digital bits are intensity modulated;
iv) Integrate-and-dump filter is used at the receiver to improve the error rate;
v) Receiver is alternating current (ac) coupled;
vi) All signal sources have the same bit rate;
vii) Signal-spontaneous beat noise is the dominant noise effect.

These assumptions fit systems with optical amplifier whose spontaneous emission appears as noise. If the amplifier gain is reasonably large (>10 db), which is normally the case for optical cross-connect systems, the receiver noise is negligible compare to the signal-spontaneous and spontaneous-spontaneous beat noise resulting from the amplifiers. The spontaneous-spontaneous beat noise can be made very small by reducing the optical bandwidth. The dominant noise is, therefore, signal-spontaneous beat noise. Since the noise is signal dependent, a simple ac-coupled receiver will set its decision threshold corresponding to average received current level [13].

3.4 Power Penalty

The impact of crosstalk in a wavelength division multiplexing (WDM) system may be quantified by considering the crosstalk power penalty (PP). The crosstalk PP is defined as the additional power (In decibels) needed for the signal to achieve the same error rate as that without crosstalk.

That is, $PP = P_{rec\ (with\ crosstalk)} - P_{rec\ (without\ crosstalk)}$

3.5 Coherence Property

The variance of the output signal depends on the coherence relation of the various components and this relation may change with the relative delays of the components. The laser output, for instance, which is the result of electron state transition from one energy band to another, is coherent only with in a characteristic time, called coherence time. It is emitted at a specific wavelength corresponding to resonance mode in the laser's cavity, but this wave will actually fluctuate around a center wavelength because electrons can leave and enter slightly different energy level within the same band. The amount of fluctuation in the wavelength is called linewidth and can be accounted for by the laser phase noise. The length of time that coherence is maintained is called coherence time. The length that the signal may travel in vacuum during that time is called the coherence length. In statistical terms, a random function becomes incoherent when its autocorrelation vanishes. Statistically, the coherence time and linewidth are related by

$$\text{Coherence time} = \frac{\lambda^2}{c\Delta\lambda}$$

Where λ is the center wavelength, Δλ is the line width and c is the speed of light in vacuum. A simple laser may have a coherence time of 0.5 ns and a coherence length of 15 cm. A vary good-quality narrow-line width laser may have a coherence time of 1 μs and coherence length of upto 300 m . The delay τ experienced by the various components depends on the OXC hardware, e.g., the length of the patch fiber. For a high-speed communication system, the bit duration T may be less than the laser coherence time, e.g.,T=0.4 ns for 2.5 Gb/s transmission.

The possible cases can, thus, be identified as

Case 1: $\tau < \tau_{coherent}$ and $\tau << T$, Bit period or Coherent case

Case 2: $\tau < \tau_{coherent}$ and $\tau > T$, Bit period or Incoherent case

3.6. Analysis of Crosstalk in an L-WIXC

The instantaneous electrical field of a signal with center frequency ω coming from port í of an OXC can be expressed as

$$\overrightarrow{E_0(t)} = Eb_i(t)\cos[\omega t + \Phi_i(t)]\ \vec{P}_i \quad (3.1)$$

Where E is the signal field amplitude that is assumed to be constant with respect to time, $b_i(t)$ is the binary data sequence with values of 0 or 1 in a bit period T, Φ_i is the phase noise of the laser and $\vec{P}_i$ is the unit-polarization vector of the signal..

For each architecture the amount of crosstalk power will be analyzed in detail. In each case the signal at ω entering from port 1 is chosen as the signal in question and inband crosstalk which has the same wavelength as the desired signal will be considered.

This architecture consists of star couplers, Tunable Filters and space division switches. The crosstalk mechanism in different optical components of this architecture is explained bellow.

3.6.1 Architecture-1 Share Per Node

A. Tunable Filter

The actual signal in question is combined with M-1 signals at different wavelengths by a star coupler at the output of fig-3.2. These signals carry with them crosstalk components having the same wavelength as the actual signal, which can be traced back to the tunable filters. Due to imperfect filtering, M-1 crosstalk components at ω leaked through the filters and mix with the actual signal at the star coupler after passing through the switches as shown in fig-3.2. Let X_i (i=1, 2,……, N) be the number of crosstalk components at ω that are leakages of the signal entering the OXC at input port i, than, each X_i is an integer satisfying

$$\sum_{i=1}^{N} X_i = M - 1,\ 1 \le X_i \le M\text{-}1 \quad (3.2)$$

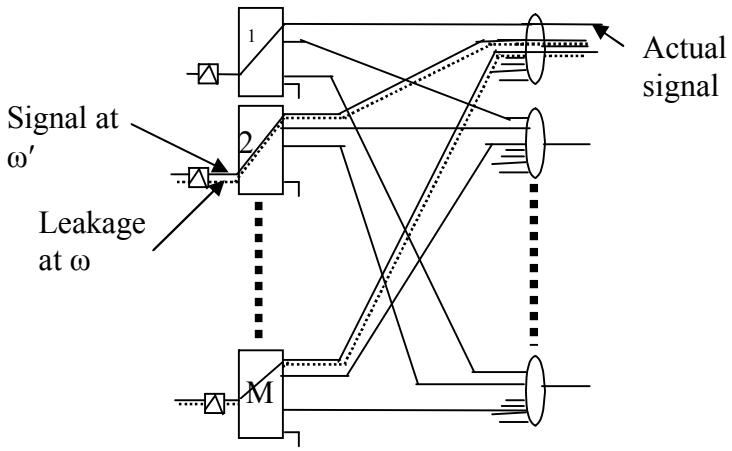

Fig**. 3.2** Crosstalk leaked from tunable filters.

B. Space-Division Switch

In a real SDS, each crosstalk will leak to the unattended outputs, including crosstalk to the actual signal. In fig-3.3, there are N-1 inband crosstalk components at ω leaking from the first stage switches. These are contributed by signals entering from different input ports, as shown in fig-3.3.

In the wave length converter for a signal converted to ω, there must be another signal originally at ω being converted to another wavelength. Therefore, in the worst case, assuming V converters, there are K crosstalk components, with K= min (N-1, $\lfloor V/2 \rfloor$) which leak from the second stage switches. Assuming the converted signal is free from the crosstalk carried with it before wavelength conversion.

Assuming that the OXC is fully loaded, in the worst case, the actual signal will be interfered by M-1 crosstalk components leaking from the tunable filters, another N-1 crosstalk components leaking from the switches and K components leaking from the second stage switches. The components traverse the OXC via different paths and, thus, have different propagation delays. Assuming intensity modulation, the electric field, which includes the influence of the crosstalk, is given by

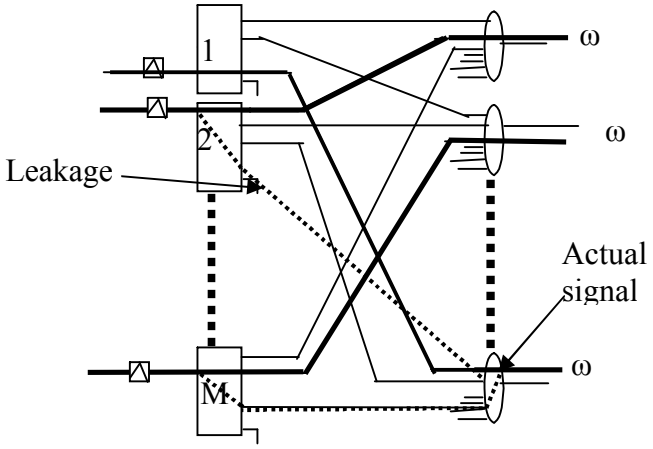

Fig. **3.3** Crosstalk leaked by Switches

$$\overrightarrow{E(t)} = Eb_1(t)\cos[\omega t + \varphi_1(t)]\ \overrightarrow{P_1} + \sum_{i=1}^{N}\sum_{j=1}^{X_i}\sqrt{\delta}Eb_i(t-\tau_{ij})\cos[\omega(t-\tau_{ij}) + \varphi_i(t-\tau_{ij})]\ \overrightarrow{P_{ij}}$$

$$+ \sum_{i=2}^{N}\sqrt{\varepsilon}Eb_i(t-\tau_{ix})\cos[\omega(t-\tau_{ix}) + \varphi_i(t-\tau_{ix})]\ \overrightarrow{P_{ix}}$$

$$+ \sum_{i=2}^{K}\sqrt{\varepsilon'}Eb'_i(t-\tau'_i)\cos[\omega(t-\tau'_i) + \varphi'_i(t-\tau'_i)]\ \overrightarrow{P'_i} \qquad (3.3)$$

That is,

$$\overrightarrow{E(t)} = Eb_1(t)\cos[\omega t + \varphi_1(t)]\ \overrightarrow{P_1} + E\sum_{j=1}^{X_1}\sqrt{\delta}b_1(t-\tau_{1j})\cos[\omega(t-\tau_{1j}) + \varphi_1(t-\tau_{1j})]\ \overrightarrow{P_{1j}}$$

$$+ \sum_{i=2}^{N}E\{\sum_{j=1}^{X_i}\sqrt{\delta}b_i(t-\tau_{ij})\cos[\omega(t-\tau_{ij}) + \varphi_i(t-\tau_{ij})]\ \overrightarrow{P_{ij}}$$

$$+ \sqrt{\varepsilon}b_i(t-\tau_{ix})\cos[\omega(t-\tau_{ix}) + \varphi_i(t-\tau_{ix})]\ \overrightarrow{P_{ix}}\ \}$$

$$+ \mathrm{E}\sum_{i=2}^{K}\sqrt{\varepsilon'}b'_i(t-\tau'_i)\cos[\omega(t-\tau'_i) + \varphi'_i(t-\tau'_i)]\ \overrightarrow{P'_i} \qquad (3.4)$$

Where τ_{ij}, $\overrightarrow{P_{ij}}$, τ_{ix}, $\overrightarrow{P_{ix}}$, δ and ε are as follows.

τ_{ij} = Propagation delay relative to the actual signal of the jth crosstalk component leaking from the signal entering from port *i* of the OXC at the tunable filter.

$\overrightarrow{P_{ij}}$ = The unit polarization vector of crosstalk component having delay τ_{ij}.

τ_{ix} = Propagation delay relative to the actual signal of the crosstalk component leaking from the signal entering from port *i* of the OXC at the first stage optical switch.

$\overrightarrow{P_{ix}}$ = The unit polarization vector of crosstalk component having delay τ_{ix}.

τ'_i = Propagation delay relative to the actual signal of the crosstalk component leaking from the signal entering from port *i* of the second stage optical switch

$\overrightarrow{P_{i'}}$ = The unit polarization vector of crosstalk component having delay τ'_i.

δ= Optical power relative to the actual signal for the crosstalk components leaked at a tunable filter.

ε = Optical power relative to the actual signal for the crosstalk components leaked at first stage optical switch.

ε′ = Optical power relative to the actual signal for the crosstalk components leaked at second stage switch.

The first term in equation (3.4) is the actual signal while the second and third terms are the crosstalk contribution due to filters; the fourth terms correspond to the crosstalks contributed by leakages from the first stage switches and fifth term for the second stage switches respectively. In the second term $E\sum_{j=1}^{X_i}\sqrt{\delta}b_i(t-\tau_{ij})\cos[\omega(t-\tau_{ij}) + \varphi_i(t-\tau_{ij})]\overrightarrow{P_{ij}}$ is the leakage contributed by the signal from the input link *i.* These components may mix coherently with each other, since they have originated from the same signal and their phases are correlated.

Since the delays are less than laser coherence time, some of the crosstalk components originate from the same signal and their phases are correlated. In this case, the time delay terms cannot be neglected, but the $\Phi(t-\tau)$ terms can be approximated by $\Phi(t)$.Equation (3.4) can be written as (3.5)

$$\overrightarrow{E(t)} = Eb_1(t)\cos[\omega t + \varphi_1(t)]\ \overrightarrow{P_1} + E\sum_{j=1}^{X_1}\sqrt{\delta}b_1(t-\tau_{1j})\cos[\omega(t-\tau_{1j}) + \varphi_1(t)]\ \overrightarrow{P_{1j}}$$

$$+ \sum_{i=2}^{N} E\{\sum_{j=1}^{X_i}\sqrt{\delta}b_i(t-\tau_{ij})\cos[\omega(t-\tau_{ij}) + \varphi_i(t)]\ \overrightarrow{P_{ij}}$$

$$+ \sqrt{\varepsilon}b_i(t-\tau_{ix})\cos[\omega(t-\tau_{ix}) + \varphi_i(t)]\ \overrightarrow{P_{ix}}\ \}$$

$$+ \mathrm{E}\sum_{i=2}^{K}\sqrt{\varepsilon'}b'_i(t-\tau'_i)\cos[\omega(t-\tau'_i) + \varphi'_i(t)]\ \overrightarrow{P'_i} \qquad (3.5)$$

The second term in equation (3.5) represents the composite crosstalk that consists of the components leaking from the actual signal and is, therefore, coherent with the actual signal. The other composite crosstalk contributions are incoherent, each of which is a coherent combination of a number of crosstalks leaking from the same signal. The decision variable J is given by

$$\mathrm{J} \approx \frac{1}{T}\int_{nT}^{(n+1)T} b_1^2(t)dt + \frac{2}{T}\sum_{j=1}^{X_1}\sqrt{\delta}\int_{nT}^{(n+1)T} b_1(t)b_1(t-\tau_{1j})dt\cos D_{1j}\cos v_{1j} +$$

$$\frac{2}{T}\sum_{i=2}^{N}\{\sum_{j=1}^{X_i}\sqrt{\delta}\int_{nT}^{(n+1)T} b_1(t)b_i(t-\tau_{ij})dt\cos[\varphi_1(t)-\varphi_i(t)+D_{ij}]\cos v_{ij} +$$

$$\sqrt{\varepsilon}\int_{nT}^{(n+1)T} b_1(t)b_i(t-\tau_{ix})dt\cos[\varphi_1(t)-\varphi_i(t)+D_{ix}]\cos v_{ix}\} +$$

$$\frac{2}{T}\sum_{i=2}^{K}\sqrt{\varepsilon'}\int_{nT}^{(n+1)T} b_1(t)b_1(t-\tau'_i)dt\cos[\varphi_1(t)-\varphi'_i(t)+D'_i]\cos v'_i \qquad (3.6)$$

Where $D_{ij}=\omega\tau_{ij}$, $D_{ix}=\omega\tau_{ix}$, $D'_i=\omega\tau'_i$ and $Cosv_{ij}=\overrightarrow{P_1}\cdot\overrightarrow{P_{ij}}$, $Cosv_{ix}=\overrightarrow{P_1}\cdot\overrightarrow{P_{ix}}$, $Cosv'_i=\overrightarrow{P_1}\,\overrightarrow{P_{i'}}$.

The case of interest is when $b_1(t)=1$. The PP can be estimated by considering the worst case when J fades to its minimum. The results for two different scenarios of interest are given bellow

Case 1: $\tau < \tau_{\text{coherent}}$ and $\tau \ll T$, Bit period or Coherent case

In this special case in which the relative delays are negligible, bit patterns of the components from the same source are almost identical. All b(t-τ) are approximately equal to b(t). This is the case when the components are delayed by almost the same amount and they interfere with other constructively to produce high power. From

(3.6) We get the mean and variance of J

$$E(J) = 1 + 2\sqrt{\delta} \sum_{j=1}^{X_1} \cos D_{1j} \cos v_{1j} \tag{3.7}$$

$$\sigma^2 = \frac{2}{3} \sum_{i=2}^{N} (\sqrt{\delta} \sum_{j=1}^{X_i} \cos D_{ij} \cos v_{ij} + \sqrt{\varepsilon} \cos D_{ix} \cos v_{ix})^2 +$$

$$\frac{2}{3} \sum_{i=2}^{N} (\sqrt{\delta} \sum_{j=1}^{X_i} \sin D_{ij} \cos v_{ij} + \sqrt{\varepsilon} \sin D_{ix} \cos v_{ix})^2 + \frac{2}{3} \sum_{i=1}^{K} \varepsilon' \cos^2 v'_i \tag{3.8}$$

The Crosstalk incurs maximum PP when all Cos υ terms are equal to 1 or -1 and X_1=0, which gives E(J) =1.

It can be shown that

$$\max \sum_{i=1}^{n} (Ax_i + B)^2 = (AL_n + B)^2 + (n-1)B^2 \text{ , } [\sum_{i=1}^{n} x_i = L_n]$$

and

$$\max (\sum_{i=1}^{n} A_j \cos\theta_j)^2 + (\sum_{i=1}^{n} A_j \sin\theta_j)^2 = (\sum_{i=1}^{n} A_j)^2$$

Applying this, we have

$$\max (\sigma^2) = \max [\frac{2}{3} \{ \sum_{i=2}^{N} (X_i \sqrt{\delta} + \sqrt{\varepsilon})^2 + K\varepsilon' \}]$$

$$= \frac{2}{3}[(M-1)\sqrt{\delta} + \sqrt{\varepsilon}]^2 + \frac{2}{3}(N-2)\varepsilon + \frac{2}{3}k\varepsilon' \tag{3.9}$$

Case 2: $\tau < \tau_{coherent}$ and $\tau > T$, Bit period or Incoherent case:

The delays experienced by any two components differ from each other by more than one bit period. All b(t-τ) become uncorrelated with each other and with the actual signal $b_1(t)$. So from equation (3.6) the mean and variance

$$E(J) = 1 + \sqrt{\delta} \sum_{j=1}^{X_1} \cos D_{1j} \cos v_{1j} \tag{3.10}$$

$$\sigma^2 = \frac{1}{3}\ \delta(\sum_{j=1}^{X_1} \cos^2 D_{1j} \cos^2 v_{1j}) + \frac{1}{2} \sum_{i=2}^{N} (\sqrt{\delta} \sum_{j=1}^{X_i} \cos D_{ij} \cos v_{ij} + \sqrt{\varepsilon} \cos D_{ix} \cos v_{ix})^2 \ +$$

$$\frac{1}{2} \sum_{i=2}^{N} (\sqrt{\delta} \sum_{j=1}^{X_i} \sin D_{ij} \cos v_{ij} + \sqrt{\varepsilon} \sin D_{ix} \cos v_{ix})^2 \ +$$

$$\frac{1}{6} \sum_{i=2}^{N} (\delta \sum_{i=1}^{X_i} \cos^2 v_{ij} + \varepsilon \cos^2 v_{ix}) \ + \frac{2}{3} \sum_{i=1}^{K} \varepsilon' \cos^2 v'_i \tag{3.11}$$

When all Cos υ terms are equal to 1 or -1 and X_1 = o, the PP is at its maximum. Applying

$$\max(\sigma^2) = \max\ [\frac{1}{2} \sum_{i=2}^{N} (X_i \sqrt{\delta} + \sqrt{\varepsilon})^2 + \frac{1}{6} \sum_{i=2}^{N} (X_i \delta + \varepsilon) + \frac{2}{3} K\varepsilon']$$

$$= \frac{1}{2}[(M-1)\sqrt{\delta} + \sqrt{\varepsilon}]^2 + \frac{1}{2}(N-2)\varepsilon + \frac{1}{6}(M-1)\delta + \frac{1}{6}(N-1)\varepsilon + \frac{2}{3}k\varepsilon'$$

$$= \frac{1}{2}[(M-1)\sqrt{\delta} + \sqrt{\varepsilon}]^2 + \frac{1}{6}(4N-7)\varepsilon + \frac{1}{6}(M-1)\delta + \frac{2}{3}k\varepsilon' \tag{3.12}$$

3.6.2 Architecture -2 Share per Link

Compared to Architecture-1, In this architecture there are dedicated set of converters for each link and before space division switches the signals that need wavelength conversion have to go through wavelength converter. The crosstalk analysis and their sources in this architecture are given bellow

A . Tunable Filter

As like the previous case in this architecture the actual signal is also combined with M-1 signals at different wavelengths by a star coupler at the output. These signals also carry with them inband crosstalk components, which can be traced back to the tunable filters. Due to imperfect filtering, M-1 crosstalk components at ω leaked through the filters. The signals which go through the conversion process are free from crosstalk. So there is M-V_n

inband crosstalk components that actually mix with the actual signal at the star coupler after passing through the switches. Let X_i (i=1,2,……,N) be the number of crosstalk components at ω that are leakages of the signal entering the OXC at input port *i,* than, each X_i is an integer satisfying

$$\sum_{i=1}^{N} Xi = \text{M-V}_n,\ 1 \le \text{Xi} \le \text{M-V}_n. \tag{3.13}$$

B. Space-Division Switch

In a real SDS, each crosstalk will leak to the unattended outputs, including crosstalk to the actual signal. In this case there are N-1 inband crosstalk components at ω leaking from the switches. These are contributed by signal entering from different input ports.

In this case we also assume that the OXC is fully loaded, in the worst case, the actual signal will be interfered by M- V_n crosstalk components leaking from the tunable filters and another N-1 crosstalk components leaking from the switches. The components traverse the OXC via different paths and, thus, have different propagation delays. Assuming intensity modulation, the electric field, which includes the influence of the crosstalk, is given by

$$\overrightarrow{E(t)} = Eb_1(t)\cos[\omega t + \varphi_1(t)]\ \overrightarrow{P_1} + \sum_{i=1}^{N}\sum_{j=1}^{X_i}\sqrt{\delta}Eb_i(t-\tau_{ij})\cos[\omega(t-\tau_{ij}) + \varphi_i(t-\tau_{ij})]\ \overrightarrow{P_{ij}}$$

$$+ \sum_{i=2}^{N}\sqrt{\varepsilon}Eb_i(t-\tau_{ix})\cos[\omega(t-\tau_{ix}) + \varphi_i(t-\tau_{ix})]\ \overrightarrow{P_{ix}} \tag{3.14}$$

That is,

$$\overrightarrow{E(t)} = Eb_1(t)\cos[\omega t + \varphi_1(t)]\ \overrightarrow{P_1} + E\sum_{j=1}^{X_1}\sqrt{\delta}Eb_1(t-\tau_{1j})\cos[\omega(t-\tau_{1j}) + \varphi_1(t-\tau_{1j})]\ \overrightarrow{P_{1j}}$$

$$+ \sum_{i=2}^{N} E\{\sum_{j=2}^{X_i}\sqrt{\delta}b_i(t-\tau_{ij})\cos[\omega(t-\tau_{ij}) + \varphi_i(t-\tau_{ij})]\ \overrightarrow{P_{ij}}$$

$$+ \sqrt{\varepsilon}Eb_i(t-\tau_{ix})\cos[\omega(t-\tau_{ix}) + \varphi_i(t-\tau_{ix})]\ \overrightarrow{P_{ix}}\ \} \tag{3.15}$$

Where τ_{ij}, $\overrightarrow{P_{ij}}$, τ_{ix}, $\overrightarrow{P_{ix}}$, δ and ε are as follows.

τ_{ij} = Propagation delay relative to the actual signal of the jth crosstalk component leaking from the signal entering from port *i* of the OXC at the tunable filter.

$\overrightarrow{P_{ij}}$ = The unit polarization vector of crosstalk component τ_{ij}.

τ_{ix} = Propagation delay relative to the actual signal of the crosstalk component leaking from the signal entering from port *i* of the OXC at the optical switch.

$\overrightarrow{P_{ix}}$ = The unit polarization vector of crosstalk component τ_{ix}.

δ= Optical power relative to the actual signal for the crosstalk components leaked at a tunable filter.

ε = Optical power relative to the actual signal for the crosstalk components leaked at an optical switch.

Here the first term in equation (3.15) is the actual signal while the second and third terms correspond to the crosstalks contributed by leakages from the filters and forth term due to the switches. In the second term $E\sum_{j=1}^{X_i}\sqrt{\delta}b_i(t-\tau_{ij})\cos[\omega(t-\tau_{ij}) + \varphi_i(t-\tau_{ij})]\ \overrightarrow{P_{ij}}$ is the leakage contributed by the signal from the input link *i.* These components may mix coherently with each other, since they have originated from the same signal and their phases are correlated.

Since the delays are less than laser coherence time, some of the crosstalk components originate from the same signal and there phase are correlated. In this case, the time delay terms cannot be neglected, but the $\Phi(t-\tau)$ terms can be approximated by $\Phi(t)$.Equation (3.15) can be written as (3.16)

$$\overrightarrow{E(t)} = Eb_1(t)\cos[\omega t + \varphi_1(t)]\ \overrightarrow{P_1} + E\sum_{j=1}^{X_1}\sqrt{\delta}b_1(t-\tau_{1j})\cos[\omega(t-\tau_{1j}) + \varphi_1(t)]\ \overrightarrow{P_{1j}}$$

$$+ \sum_{i=2}^{N} E\{\sum_{j=1}^{X_i}\sqrt{\delta}b_i(t-\tau_{ij})\cos[\omega(t-\tau_{ij}) + \varphi_i(t)]\ \overrightarrow{P_{ij}}$$

$$+ \sqrt{\varepsilon}b_i(t-\tau_{ix})\cos[\omega(t-\tau_{ix}) + \varphi_i(t)]\ \overrightarrow{P_{ix}}\ \} \qquad (3.16)$$

The second term in equation (3.16) represents the composite crosstalk that consists of the components leaking from the actual signal and is, therefore, coherent with the actual signal. The other composite crosstalk contributions are incoherent, each of which is a coherent combination of a number of crosstalks leaking from the same signal. The decision variable J is given by

$$J \approx \frac{1}{T}\int_{nT}^{(n+1)T} b_1^2(t)dt + \frac{2}{T}\sum_{j=1}^{X_1}\sqrt{\delta}\int_{nT}^{(n+1)t} b_1(t)b_1(t-\tau_{1j})dt\cos D_{1j}\cos v_{1j} +$$

$$\frac{2}{T}\sum_{i=2}^{N}\{\sum_{j=1}^{Xi}\sqrt{\delta}\int_{nT}^{(n+1)T} b_1(t)b_i(t-\tau_{ij})dt\cos[\phi_1(t)-\phi_i(t)+D_{ij}]\cos v_{ij}$$

$$+\sqrt{\varepsilon}\int_{nT}^{(n+1)T} b_1(t)b_i(t-\tau_{ix})dt\cos[\phi_1(t)-\phi_i(t)+D_{ix}]\cos v_{ix}\} \qquad (3.17)$$

Where $D_{ij}=\omega\tau_{ij}$, $D_{ix}=\omega\tau_{ix}$, *and* $Cosv_{ij}=\overrightarrow{P_1}.\overrightarrow{P_{ij}}$, $cosv_{ix}=\overrightarrow{P_1}$.

The case of interest is when $b_1(t)=1$. The PP can be estimated by considering the worst case when J fades to its minimum. The results for two different scenarios of interest are given bellow

Case 1: $\tau < \tau_{coherent}$ and $\tau \ll T$, Bit period or Coherent case

In this special case in which the relative delays are negligible, bit patterns of the components from the same source are almost identical. All $b(t-\tau)$ are approximately equal to $b(t)$. This is the case when the components are delayed by almost the same amount and they interfere with other constructively to produce high power. From

(3.17) We get the mean and variance of J

$$E(J) = 1 + 2\sqrt{\delta}\sum_{j=1}^{X_1}\cos D_{1j}\cos v_{1j} \qquad (3.18)$$

$$\sigma^2 = \frac{2}{3}\sum_{i=2}^{N}(\sqrt{\delta}\sum_{j=1}^{X_i}\cos D_{ij}\cos v_{ij} + \sqrt{\varepsilon}\cos D_{ix}\cos v_{ix})^2 +$$

$$\frac{2}{3}\sum_{i=2}^{N}(\sqrt{\delta}\sum_{j=1}^{X_i}\sin D_{ij}\cos v_{ij} + \sqrt{\varepsilon}\sin D_{ix}\cos v_{ix})^2 \qquad (3.19)$$

The Crosstalk incurs maximum PP when all Cos υ terms are equal to 1 or -1 and $X_1=0$, which gives E(J) =1.

It can be shown that

$$\max \sum_{i=1}^{n}(Ax_i + B)^2 = (AL_n + B)^2 + (n-1)B^2 \text{ , } [\ \sum_{i=1}^{n} x_i = L_n\ ]$$

and

$$\max (\sum_{i=1}^{n} A_j \cos\theta_j)^2 + (\sum_{i=1}^{n} A_j \sin\theta_j)^2 = (\sum_{i=1}^{n} A_j)^2$$

Applying this, we have

$$\max (\sigma^2) = \max\ [\frac{2}{3}\sum_{i=2}^{N}(X_i\sqrt{\delta} + \sqrt{\varepsilon})^2]$$

$$= \frac{2}{3}[(M - V_n)\sqrt{\delta} + \sqrt{\varepsilon}]^2 + \frac{2}{3}(N-2)\varepsilon \qquad (3.20)$$

Case 2: $\tau < \tau_{coherent}$ and $\tau > T$, Bit period or Incoherent case :

The delays experienced by any two components differ from each other by more than one bit period. All b(t-τ) become uncorrelated with each other and with the actual signal the actual signal $b_1(t)$. So from equation (3.17) the mean and variance

$$E(J) = 1 + \sqrt{\delta}\ \sum_{j=1}^{X_1}\cos D_{1j}\cos v_{1j} \qquad (3.21)$$

$$\sigma^2 = \frac{1}{3}\delta(\sum_{j=1}^{X_1}\cos^2 D_{1j}\cos v_{ij}^2) + \frac{1}{2}\sum_{i=2}^{N}\ (\sqrt{\delta}\ \sum_{j=1}^{X_i}\cos D_{ij}\cos v_{ij} + \sqrt{\varepsilon}\cos D_{ix}\cos v_{ix})^2$$

$$+\frac{1}{2}\sum_{i=2}^{N}(\sqrt{\delta}\ \sum_{j=1}^{X_i}\sin D_{ij}\cos v_{ij} + \sqrt{\varepsilon}\sin D_{ix}\cos v_{ix})^2$$

$$+\frac{1}{6}\sum_{i=2}^{N}(\delta\ \sum_{j=1}^{X_i}\cos^2 v_{ij} + \varepsilon\cos^2 v_{ix}) \qquad (3.22)$$

When all Cos υ terms are equal to 1 or -1 and $X_1 = 0$, the PP is at its maximum. Applying

$$\max (\sigma^2) = \max\ [\frac{1}{2}\sum_{i=2}^{N}(X_i\sqrt{\delta} + \sqrt{\varepsilon})^2 + \frac{1}{6}\sum_{i=2}^{N}(X_i\delta + \varepsilon)]$$

$$= \frac{1}{2}[(M - V_n)\sqrt{\delta} + \sqrt{\varepsilon}]^2 + \frac{1}{2}(N-2)\varepsilon + \frac{1}{6}(M - V_n)\delta + \frac{1}{6}(N-1)\varepsilon$$

$$= \frac{1}{2}[(M - V_n)\sqrt{\delta} + \sqrt{\varepsilon}]^2 + \frac{1}{6}(4N-7)\varepsilon + \frac{1}{6}(M - V_n)\delta \quad (3.23)$$

3.6.3 DCS-1 Architecture

This architecture is as same as Share per Node architecture but instead of Space switch Delivery-and –coupling switch is used. The crosstalk mechanism in different optical components are given bellow

A. Tunable Filter

The actual signal in question is combined with M-1 signals at different wavelengths by a star coupler at the output. These signals carry with them crosstalk components having the same wavelength as the actual signal, which can be traced back to the tunable filters. Due to imperfect filtering, M-1 crosstalk components at ω leaked through the filters and mix with the actual signal at the star coupler after passing through the switches. Let X_i (i=1,2,……,N) be the number of crosstalk components at ω that are leakages of the signal entering the OXC at input port *i,* than, each X_i is an integer satisfying

$$\sum_{i=1}^{N} X_i = \text{M-1},\ 1 \le X_i \le \text{M-1}. \quad (3.24)$$

B. Delivery-and –coupling switch

In a real SDS, each crosstalk will leak to the unattended outputs, including crosstalk to the actual signal. In fig-3.4 , there are N-1 inband crosstalk components at ω leaking from the first stage switches. These are contributed by signal entering from different input ports.

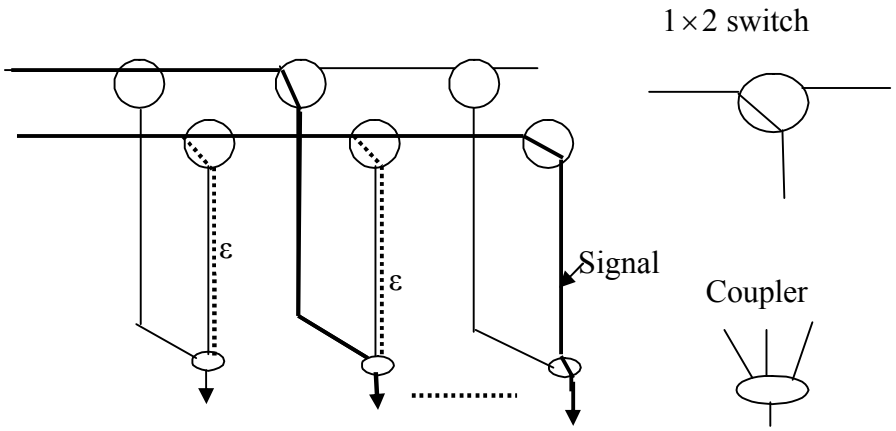

Fig. **3.4** Crosstalk in DCS.

In the wavelength converter for a signal converted to ω, there must be another signal originally at ω being converted to another wavelength. Therefore, in the worst case, assuming V converters, there are K crosstalk components, with K= min (N-1, $\lfloor V/2 \rfloor$) which leak from the second stage switches. The converted signal is free from the crosstalk carried with it before wavelength conversion.

Assuming that the OXC is fully loaded, in the worst case, the actual signal will be interfered by M-1 crosstalk components leaking from the tunable filters, another N-1 crosstalk components leaking from the switches and K components leaking from the second stage switches. The components traverse the OXC via different paths and, thus, have different propagation delays. Assuming intensity modulation, the electric field, which includes the influence of the crosstalk, is given by

$$\overrightarrow{E(t)} = Eb_1(t)\cos[\omega t + \varphi_1(t)]\ \overrightarrow{P_1} + \sum_{i=1}^{N}\sum_{j=1}^{X_i}\sqrt{\delta}\,Eb_i(t-\tau_{ij})\cos[\omega(t-\tau_{ij}) + \varphi_i(t-\tau_{ij})]$$

$$\overrightarrow{P_{ij}} + \sum_{i=2}^{N}\sqrt{\varepsilon}\,Eb_i(t-\tau_{ix})\cos[\omega(t-\tau_{ix}) + \varphi_i(t-\tau_{ix})]\ \overrightarrow{P_{ix}}$$

$$+ \sum_{i=2}^{K}\sqrt{\varepsilon'}Eb'_i(t-\tau'_i)\cos[\omega(t-\tau'_i) + \varphi'_i(t-\tau'_i)]\ \overrightarrow{P'_i} \qquad (3.25)$$

That is,

$$\overrightarrow{E(t)} = Eb_1(t)\cos[\omega t + \varphi_1(t)]\ \overrightarrow{P_1} + E\sum_{j=1}^{X_1}\sqrt{\delta}b_1(t-\tau_{1j})\cos[\omega(t-\tau_{1j}) + \varphi_1(t-\tau_{1j})]\ \overrightarrow{P_{1j}}$$

$$+ \sum_{i=2}^{N} E\{\sum_{j=1}^{X_i}\sqrt{\delta}b_i(t-\tau_{ij})\cos[\omega(t-\tau_{ij}) + \varphi_i(t-\tau_{ij})]\ \overrightarrow{P_{ij}}$$

$$+ \sqrt{\varepsilon}b_i(t-\tau_{ix})\cos[\omega(t-\tau_{ix}) + \varphi_i(t-\tau_{ix})]\ \overrightarrow{P_{ix}}\ \}$$

$$+ \mathrm{E}\sum_{i=2}^{K}\sqrt{\varepsilon'}b'_i(t-\tau'_i)\cos[\omega(t-\tau'_i) + \varphi'_i(t-\tau'_i)]\ \overrightarrow{P'_i} \qquad (3.26)$$

Where τ_{ij}, $\overrightarrow{P_{ij}}$, τ_{ix}, $\overrightarrow{P_{ix}}$, δ and ε are as follows.

τ_{ij} = Propagation delay relative to the actual signal of the jth crosstalk component leaking from the signal entering from port *i* of the OXC at the tunable filter.

$\overrightarrow{P_{ij}}$ = The unit polarization vector of crosstalk component τ_{ij}.

τ_{ix} = Propagation delay relative to the actual signal of the crosstalk component leaking from the signal entering from port *i* of the OXC at the first stage optical switch.

$\overrightarrow{P_{ix}}$ = The unit polarization vector of crosstalk component τ_{ix}.

τ'_i = Propagation delay relative to the actual signal of the crosstalk component leaking from the signal entering from port *i* of the second stage optical switch

$\overrightarrow{P_{i'}}$ = The unit polarization vector of crosstalk component τ'_i.

δ= Optical power relative to the actual signal for the crosstalk components leaked at a tunable filter.

ε = Optical power relative to the actual signal for the crosstalk components leaked at first stage optical switch.

ε′ = Optical power relative to the actual signal for the crosstalk components leaked at second stage switch.

The first term in equation (3.26) is the actual signal while the second and third terms are the crosstalk contribution due to filters; the fourth terms correspond to the crosstalks contributed by leakages the first stage switches and fifth term for the second stage switches respectively. In the second term $E\sum_{j=1}^{X_i}\sqrt{\delta}b_i(t-\tau_{ij})\cos[\omega(t-\tau_{ij}) + \varphi_i(t-\tau_{ij})]\ \overrightarrow{P_{ij}}$ is the

leakage contributed by the signal from the input link *i*. These components may mix coherently with each other, since they have originated from the same signal and their phases are correlated.

Since the delays are less than laser coherence time, some of the crosstalk components originate from the same signal and there phase are correlated. In this case, the time delay terms cannot be neglected, but the $\Phi(t-\tau)$ terms can be approximated by $\Phi(t)$.Equation (3.26) can be written as (3.27)

$$\overrightarrow{E(t)} = Eb_1(t)\cos[\omega t + \varphi_1(t)]\ \overrightarrow{P_1} + E\sum_{j=1}^{X_1}\sqrt{\delta}\,b_1(t-\tau_{1j})\cos[\omega(t-\tau_{1j}) + \varphi_1(t)]\ \overrightarrow{P_{1j}}$$

$$+ \sum_{i=2}^{N} E\{\sum_{j=1}^{X_i}\sqrt{\delta}\,b_i(t-\tau_{ij})\cos[\omega(t-\tau_{ij}) + \varphi_i(t)]\ \overrightarrow{P_{ij}}$$

$$+ \sqrt{\varepsilon}\,b_i(t-\tau_{ix})\cos[\omega(t-\tau_{ix}) + \varphi_i(t)]\ \overrightarrow{P_{ix}}\ \}$$

$$+ \mathrm{E}\sum_{i=2}^{K}\sqrt{\varepsilon'}\,b'_i(t-\tau'_i)\cos[\omega(t-\tau'_i) + \varphi'_i(t)]\ \overrightarrow{P'_i} \qquad (3.27)$$

The second term in equation (3.27) represents the composite crosstalk that consists of the components leaking from the actual signal and is, therefore, coherent with the actual signal. The other composite crosstalk contributions are incoherent, each of which is a coherent combination of a number of crosstalks leaking from the same signal. The decision variable J is given by

$$\mathrm{J} \approx \frac{1}{T}\int_{nT}^{(n+1)T} b_1^2(t)dt + \frac{2}{T}\sum_{j=1}^{X_1}\sqrt{\delta}\int_{nT}^{(n+1)T} b_1(t)b_1(t-\tau_{1j})dt\cos D_{1j}\cos v_{1j} +$$

$$\frac{2}{T}\sum_{i=2}^{N}\{\sum_{j=1}^{X_i}\sqrt{\delta}\int_{nT}^{(n+1)T} b_1(t)b_i(t-\tau_{ij})dt\cos[\varphi_1(t)-\varphi_i(t)+D_{ij}]\cos v_{ij} +$$

$$\sqrt{\varepsilon}\int_{nT}^{(n+1)T} b_1(t)b_i(t-\tau_{ix})dt\cos[\varphi_1(t)-\varphi_i(t)+D_{ix}]\cos v_{ix}\} +$$

$$\frac{2}{T}\sum_{i=2}^{K}\sqrt{\varepsilon'}\int_{nT}^{(n+1)T} b_1(t)b_1(t-\tau'_i)dt\cos[\varphi_1(t)-\varphi'_i(t)+D'_i]\cos v'_i \qquad (3.28)$$

Where $D_{ij}=\omega\tau_{ij}$, $D_{ix}=\omega\tau_{ix}$, $D'_i=\omega\tau'_i$ and $Cosv_{ij}=\overrightarrow{P_1}\,.\,\overrightarrow{P_{ij}}$, $Cosv_{ix}=\overrightarrow{P_1}\,.\,\overrightarrow{P_{ix}}$, $Cosv'_i=\overrightarrow{P_1}\,\overrightarrow{P_{i'}}$.

The case of interest is when $b_1(t) = 1$. The PP can be estimated by considering the worst case when J fades to its minimum. The results for two different scenarios of interest are given bellow

Case 1: $\tau < \tau_{coherent}$ and $\tau << T$, Bit period or Coherent case

In this special case in which the relative delays are negligible, bit patterns of the components from the same source are almost identical. All $b(t-\tau)$ are approximately equal to b(t). This is the case when the components are delayed by almost the same amount and they interfere with other constructively to produce high power. From

(3.28) We get the mean and variance of J

$$E(J) = 1 + 2\sqrt{\delta}\sum_{j=1}^{X_1}\cos D_{ij}\cos v_{ij} \tag{3.29}$$

$$\sigma^2 = \frac{2}{3}\sum_{i=2}^{N}(\sqrt{\delta}\sum_{j=1}^{X_i}\cos D_{ij}\cos v_{ij} + \sqrt{\varepsilon}\cos D_{ix}\cos v_{ix})^2 +$$

$$\frac{2}{3}\sum_{i=2}^{N}(\sqrt{\delta}\sum_{j=1}^{X_i}\sin D_{ij}\cos v_{ij} + \sqrt{\varepsilon}\sin D_{ix}\cos v_{ix})^2 + \frac{2}{3}\sum_{i=1}^{K}\varepsilon'\cos^2 v'_i \tag{3.30}$$

The Crosstalk incurs maximum PP when all Cos υ terms are equal to 1 or -1 and $X_1 = 0$, which gives E(J) =1.

It can be shown that

$$\max \sum_{i=1}^{n}(Ax_i + B)^2 = (AL_n + B)^2 + (n-1)B^2 \text{ , } [\ \sum_{i=1}^{n}x_i = L_n\ ]$$

and

$$\max (\sum_{i=1}^{n}A_j\cos\theta_j)^2 + (\sum_{i=1}^{n}A_j\sin\theta_j)^2 = (\sum_{i=1}^{n}A_j)^2$$

Applying this, we have

$$\max(\sigma^2) = \max\ [\frac{2}{3}\{\sum_{i=2}^{N}(X_i\sqrt{\delta} + \sqrt{\varepsilon})^2 + K\varepsilon'\}]$$

$$= \frac{2}{3}[(M-1)\sqrt{\delta} + \sqrt{\varepsilon}]^2 + \frac{2}{3}(N-2)\varepsilon + \frac{2}{3}k\varepsilon' \tag{3.31}$$

Case 2: $\tau < \tau_{coherent}$ and $\tau > T$, Bit period or Incoherent case:

The delays experienced by any two components differ from each other by more than one bit period. All b(t-τ) become uncorrelated with each other and with the actual signal the actual signal $b_1(t)$. So from equation (3.28) the mean and variance

$$E(J) = 1 + \sqrt{\delta} \sum_{j=1}^{X_1} \cos D_{1j} \cos v_{1j} \tag{3.32}$$

$$\sigma^2 = \frac{1}{3}\ \delta(\sum_{j=1}^{X_1} \cos^2 D_{1j} \cos^2 v_{1j}) + \frac{1}{2} \sum_{i=2}^{N} (\sqrt{\delta} \sum_{j=1}^{X_i} \cos D_{ij} \cos v_{ij} + \sqrt{\varepsilon} \cos D_{ix} \cos v_{ix})^2 \ +$$

$$\frac{1}{2} \sum_{i=2}^{N} (\sqrt{\delta} \sum_{j=1}^{X_i} \sin D_{ij} \cos v_{ij} + \sqrt{\varepsilon} \sin D_{ix} \cos v_{ix})^2 \ +$$

$$\frac{1}{6} \sum_{i=2}^{N} (\delta \sum_{i=1}^{X_i} \cos^2 v_{ij} + \varepsilon \cos^2 v_{ix}) \ + \frac{2}{3} \sum_{i=1}^{K} \varepsilon' \cos^2 v'_i \tag{3.33}$$

When all Cos υ terms are equal to 1 or -1 and X_1 = o, the PP is at its maximum. Applying

$$\max(\sigma^2) = \max\ [\frac{1}{2} \sum_{i=2}^{N} (X_i \sqrt{\delta} + \sqrt{\varepsilon})^2 + \frac{1}{6} \sum_{i=2}^{N} (X_i \delta + \varepsilon) + \frac{2}{3} K\varepsilon']$$

$$= \frac{1}{2}[(M-1)\sqrt{\delta} + \sqrt{\varepsilon}]^2 + \frac{1}{2}(N-2)\varepsilon + \frac{1}{6}(M-1)\delta + \frac{1}{6}(N-1)\varepsilon + \frac{2}{3}k\varepsilon'$$

$$= \frac{1}{2}[(M-1)\sqrt{\delta} + \sqrt{\varepsilon}]^2 + \frac{1}{6}(4N-7)\varepsilon + \frac{1}{6}(M-1)\delta + \frac{2}{3}k\varepsilon' \tag{3.34}$$

3.6.4 DCS-2 Architecture

This architecture is also same as Share Per Link architecture but instead of Space switch Delivery-and –coupling switch is used. , In this architecture there are dedicated set of converters for each link and before DCS switches the signals that need wavelength conversion have to go through the wavelength converters. The crosstalk mechanism in different optical components are given bellow

A. Tunable Filter

As like the previous case in this architecture the actual signal is also combined with M-1 signals at different wavelengths by a star coupler at the output. These signals also carry with them inband crosstalk components, which can be traced back to the tunable filters. Due to imperfect filtering, M-1 crosstalk components at ω leaked through the filters. The signals which go through the conversion process are free from crosstalk. So there is M- V_n inband crosstalk components that actually mix with the actual signal at the star coupler after passing through the switches. Let X_i (i=1,2,……,N) be the number of crosstalk components at ω that are leakages of the signal entering the OXC at input port *i,* than, each X_i is an integer satisfying

$$\sum_{i=1}^{N} X_i = \text{M- } V_n,\ 1 \le X_i \le \text{M- } V_n. \tag{3.35}$$

B. Space-Division Switch

In a real SDS, each crosstalk will leak to the unattended outputs, including crosstalk to the actual signal. In this case there are also N-1 inband crosstalk components at ω leaking from the switches. These are contributed by signal entering from different input ports.

In this case we also assume that the OXC is fully loaded, in the worst case, the actual signal will be interfered by M-V crosstalk components leaking from the tunable filters and another N-1 crosstalk components leaking from the switches. The components traverse the OXC via different paths and, thus, have different propagation delays. Assuming intensity modulation, the electric field, which includes the influence of the crosstalk, is given by

$$\overrightarrow{E(t)} = Eb_1(t)\cos[\omega t + \varphi_1(t)]\ \overrightarrow{P_1} + \sum_{i=1}^{N}\sum_{j=1}^{X_i}\sqrt{\delta}\,Eb_i(t-\tau_{ij})\cos[\omega(t-\tau_{ij}) + \varphi_i(t-\tau_{ij})]\ \overrightarrow{P_{ij}}$$

$$+ \sum_{i=2}^{N}\sqrt{\varepsilon}\,Eb_i(t-\tau_{ix})\cos[\omega(t-\tau_{ix}) + \varphi_i(t-\tau_{ix})]\ \overrightarrow{P_{ix}} \tag{3.36}$$

That is,

$$\overrightarrow{E(t)} = Eb_1(t)\cos[\omega t + \varphi_1(t)]\ \overrightarrow{P_1} + E\sum_{j=1}^{X_1}\sqrt{\delta}\,Eb_1(t-\tau_{1j})\cos[\omega(t-\tau_{1j}) + \varphi_1(t-\tau_{1j})]\ \overrightarrow{P_{1j}}$$

$$+ \sum_{i=2}^{N} E\{ \sum_{j=2}^{X_i} \sqrt{\delta} b_i(t-\tau_{ij}) \cos[\omega(t-\tau_{ij}) + \varphi_i (t-\tau_{ij})] \ \overrightarrow{P_{ij}}$$

$$+ \sqrt{\varepsilon} E b_i(t-\tau_{ix}) \cos[\omega(t-\tau_{ix}) + \varphi_i (t-\tau_{ix})] \ \overrightarrow{P_{ix}} \ \} \quad (3.37)$$

Where τ_{ij}, $\overrightarrow{P_{ij}}$, τ_{ix}, $\overrightarrow{P_{ix}}$,δ and ε are as follows.

τ_{ij} = Propagation delay relative to the actual signal of the jth crosstalk component leaking from the signal entering from port *i* of the OXC at the tunable filter.

$\overrightarrow{P_{ij}}$ = The unit polarization vector of crosstalk component τ_{ij}.

τ_{ix} = Propagation delay relative to the actual signal of the crosstalk component leaking from the signal entering from port *i* of the OXC at the optical switch.

$\overrightarrow{P_{ix}}$ = The unit polarization vector of crosstalk component τ_{ix}.

δ= Optical power relative to the actual signal for the crosstalk components leaked at a tunable filter.

ε = Optical power relative to the actual signal for the crosstalk components leaked at an optical switch.

Here the first term in equation (3.37) is the actual signal while the second and third terms correspond to the crosstalks contributed by leakages from the filters and forth term due to the switches. In the second term $E \sum_{j=1}^{X_i} \sqrt{\delta} b_i(t-\tau_{ij}) \cos[\omega(t-\tau_{ij}) + \varphi_i (t-\tau_{ij})] \ \overrightarrow{P_{ij}}$ is the leakage contributed by the signal from the input link *i.* These components may mix coherently with each other, since they have originated from the same signal and their phases are correlated.

Since the delays are less than laser coherence time, some of the crosstalk components originate from the same signal and there phase are correlated. In this case, the time delay terms cannot be neglected, but the $\Phi(t-\tau)$ terms can be approximated by $\Phi(t)$.Equation (3.37) can be written as (3.38)

$$\overrightarrow{E(t)} = E b_1(t) \cos[\omega t + \varphi_1 (t)] \ \overrightarrow{P_1} + E \sum_{j=1}^{X_1} \sqrt{\delta} b_1(t-\tau_{1j}) \cos[\omega(t-\tau_{1j}) + \varphi_1 (t)] \ \overrightarrow{P_{1j}}$$

$$+ \sum_{i=2}^{N} E\{ \sum_{j=1}^{X_i} \sqrt{\delta} b_i(t-\tau_{ij}) \cos[\omega(t-\tau_{ij}) + \varphi_i(t)] \overrightarrow{P_{ij}}$$

$$+ \sqrt{\varepsilon} b_i(t-\tau_{ix}) \cos[\omega(t-\tau_{ix}) + \varphi_i(t)] \quad \overrightarrow{P_{ix}} \quad \} \tag{3.38}$$

The second term in equation (3.38) represents the composite crosstalk that consists of the components leaking from the actual signal and is, therefore, coherent with the actual signal. The other composite crosstalk contributions are incoherent, each of which is a coherent combination of a number of crosstalks leaking from the same signal. The decision variable J is given by

$$J \approx \frac{1}{T} \int_{nT}^{(n+1)T} b_1^2(t)dt + \frac{2}{T} \sum_{j=1}^{X_1} \sqrt{\delta} \int_{nT}^{(n+1)t} b_1(t) b_1(t-\tau_{1j}) dt \cos D_{1j} \cos v_{1j} +$$

$$\frac{2}{T} \sum_{i=2}^{N} \{ \sum_{j=1}^{Xi} \sqrt{\delta} \int_{nT}^{(n+1)T} b_1(t) b_i(t-\tau_{ij}) dt \cos[\phi_1(t) - \phi_i(t) + D_{ij}] \cos v_{ij}$$

$$+ \sqrt{\varepsilon} \int_{nT}^{(n+1)T} b_1(t) b_i(t-\tau_{ix}) dt \cos[\phi_1(t) - \phi_i(t) + D_{ix}] \cos v_{ix} \} \tag{3.39}$$

Where $D_{ij} = \omega\tau_{ij}$, $D_{ix} = \omega\tau_{ix}$, *and* $\cos v_{ij} = \overrightarrow{P_1} . \overrightarrow{P_{ij}}$, $\cos v_{ix} = \overrightarrow{P_1} . \overrightarrow{P_{ix}}$

The case of interest is when $b_1(t) = 1$. The PP can be estimated by considering the worst case when J fades to its minimum. The results for two different scenarios of interest are given bellow

Case 1: $\tau < \tau_{coherent}$ and $\tau << T$, Bit period or Coherent case

In this special case in which the relative delays are negligible, bit patterns of the components from the same source are almost identical. All $b(t-\tau)$ are approximately equal to $b(t)$. This is the case when the components are delayed by almost the same amount and they interfere with other constructively to produce high power. From equation (3.39) We get the mean and variance of J

$$E(J) = 1 + 2\sqrt{\delta} \sum_{j=1}^{X_1} \cos D_{1j} \cos v_{1j} \tag{3.40}$$

$$\sigma^2 = \frac{2}{3} \sum_{i=2}^{N} (\sqrt{\delta} \sum_{j=1}^{X_i} \cos D_{ij} \cos v_{ij} + \sqrt{\varepsilon} \cos D_{ix} \cos v_{ix})^2 +$$

$$\frac{2}{3}\sum_{i=2}^{N}(\sqrt{\delta}\sum_{j=1}^{X_i}\sin D_{ij}\cos v_{ij}+\sqrt{\varepsilon}\sin D_{ix}\cos v_{ix})^2 \qquad (3.41)$$

The Crosstalk incurs maximum PP when all Cos υ terms are equal to 1 or -1 and X_1=0 , which gives E(J) =1.

It can be shown that

$$\max\ \sum_{i=1}^{n}(Ax_i+B)^2=(AL_n+B)^2+(n-1)B^2\ ,\ [\ \sum_{i=1}^{n}x_i=L_n\ ]$$

and

$$\max\ (\sum_{i=1}^{n}A_j\cos\theta_j)^2+(\sum_{i=1}^{n}A_j\sin\theta_j)^2=(\sum_{i=1}^{n}A_j)^2$$

Applying this, we have

$$\max\ (\sigma^2)=\max\ [\frac{2}{3}\sum_{i=2}^{N}(X_i\sqrt{\delta}+\sqrt{\varepsilon})^2]$$

$$=\frac{2}{3}[(M-V_n)\sqrt{\delta}+\sqrt{\varepsilon}]^2+\frac{2}{3}(N-2)\varepsilon \qquad (3.42)$$

Case 2: $\tau<\tau_{coherent}$ and $\tau>$ T, Bit period or Incoherent case :

The delays experienced by any two components differ from each other by more than one bit period. All b(t-τ) become uncorrelated with each other and with the actual signal the actual signal $b_1(t)$. So from equation (3.39) the mean and variance

$$E(J)=1+\ \sqrt{\delta}\ \sum_{j=1}^{X_1}\cos D_{1j}\cos v_{1j} \qquad (3.43)$$

$$\sigma^2=\frac{1}{3}\delta(\sum_{j=1}^{X_1}\cos^2 D_{1j}\cos v_{ij}^2)+\frac{1}{2}\sum_{i=2}^{N}\ (\sqrt{\delta}\ \sum_{j=1}^{X_i}\cos D_{ij}\cos v_{ij}+\sqrt{\varepsilon}\cos D_{ix}\cos v_{ix})^2$$

$$+\frac{1}{2}\sum_{i=2}^{N}(\sqrt{\delta}\ \sum_{j=1}^{X_i}\sin D_{ij}\cos v_{ij}+\sqrt{\varepsilon}\sin D_{ix}\cos v_{ix})^2$$

$$+\frac{1}{6}\sum_{i=2}^{N}(\delta\ \sum_{j=1}^{X_i}\cos^2 v_{ij}+\varepsilon\cos^2 v_{ix}) \qquad (3.44)$$

When all Cos υ terms are equal to 1 or -1 and X_1 = 0, the PP is at its maximum. Applying

$$\max(\sigma^2) = \max\ [\frac{1}{2}\sum_{i=2}^{N}(X_i\sqrt{\delta}+\sqrt{\varepsilon})^2+\frac{1}{6}\sum_{i=2}^{N}(X_i\delta+\varepsilon)]$$

$$=\frac{1}{2}[(M-V_n)\sqrt{\delta}+\sqrt{\varepsilon}]^2+\frac{1}{2}(N-2)\varepsilon+\frac{1}{6}(M-V_n)\delta+\frac{1}{6}(N-1)\varepsilon$$

$$=\frac{1}{2}[(M-V_n)\sqrt{\delta}+\sqrt{\varepsilon}]^2+\frac{1}{6}(4N-7)\varepsilon+\frac{1}{6}(M-V_n)\delta \qquad (3.45)$$

3.6.5 Multi-wavelength Selective filters Optical Cross-connect Architecture

This architecture composed of multi-wavelength selective filter (MWSF), tunable filters & star couplers. The MWSFs will be configured such that signals of same wavelength are never led to the same coupler. There are N identical intermediate modules. In each of the modules only V_n tunable filters are followed by wavelength converters.

There are leakages in the MWSF & the tunable filter. Let X_i (i=1,2,3,……..,N) be the number of crosstalk component at ω, leaked from the signal entering the OXC at input port i .Each X_i is then an integer satisfying $\sum X_i$ =M-1,where $1 \le X_i \le M-1$.As in each of the modules V_n tunable filters are followed by wavelength converters then the number of crosstalk component at the output equal to M-V_n which leak from the same signal.

There are also N-1 crosstalk components that leak from different input ports having same wavelength as the main signal.

The total electric field at a output port of the OXC which includes the influence of crosstalk, is given by

$$\overrightarrow{E(t)} = Eb_1(t)\cos[\omega t + \varphi_1(t)]\ \overrightarrow{P_1} + E\sum_{i=2}^{N}\sqrt{\delta}b_i(t)\cos[\omega t + \varphi_i(t)]\ \overrightarrow{P_i}$$

$$+ E\sum_{i=1}^{N}\sum_{j=1}^{X_i}\sqrt{\delta}b_i(t-\tau_{ij})\cos[\omega(t-\tau_{ij}) + \varphi_i(t-\tau_{ij})]\ \overrightarrow{P_{ij}}$$

$$+ E\sum_{i=2}^{N}\sqrt{\delta}b'_i(t-\tau'_i)\cos[\omega(t-\tau'_i) + \varphi_i(t-\tau'_i)]\ \overrightarrow{P_{i'}} \qquad (3.46)$$

Where τ_j, $\overrightarrow{P_i}$, τ_{ij}, $\overrightarrow{P_{ij}}$, τ'_i, $\overrightarrow{P_{i'}}$, δ and ε are as follows.

τ_{ij} = Propagation delay relative to the actual signal of the jth crosstalk component leaking from the signal entering from port *i* of the OXC at the tunable filter.

$\overrightarrow{P_{ij}}$ = The unit polarization vector of crosstalk component τ_{ij}.

τ_i = Propagation delay relative to the actual signal of the crosstalk component leaking from the signal entering from other port of the first stage MWSF.

$\overrightarrow{P_i}$ = The unit polarization vector of crosstalk component τ_i.

τ_i' = Propagation delay relative to the actual signal of the crosstalk component leaking from the signal entering from other port of the second stage MWSF.

$\overrightarrow{P_{i'}}$ = The unit polarization vector of crosstalk component $\tau_{i'}$.

δ= Optical power relative to the actual signal for the crosstalk components leaked at a tunable filter.

The first term in equation (3.46) is the main signal; the second is the leakage from the first stage MWSF and the third and fourth term are the leakage from the second stage MWSF.In the third term $E\sum_{j=1}^{X_i}\sqrt{\delta}b_i(t-\tau_{ij})\cos[\omega(t-\tau_{ij}) + \varphi_i(t-\tau_{ij})]\ \overrightarrow{P_{ij}}$ is the leakage contributed by the signal from the input link *i*. These components may mix coherently with each other, since they have originated from the same signal and their phases are correlated.

Since the delays are less than laser coherence time, some of the crosstalk components originate from the same signal and there phase are correlated. In this case, the time delay terms cannot be neglected, but the $\Phi(t-\tau)$ terms can be approximated by $\Phi(t)$.Equation (3.46) can be written as (3.47)

$$\begin{aligned}\overrightarrow{E(t)} = {} & Eb_1(t)\cos[\omega t + \varphi_1(t)]\ \overrightarrow{P_1} + E\sum_{i=2}^{N}\sqrt{\delta}b_i(t)\cos[\omega t + \varphi_i(t)]\ \overrightarrow{P_i} \\ & + E\sum_{j=1}^{X_i}\sqrt{\delta}b_1(t-\tau_{1j})\cos[\omega(t-\tau_{1j}) + \varphi_1(t)]\ \overrightarrow{P_{1j}} \\ & + E\sum_{i=2}^{N}\sum_{j=1}^{X_i}\sqrt{\delta}b_i(t-\tau_{ij})\cos[\omega(t-\tau_{ij}) + \varphi_i(t-\tau_{ij})]\ \overrightarrow{P_{ij}} \\ & + E\sum_{i=2}^{N}\sqrt{\delta}b'_i(t-\tau'_i)\cos[\omega(t-\tau'_i) + \varphi_i(t-\tau'_i)]\ \overrightarrow{P_{i'}} \end{aligned} \quad (3.47)$$

The third term in equation (3.47) represents the composite crosstalk that consists of the components leaking from the actual signal and is, therefore, coherent with the actual signal. The other composite crosstalk contributions are incoherent, each of which is a coherent combination of a number of crosstalks leaking from the same signal

Decision variable

$$J \approx \frac{1}{T}\int_{nT}^{(n+1)T} b^2{}_1(t)dt + \frac{2}{T}\sum_{j=1}^{X_1} \sqrt{\delta}\int_{nT}^{(n+1)T} b_1(t)b_1(t-\tau_{1j})dt \cos D_{1j} \cos v_{1j}$$

$$+\frac{2}{T}\sum_{i=2}^{N}\{\sum_{j=1}^{Xi} \sqrt{\delta}\int_{nT}^{(n+1)T} b_1(t)b_i(t-\tau_{ij})dt \cos[\varphi_1(t)-\varphi_{ij}(t) + D_{ij}] \cos v_{ij}$$

$$+\sqrt{\delta}\int_{nT}^{(n+1)T} b_1(t)b_i(t)dt \cos[\varphi_1(t)-\varphi_i(t)+D_j] \cos v_i +$$

$$\sqrt{\delta}\int_{nT}^{(n+1)T} b_1(t)b'_i(t-\tau t_i)dt \cos[\varphi_1(t)-\varphi t_i(t)+D'_i] \cos v'_i\} \qquad (3.48)$$

[D= ωτ and $\vec{P_i} \cdot \vec{P_j} = \cos \upsilon_{ij}$]

Case 1: $\tau < \tau_{coherent}$ and $\tau << T$, Bit period or Coherent case

In this special case in which the relative delays are negligible, bit patterns of the components from the same source are almost identical. All b(t-τ) are approximately equal to b(t). This is the case when the components are delayed by almost the same amount and they interfere with other constructively to produce high power. From

(3.48) we get the mean and variance of J

$$E(J) = 1 + 2\sqrt{\delta}\sum_{j=1}^{X_1}\cos D_{ij} \cos v_{ij} \qquad (4.39)$$

$$\sigma^2 = \frac{2}{3}\sum_{i=2}^{N}(\sqrt{\delta}\sum_{j=1}^{X_i}\cos D_{ij} \cos v_{ij} + \sqrt{\delta}\cos D_i \cos v_i)^2 +$$

$$\frac{2}{3}\sum_{i=2}^{N}(\sqrt{\delta}\sum_{j=1}^{X_i}\sin D_{ij} \cos v_{ij} + \sqrt{\delta}\sin D_i \cos v_i)^2 + \frac{2}{3}\sum_{i=2}^{N}\delta\cos^2 v'_i \qquad (3.50)$$

The Crosstalk incurs maximum PP when all Cos υ terms are equal to 1 or -1 and $X_1=0$, which gives E(J) =1.

It can be shown that

$$\max \sum_{i=1}^{n}(Ax_i + B)^2 = (AL_n + B)^2 + (n-1)B^2 \text{ , } [\ \sum_{i=1}^{n} x_i = L_n\ ]$$

and

$$\max (\sum_{i=1}^{n} A_j \cos\theta_j)^2 + (\sum_{i=1}^{n} A_j \sin\theta_j)^2 = (\sum_{i=1}^{n} A_j)^2$$

Applying this, we have

$$\max (\sigma^2) = \max\ [\frac{2}{3}\{\sum_{i=2}^{N}(X_i\sqrt{\delta} + \sqrt{\delta})^2] + \frac{2}{3}\sum_{i=2}^{N}\delta$$

$$= \frac{2}{3}\delta\{(M - V_n + 1)^2 + (N-2) + (N-1)\}$$

$$= \frac{2}{3}\delta\{(M - V_n + 1)^2 + (2N-3)\} \tag{3.51}$$

Case 2: $\tau < \tau_{coherent}$ and $\tau > T$, Bit period or Incoherent case :

The delays experienced by any two components differ from each other by more than one bit period. All b(t-τ) become uncorrelated with each other and with the actual signal the actual signal $b_1(t)$. So from equation (3.48) the mean and variance

$$E(J) = 1 + \sqrt{\delta}\sum_{j=1}^{X_1}\cos D_{1j}\cos v_{1j} \tag{3.52}$$

$$\sigma^2 = \frac{1}{3}\ \delta(\sum_{j=1}^{X_1}\cos^2 D_{1j}\cos^2 v_{1j}) + \frac{1}{2}\sum_{i=2}^{N}\{(\sqrt{\delta}\ \sum_{j=1}^{X_i}\cos D_{ij}\cos v_{ij} + \sqrt{\delta}\cos D_i\cos v_i)^2\ +$$

$$\frac{1}{2}\sum_{i=2}^{N}(\sqrt{\delta}\sum_{j=1}^{X_i}\sin D_{ij}\cos v_{ij} + \sqrt{\delta}\sin D_i\cos v_i)^2$$

$$+\frac{1}{6}\sum_{i=2}^{N}(\delta\sum_{i=1}^{X_i}\cos^2 v_{ij} + \delta\cos^2 v_i)\ +\ \frac{2}{3}\sum_{i=2}^{N}\varepsilon'\cos^2 v'_i \tag{3.53}$$

when all cos*v* terms are equal to 1 or -1 & $X_1 = 0$ then

we get

$$\max (\sigma^2) = \max\ [\frac{1}{2}\sum_{i=2}^{N}(X_i\sqrt{\delta} + \sqrt{\delta})^2 + \frac{1}{6}\sum_{i=2}^{N}(X_i\delta + \delta)] + \sum_{i=2}^{N}\delta$$

$$= \frac{1}{2}\delta(M - V_n + 1)^2 + \frac{1}{2}(N-2)\delta + \frac{1}{6}(M - V_n + 1)\delta + \frac{1}{6}(N-2)\delta + \frac{2}{3}(N-1)\delta$$

$$= \frac{1}{2}\delta(M - V_n + 1)^2 + \frac{2}{3}(2N - 3)\delta + \frac{1}{6}(M - V_n + 1)\delta \quad (3.54)$$

3.6.6 Wavelength Switch Optical Cross-Connect

In this architecture the signals have to go through two stage switching structure before combined at the output star coupler. The various crosstalk sources and their effect are describing bellow .

A. First stage Space-Division Switch

In First stage Space-Division Switch there are N-1 inband crosstalk components due to leakage to the unattended output which include crosstalk to the actual signal. These are contributed by signal entering from different input ports,

B. Tunable Filter

The actual signal is also combined with M-1 signals at different wavelengths by a star coupler at the output. These signals also carry with them inband crosstalk components, due to imperfect filtering. M-1 crosstalk components at ω leaked through the filters. The signals which go through the conversion process are free from crosstalk. So there is M-V inband crosstalk components that actually mix with the actual signal at the star coupler after passing through the second stage switches. Let X_i (i=1,2,……,N) be the number of crosstalk component at ω that are leakages of the signal in question entering the OXC at input port *i,* than, each X_i is an integer satisfying

$$\sum_{i=1}^{N} X_i = M - V_n \text{ , } 1 \le X_i \le M\text{-}V_n. \quad (3.55)$$

C. Second stage Space-Division Switch

In the second stage Space-Division Switch there are also N-1 leakages due to presence of other signals at wavelength ω due to Imperfect isolation. These crosstalk components also mix with the signal in question at the output of the OXC.

In this case we also assume that the OXC is fully loaded, in the worst case, the actual signal will be interfered by M-V crosstalk components leaking from the tunable filters and N-1 crosstalk components leaking from the switches each. The components traverse the OXC via different paths and, thus, have different propagation delays. Assuming intensity modulation, the electric field, which includes the influence of the crosstalk, is given by

$$\begin{aligned}\overrightarrow{E(t)} = {} & Eb_1(t)\cos[\omega t + \varphi_1(t)]\ \overrightarrow{P_1} \\ & + E\sum_{i=1}^{N}\sum_{j=1}^{X_i}\sqrt{\delta}\,b_i(t-\tau_{ij})\cos[\omega(t-\tau_{ij}) + \varphi_i(t-\tau_{ij})]\ \overrightarrow{P_{ij}} \\ & + E\sum_{i=2}^{N}\sqrt{\varepsilon}\,b_i(t-\tau_{ix})\cos[\omega(t-\tau_{ix}) + \varphi_i(t-\tau_{ix})]\ \overrightarrow{P_{ix}} \\ & + E\sum_{i=2}^{N}\sqrt{\varepsilon}\,b_i(t-\tau_{iy})\cos[\omega(t-\tau_{iy}) + \varphi_i(t-\tau_{yx})]\ \overrightarrow{P_{iy}} \end{aligned} \quad (3.56)$$

That is,

$$\begin{aligned}\overrightarrow{E(t)} = {} & Eb_1(t)\cos[\omega t + \varphi_1(t)]\ \overrightarrow{P_1} + E\sum_{j=1}^{X_1}\sqrt{\delta}\,Eb_1(t-\tau_{1j})\cos[\omega(t-\tau_{1j}) + \varphi_1(t-\tau_{1j})]\ \overrightarrow{P_{1j}} \\ & + \sum_{i=2}^{N}E\{\sum_{j=2}^{X_i}\sqrt{\delta}\,b_i(t-\tau_{ij})\cos[\omega(t-\tau_{ij}) + \varphi_i(t-\tau_{ij})]\ \overrightarrow{P_{ij}} \\ & + \sqrt{\varepsilon}\,Eb_i(t-\tau_{ix})\cos[\omega(t-\tau_{ix}) + \varphi_i(t-\tau_{ix})]\ \overrightarrow{P_{ix}} + \\ & \sqrt{\varepsilon}\,Eb_i(t-\tau_{iy})\cos[\omega(t-\tau_{iy}) + \varphi_i(t-\tau_{iy})]\ \overrightarrow{P_{iy}}\} \end{aligned} \quad (3.57)$$

Where τ_{ij}, $\overrightarrow{P_{ij}}$, τ_{ix}, $\overrightarrow{P_{ix}}$, τ_{iy}, $\overrightarrow{P_{iy}}$, δ and ε are as follows.

τ_{ij} = Propagation delay relative to the actual signal of the jth crosstalk component leaking from the signal entering from port *i* of the OXC at the tunable filter.

$\overrightarrow{P_{ij}}$ = The unit polarization vector of crosstalk component τ_{ij}.

τ_{ix} = Propagation delay relative to the actual signal of the crosstalk component leaking from other signals at wavelength ω at the first stage optical switch.

$\overrightarrow{P_{ix}}$ = The unit polarization vector of crosstalk component τ_{ix}.

τ_{iy} = Propagation delay relative to the actual signal of the crosstalk component leaking from others signals at wavelength ω at the optical switch.

$\overrightarrow{P_{iy}}$ = The unit polarization vector of crosstalk component τ_{iy}.

δ= Optical power relative to the actual signal for the crosstalk components leaked at a tunable filter.

ε = Optical power relative to the actual signal for the crosstalk components leaked at an optical switch.

Here the first term in equation (3.57) is the actual signal while the second and third terms correspond to the crosstalks contributed by leakages from the filters and forth and fifth terms due to the first and second stage the switches, respectively. In the second term $E\sum_{j=1}^{X_i}\sqrt{\delta}b_i(t-\tau_{ij})\cos[\omega(t-\tau_{ij}) + \varphi_i(t-\tau_{ij})]$ $\overrightarrow{P_{ij}}$ is the leakage contributed by the signal from the input link *i*. These components may mix coherently with each other, since they have originated from the same signal and their phases are correlated.

Since the delays are less than laser coherence time, some of the crosstalk components originate from the same signal and there phase are correlated. In this case, the time delay terms cannot be neglected, but the $\Phi(t-\tau)$ terms can be approximated by $\Phi(t)$.Equation (3.57) can be written as (3.58)

$$\begin{aligned}\overrightarrow{E(t)} = {} & Eb_1(t)\cos[\omega t + \varphi_1(t)]\ \overrightarrow{P_1} + E\sum_{i=2}^{N}\sqrt{\varepsilon}b_i(t-\tau_{ix})\cos[\omega(t-\tau_{ix})] + \varphi_i(t)]\ \overrightarrow{P_{ix}} \\ & + E\sum_{j=1}^{X_i}\sqrt{\delta}b_1(t-\tau_{1j})\cos[\omega(t-\tau_{1j}) + \varphi_1(t)]\ \overrightarrow{P_{1j}} \\ & + E\sum_{i=2}^{N}\sum_{j=1}^{X_i}\sqrt{\delta}b_i(t-\tau_{ij})\cos[\omega(t-\tau_{ij}) + \varphi_i(t-\tau_{ij})]\ \overrightarrow{P_{ij}} \\ & + E\sum_{i=2}^{N}\sqrt{\varepsilon}b_i(t-\tau_{yi})\cos[\omega(t-\tau_{yi}) + \varphi_i(t)]\ \overrightarrow{P_{iy}} \end{aligned} \quad (3.58)$$

The second term in equation (3.58) represents the composite crosstalk that consists of the components leaking from the actual signal and is, therefore, coherent with the actual signal. The other composite crosstalk composite crosstalk contributions are incoherent, each of which is a coherent combination of a number of crosstalk leaking from the same signal. The decision variable J is given by

$$J \approx \frac{1}{T}\int_{nT}^{(n+1)T} b^2{}_1(t)dt + \frac{2}{T}\sum_{j=1}^{X_1} \sqrt{\delta}\int_{nT}^{(n+1)T} b_1(t)b_1(t-\tau_{1j})dt \cos D_{1j} \cos v_{1j}$$

$$+\frac{2}{T}\sum_{i=2}^{N} E\{\sum_{j=1}^{Xi} \sqrt{\delta}\int_{nT}^{(n+1)T} b_1(t)b_i(t-\tau_{ij})dt \cos[\varphi_1(t)-\varphi_{ij}(t) + D_{ij}] \cos v_{ij}$$

$$+\sqrt{\varepsilon}\int_{nT}^{(n+1)T} b_1(t)b_i(t-\tau_{ix})dt \cos[\varphi_1(t)-\varphi_{ix}(t)+D_{ix}] \cos v_{ix} +$$

$$\sqrt{\varepsilon}\int_{nT}^{(n+1)T} b_1(t)b_{iy}(t-\tau_{iy})dt \cos[\varphi_1(t)-\varphi_{iy}(t)+D_{iy}] \cos v_{iy}\} \quad (3.59)$$

Where $D_{ij}=\omega\tau_{ij}$, $D_{ix}=\omega\tau_{ix}$ $D_{iy}=\omega\tau_{iy}$, *and* $Cos_{ij}=\overrightarrow{P_1}.\overrightarrow{P_{ij}}$, $Cosv_{ix}=\overrightarrow{P_1}.\overrightarrow{P_{ix}}$, $Cosv_{iy}=\overrightarrow{P_1}.\overrightarrow{P_{iy}}$

The case of interest is when $b_1(t) = 1$. The PP can be estimated by considering the worst case when J fades to its minimum. The results for two different scenarios of interest are given bellow

Case 1: $\tau < \tau_{coherent}$ and $\tau << T$, Bit period or Coherent case

In this special case in which the relative delays are negligible, bit patterns of the components from the same source are almost identical. All $b(t-\tau)$ are approximately equal to $b(t)$. This is the case when the components are delayed by almost the same amount and they interfere with other constructively to produce high power. From equation (3.59) we get the mean and variance of J

$$E(J) = 1 + 2\sqrt{\delta}\sum_{j=1}^{X_1}\cos D_{ij} \cos v_{ij} \quad (3.60)$$

$$\sigma^2 = \frac{2}{3}\sum_{i=2}^{N}(\sqrt{\delta}\sum_{j=1}^{X_i}\cos D_{ij}\cos v_{ij} + \sqrt{\varepsilon}\cos D_{ix}\cos v_{ix} + \sqrt{\varepsilon}\cos D_{iy}\cos v_{iy})^2 +$$

$$\frac{2}{3}\sum_{i=2}^{N}(\sqrt{\delta}\sum_{j=1}^{X_i}\sin D_{ij}\cos v_{ij} + \sqrt{\varepsilon}\sin D_{ix}\cos v_{ix} + \sqrt{\varepsilon}\sin Dy\cos v_{iy})^2 + \frac{2}{3}\sum_{i=2}^{N}\delta\cos^2 v'_i \quad (3.61)$$

The Crosstalk incurs maximum PP when all Cos υ terms are equal to 1 or -1 and $X_1=0$, which gives E(J) =1.

It can be shown that

$$\max \sum_{i=1}^{n}(Ax_i + B)^2 = (AL_n + B)^2 + (n-1)B^2 \text{ , } [\ \sum_{i=1}^{n} x_i = L_n\ ]$$

and

$$\max\left(\sum_{i=1}^{n} A_j \cos\theta_j\right)^2 + \left(\sum_{i=1}^{n} A_j \sin\theta_j\right)^2 = \left(\sum_{i=1}^{n} A_j\right)^2$$

Applying this, we have

$$\max(\sigma^2) = \max\left[\frac{2}{3}\sum_{i=2}^{N}(X_i\sqrt{\delta} + \sqrt{\varepsilon} + \sqrt{\varepsilon})^2\right]$$

$$= \frac{2}{3}[(M - V_n)\sqrt{\delta} + 2\sqrt{\varepsilon}]^2 + \frac{4}{3}(N-2)\varepsilon \tag{3.62}$$

Case 2: $\tau < \tau_{coherent}$ and $\tau > T$, Bit period or Incoherent case:

The delays experienced by any two components differ from each other by more than one bit period. All $b(t-\tau)$ become uncorrelated with each other and with the actual signal the actual signal $b_1(t)$. So from equation (3.59) the mean and variance

$$E(J) = 1 + \sqrt{\delta}\sum_{j=1}^{X_1}\cos D_{1j}\cos v_{1j} \tag{3.63}$$

$$\sigma^2 = \frac{1}{3}\delta\left(\sum_{j=1}^{X_1}\cos^2 D_{1j}\cos^2 v_{1j}\right) +$$

$$\frac{1}{2}\sum_{i=2}^{N}\left(\sqrt{\delta}\sum_{j=1}^{X_i}\cos D_{ij}\cos v_{ij} + \sqrt{\varepsilon}\cos D_{ix}\cos v_{ix} + \sqrt{\varepsilon}\cos D_{iy}\cos v_{iy}\right)^2 +$$

$$\frac{1}{2}\sum_{i=2}^{N}\left(\sqrt{\delta}\sum_{j=1}^{X_i}\sin D_{ij}\cos v_{ij} + \sqrt{\varepsilon}\sin D_{ix}\cos v_{ix} + \sqrt{\varepsilon}\sin D_{iy}\cos v_{iy}\right)^2 +$$

$$\frac{1}{6}\sum_{i=2}^{N}\left(\delta\sum_{i=1}^{X_i}\cos^2 v_{ij} + \varepsilon\cos^2 v_{ix} + \varepsilon\cos^2 v_{iy}\right) \tag{3.64}$$

When all Cos υ terms are equal to 1 or -1 and $X_1 = 0$, the PP is at its maximum. Applying

$$\max(\sigma^2) = \max\left[\frac{1}{2}\sum_{i=2}^{N}(X_i\sqrt{\delta} + \sqrt{\varepsilon} + \sqrt{\varepsilon})^2 + \frac{1}{6}\sum_{i=2}^{N}(X_i\delta + \varepsilon + \varepsilon)\right]$$

$$= \frac{1}{2}[(M - V_n)\sqrt{\delta} + 2\sqrt{\varepsilon}]^2 + (N-2)\varepsilon + \frac{1}{6}(M - V_n)\delta + \frac{1}{3}(N-1)\varepsilon$$

$$= \frac{1}{2}[(M - V_n)\sqrt{\delta} + \sqrt{\varepsilon}]^2 + \frac{1}{3}(4N-7)\varepsilon + \frac{1}{6}(M - V_n)\delta \tag{3.65}$$

CHAPTER-4
RESULT and DISCUSSION

4.1 Result

Following the analytical formulations presented in previous chapter in this chapter we will present the effect of various parameters such as input power, number of wavelength per fiber and number of fiber on the system performance. The system performance will be evaluated in terms of BER and power penalty (PP). In the following figures where not mentioned the numerical numbers suggest the cases that have been indicated to the right of the numbers.

1. Share per node coherent case
2. Share per node incoherent case
3. Share per link coherent case
4. Share per link incoherent case
5. Wavelength switch OXC coherent case
6. Wavelength switch OXC incoherent case
7. DCS-1 coherent case
8. DCS-1 incoherent case
9. DCS-2 coherent case
10. DCS-2 incoherent case
11. MWSF coherent case
12. MWSF incoherent case

4.2. Effect of input power on crosstalk for different number of wavelength per fiber with and without WC

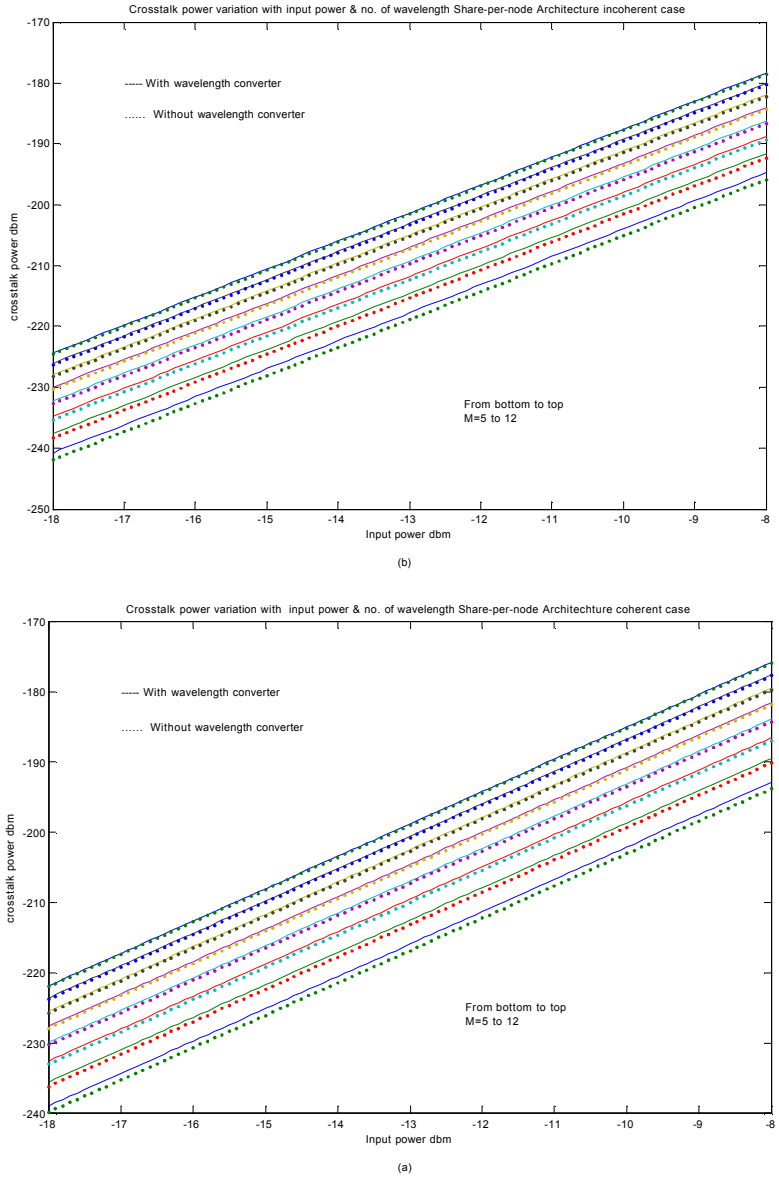

Fig. **4.1** Variation of crosstalk power with input power for different Number of wavelength per fiber M for Share-per-node architecture (a) Coherent case and (b) Incoherent case.(P_r = -19 dbm, V_n = 4, δ =-20 dbm, ε = -25 dbm and ε′= -25 dbm, N=8).

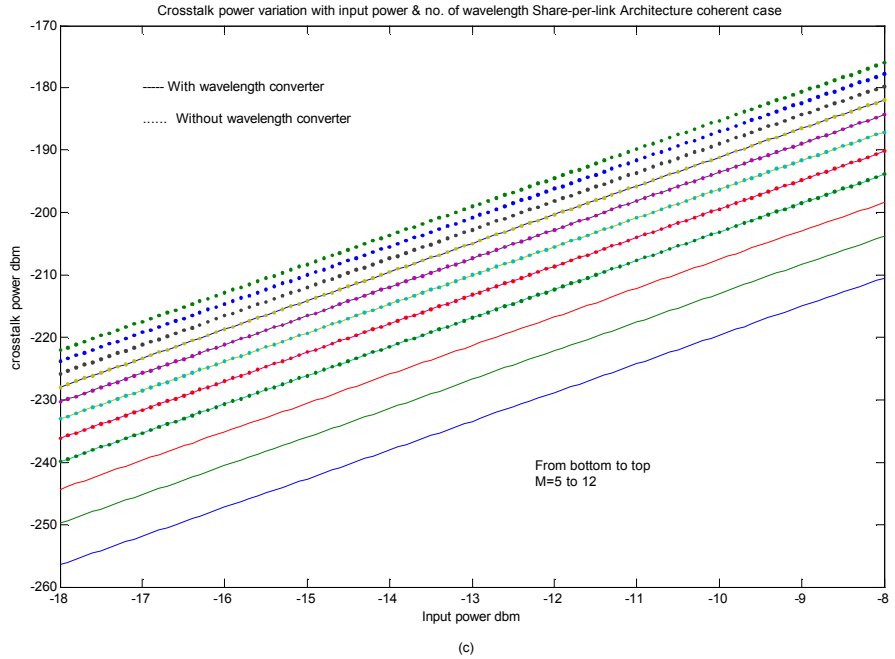

(c)

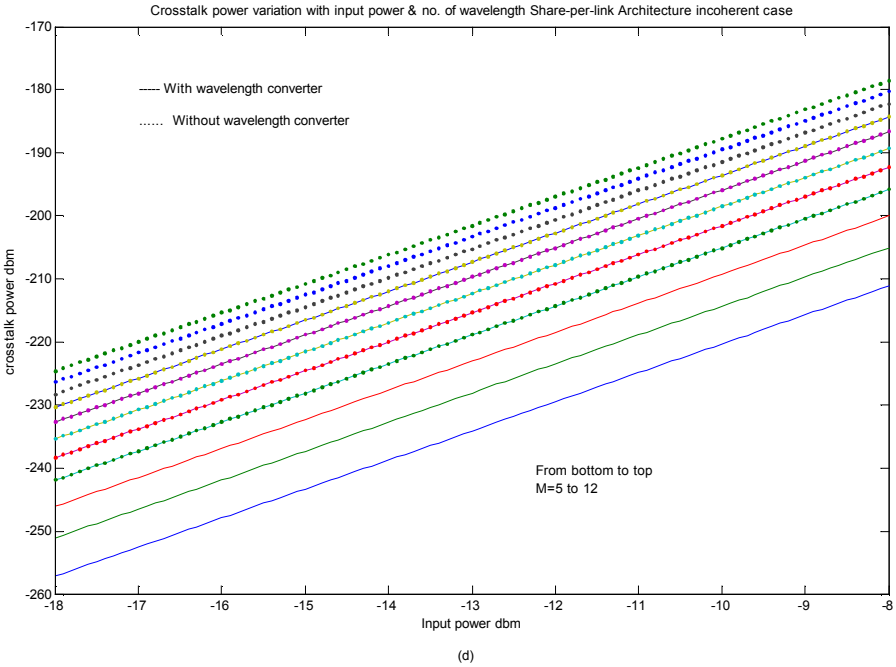

(d)

Fig. **4.2** Variation of crosstalk power with input power for different Number of wavelength per fiber M for Share-per-link architecture (a) Coherent case and (b) Incoherent case.(P_r = -19 dbm, V_n = 4, δ =-20 dbm, ε = -25 dbm and ε'= -25 dbm, N=8).

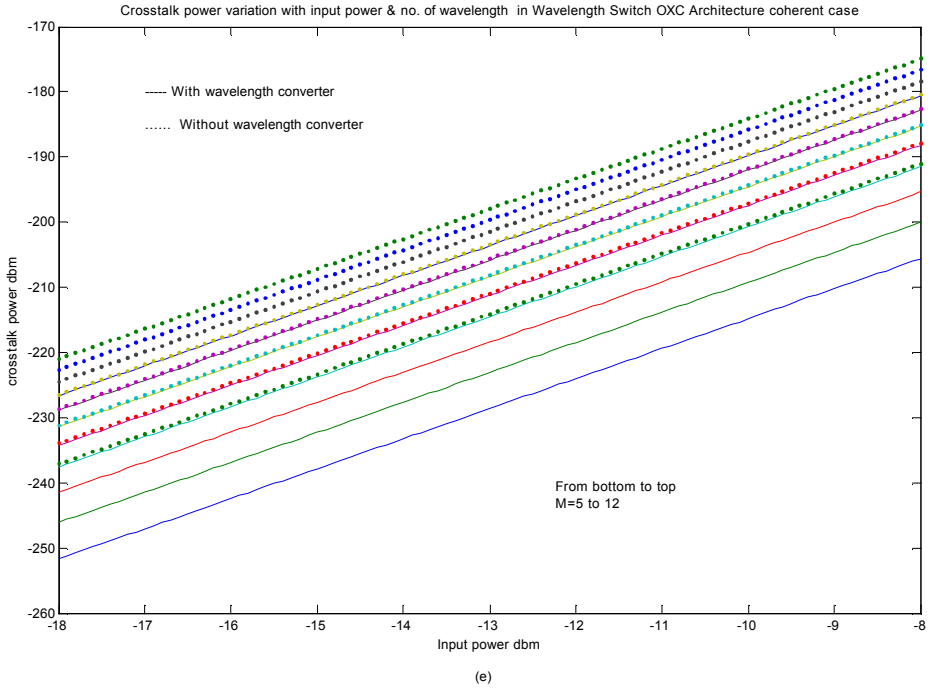

(e)

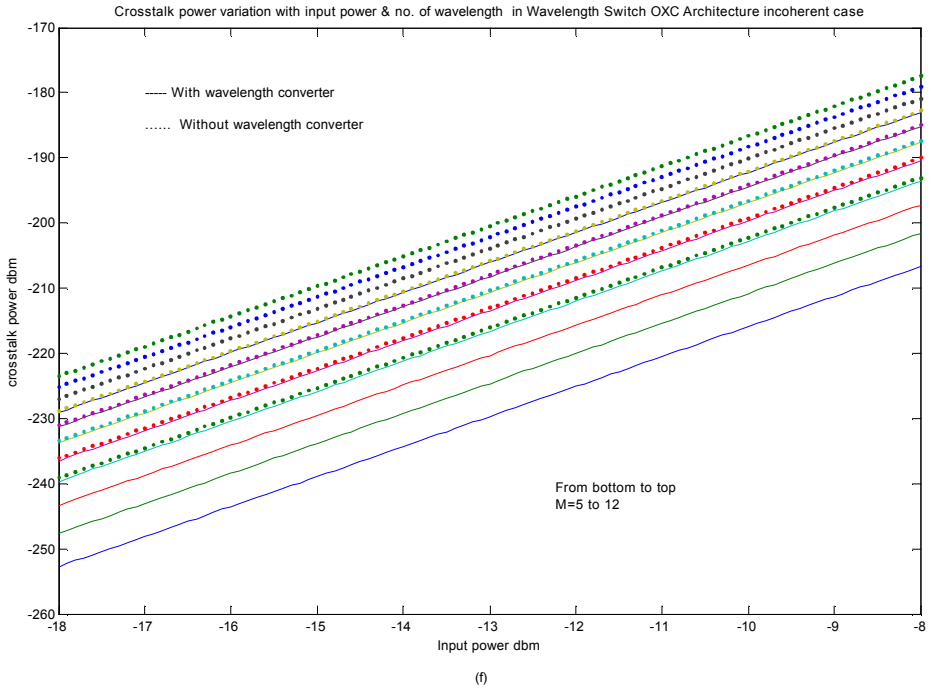

(f)

Fig. **4.3** Variation of crosstalk power with input power for different Number of wavelength per fiber M for Wavelength switch OXC architecture (a) Coherent case and (b) Incoherent case.(P_r = -19 dbm, V_n = 4, δ =-20 dbm,ε = -25 dbm and ε′= -25 dbm, N=8).

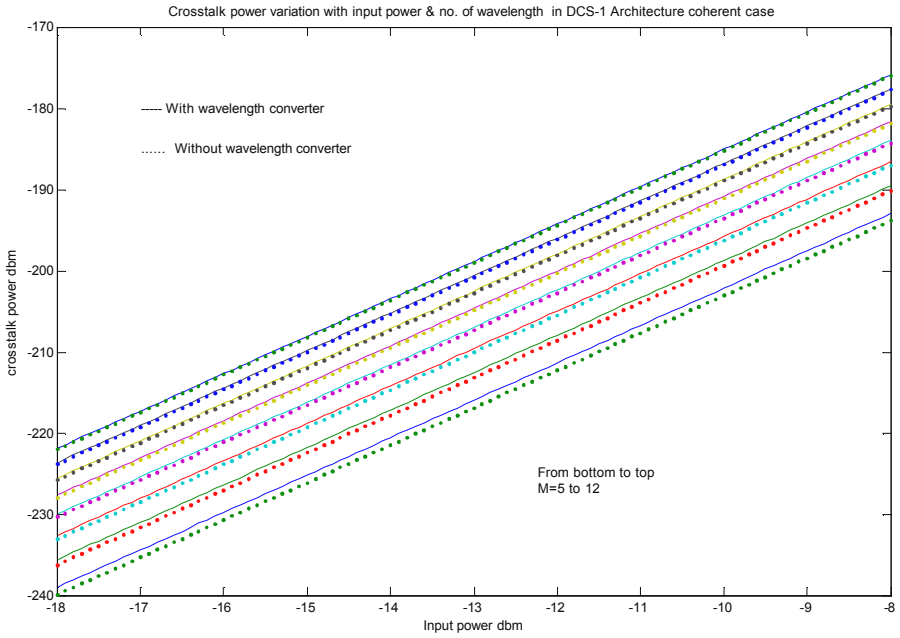

(g)

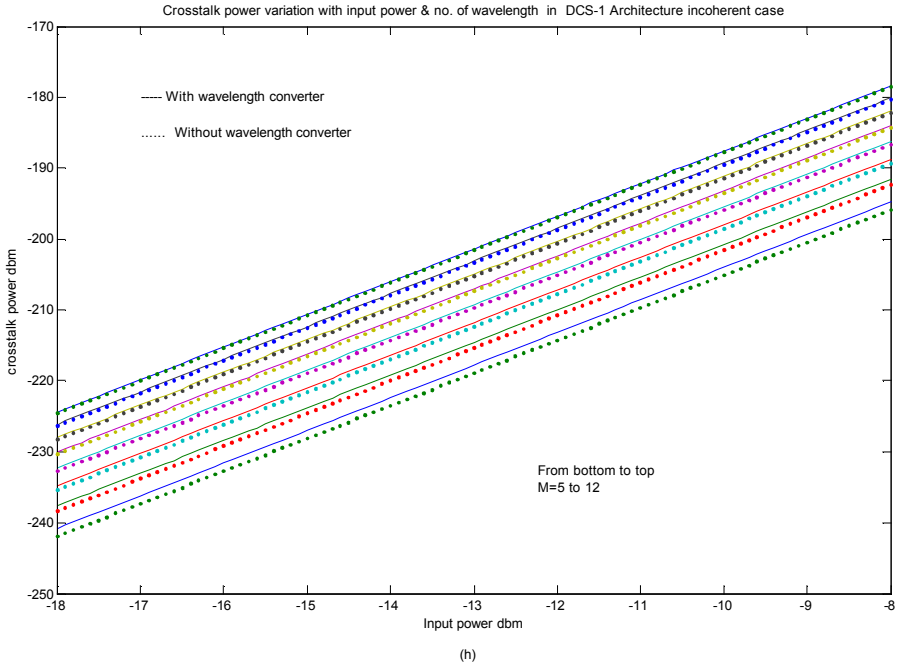

(h)

Fig. **4.4** Variation of crosstalk power with input power for different Number of wavelength per fiber M for DCS-1 architecture (a) Coherent case and (b) Incoherent case.(P_r = -19 dbm, V_n = 4, δ =-20 dbm,ε = -25 dbm and ε'= -25 dbm, N=8).

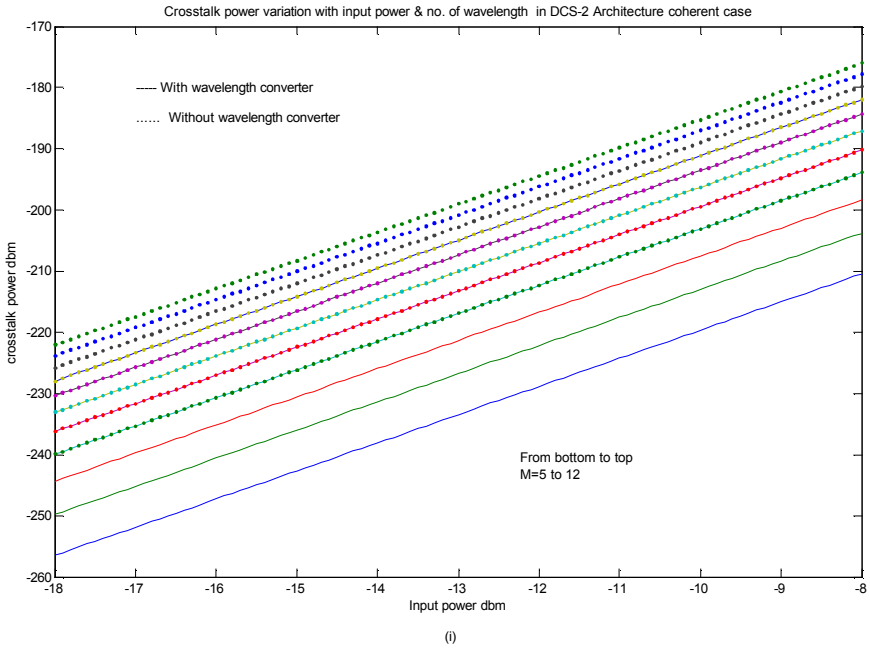

(i)

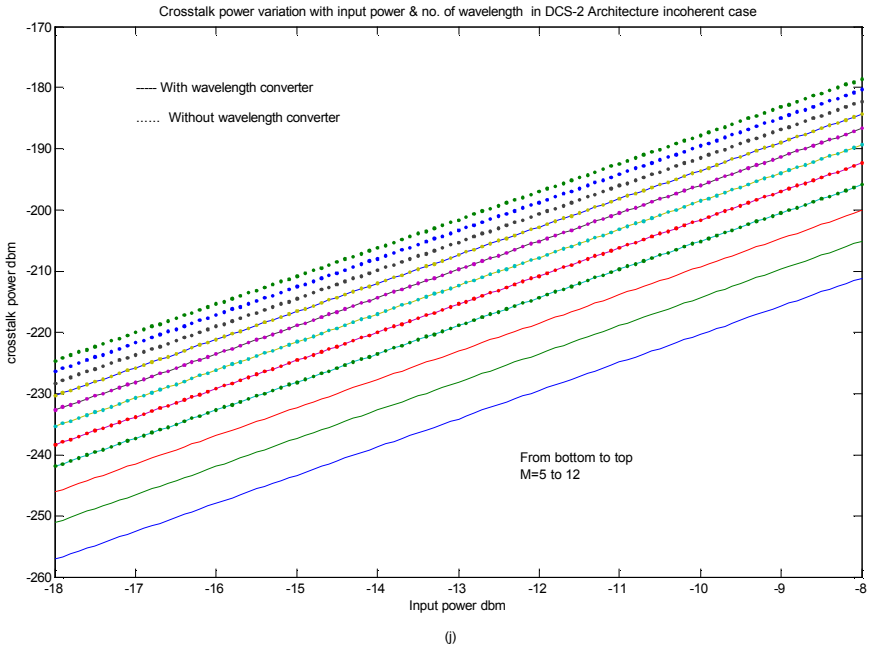

(j)

Fig. **4.5** Variation of crosstalk power with input power for different Number of wavelength per fiber M for DCS-2 architecture (a) Coherent case and (b) Incoherent case.(P_r = -19 dbm, V_n = 4, δ =-20 dbm, ε = -25 dbm and ε'= -25 dbm ,N=8).

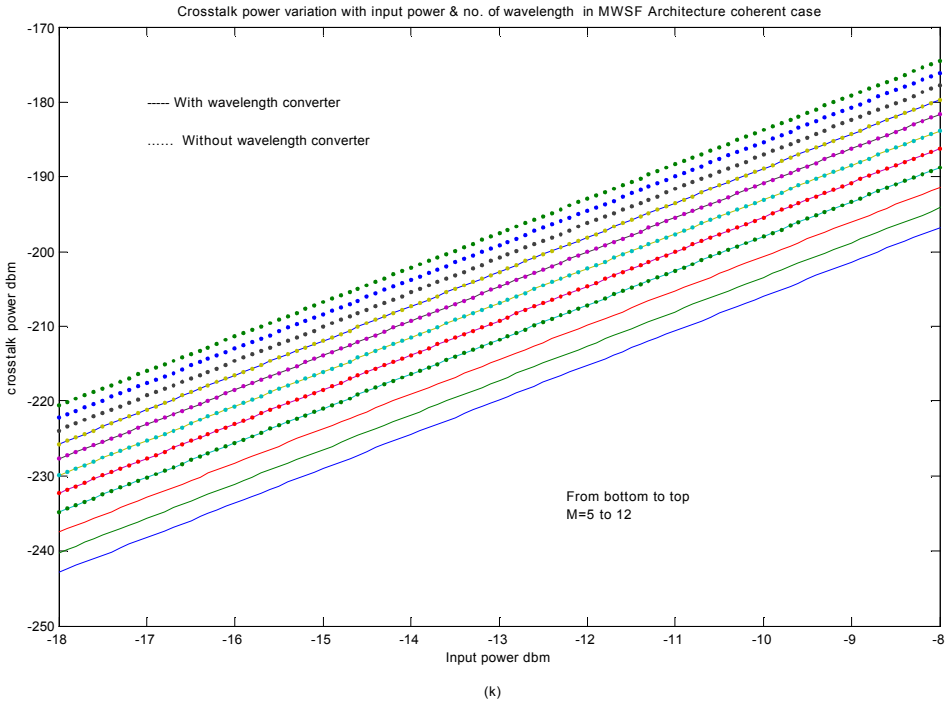

(k)

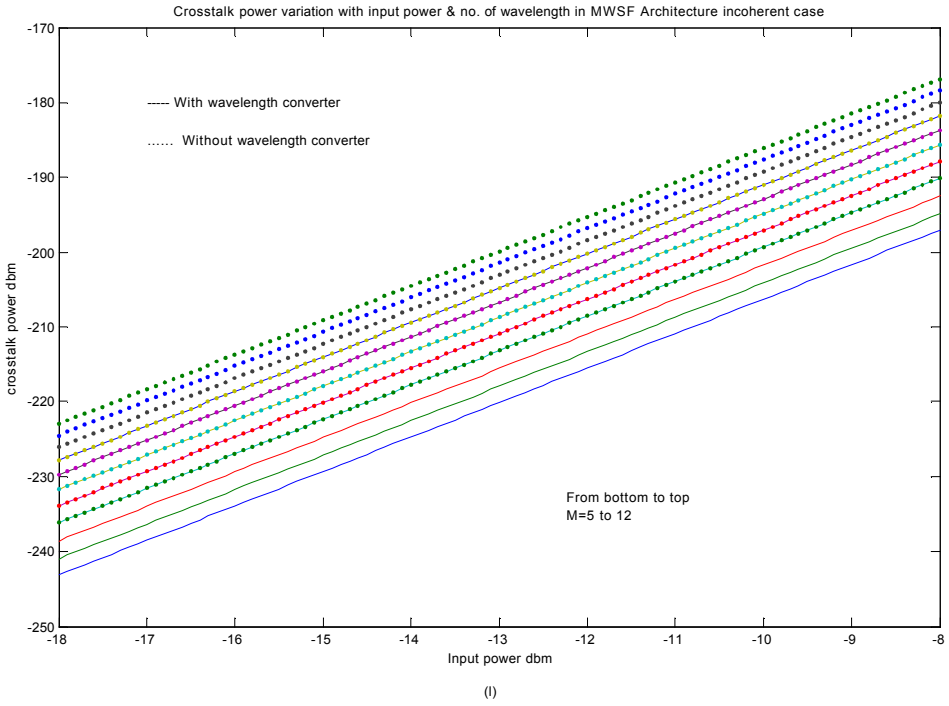

(l)

Fig. **4.6** Variation of crosstalk power with input power for different Number of wavelength per fiber M for MWSF architecture (a) Coherent case and (b) Incoherent case.(P_r = -19 dbm, V_n = 4, δ =-20 dbm, ε = -25 dbm and ε′= -25 dbm, N=8).

Fig. 4.1 to 4.6 show variation of crosstalk power with input power for different number of input wavelength per fiber. In the above figures receive power is -27 dbm, number of input fiber is N=8, number of wavelength converter per link is 4 i.e. total number of wavelength converter is $4 \times 8 = 32$; optical powers relative to the actual signal of the crosstalk contribution from the tunable filter/ Multiwavelength selective filter (MWSF), switch both first and second stage (incase of wavelength switch OXC) and second stage switch (in case of share-per-node architecture and DCS-1) are -20 dbm, -25 dbm and -25 dbm respectively.

From the crosstalk Vs input power curves we see that crosstalk power increases as input power or number of wavelength per fiber is increased and this increasing nature is quadratic. This characteristic curves diverse from each other as one of the input variables such as input power or number of wavelength per fiber M is increased.

4.3. Effect of input power on BER for different number of input wavelength per fiber with and without WC

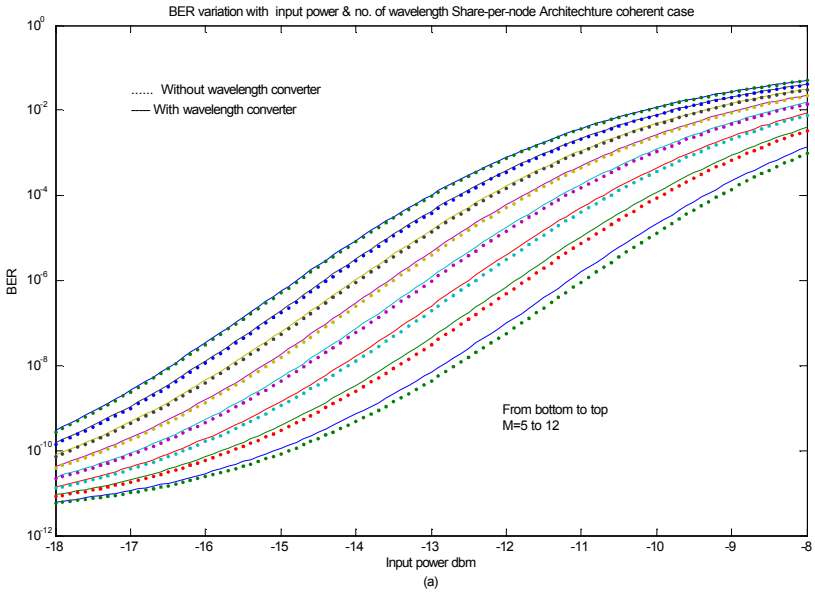

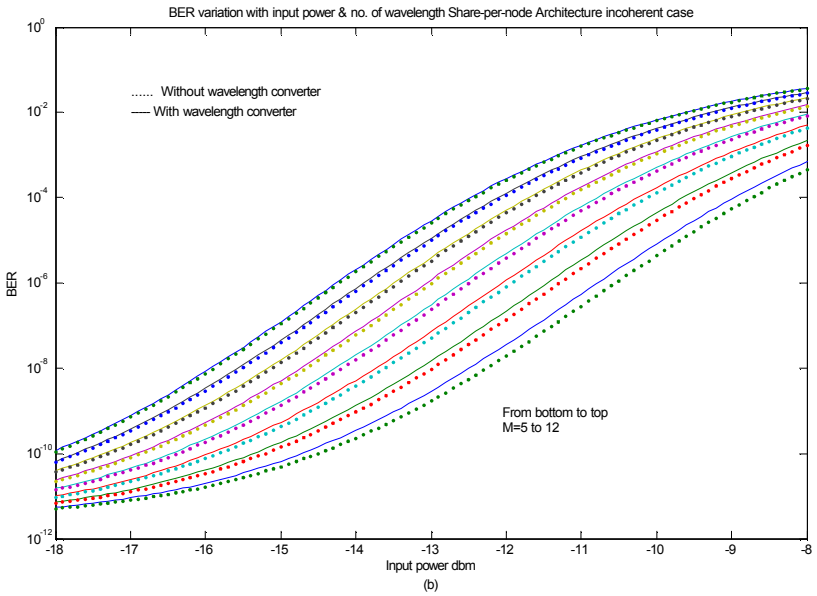

Fig. **4.7** Variation of BER with input power for different Number of wavelength per fiber M for Share-per-node architecture (a) Coherent case and (b) Incoherent case.(P_r = -19 dbm, V_n = 4, δ =-20 dbm,ε = -25 dbm and ε′= -25 dbm, N=8).

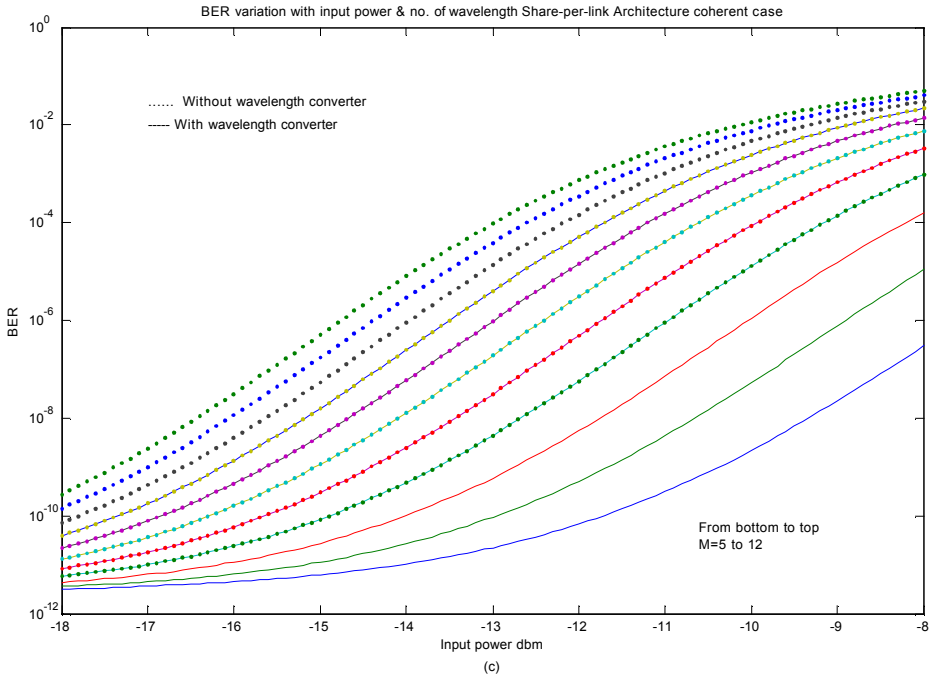

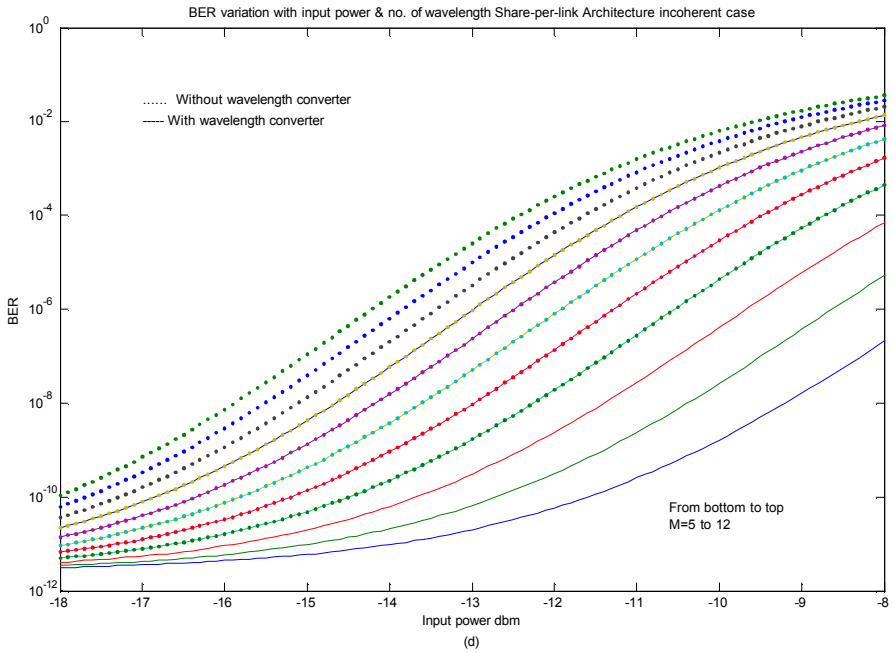

Fig. **4.8** Variation of BER with input power for different Number of wavelength per fiber M for Share-per-link architecture (a) Coherent case and (b) Incoherent case.(P_r = -19 dbm, V_n = 4, δ =-20 dbm, ε = -25 dbm and ε′= -25 dbm, N=8).

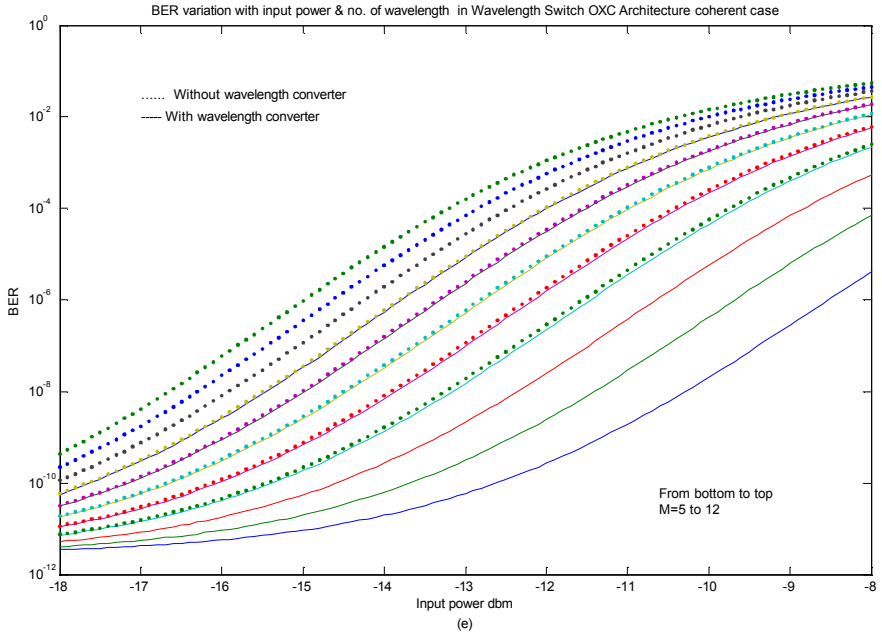

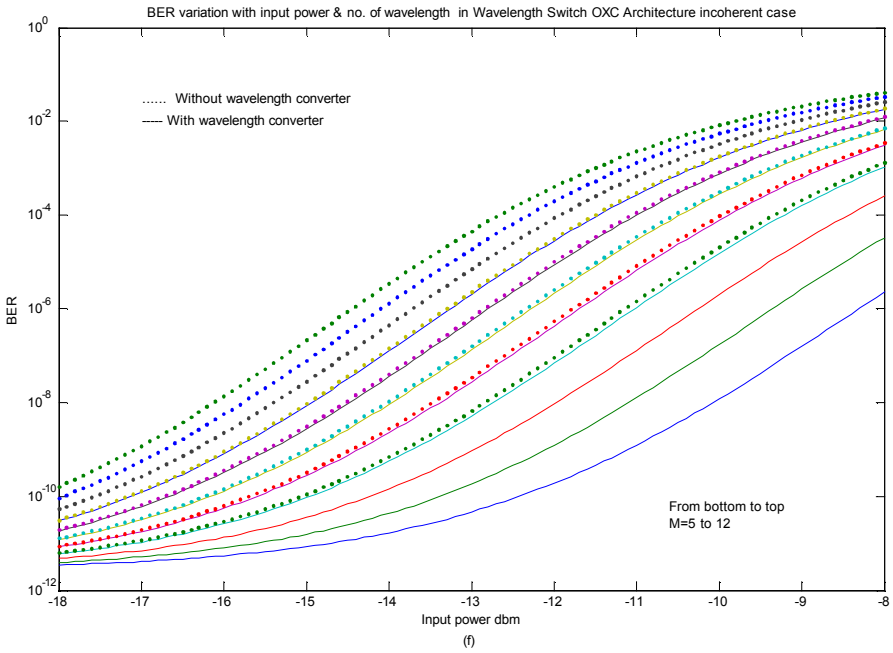

Fig. **4.9** Variation of BER with input power for different Number of wavelength per fiber M for Wavelength switch OXC architecture (a) Coherent case and (b) Incoherent case.(P_r = -19 dbm, V_n = 4, δ =-20 dbm,ε = -25 dbm and ε′= -25 dbm, N=8).

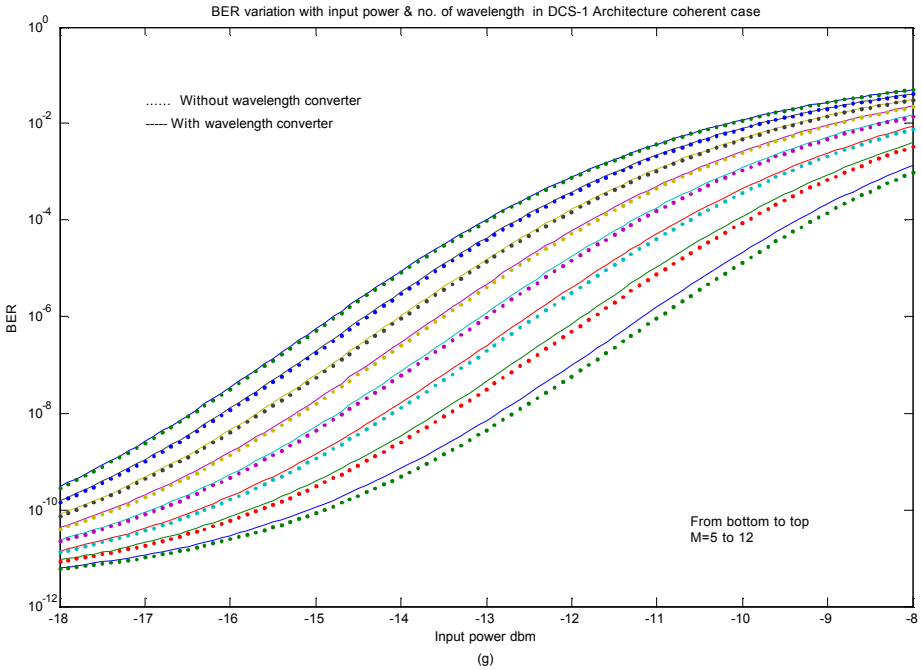

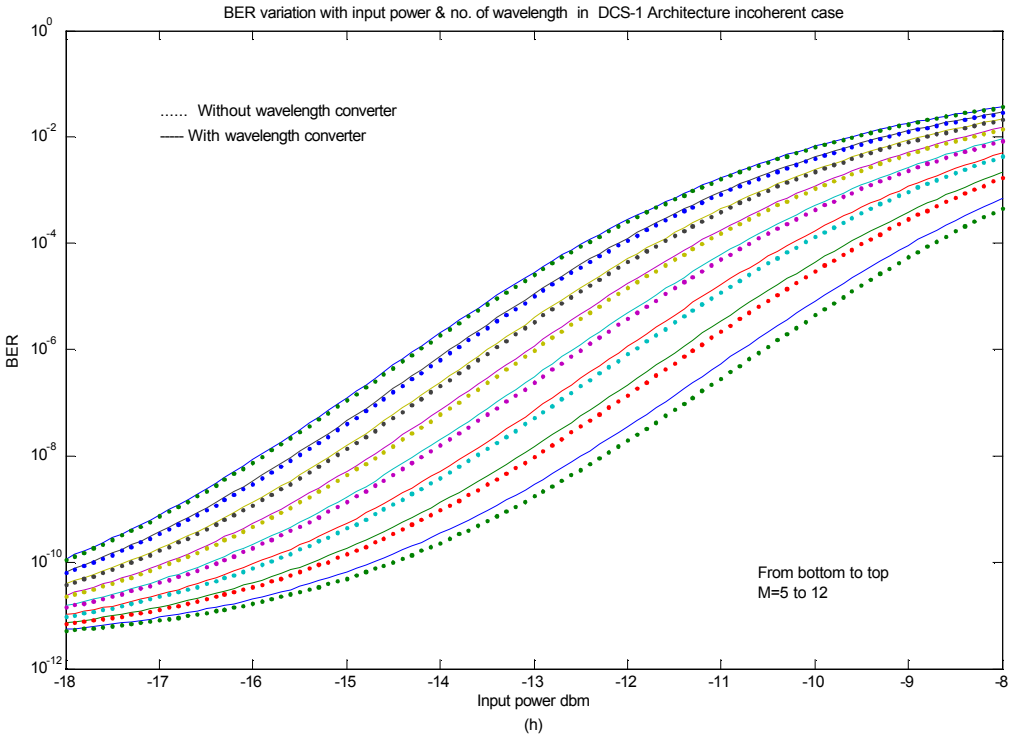

Fig. **4.10** Variation of BER with input power for different Number of wavelength per fiber M for DCS-1 architecture (a) Coherent case and (b) Incoherent case.(P_r = -19 dbm, V_n = 4, δ =-20 dbm, ε = -25 dbm and ε'= -25 dbm, N=8).

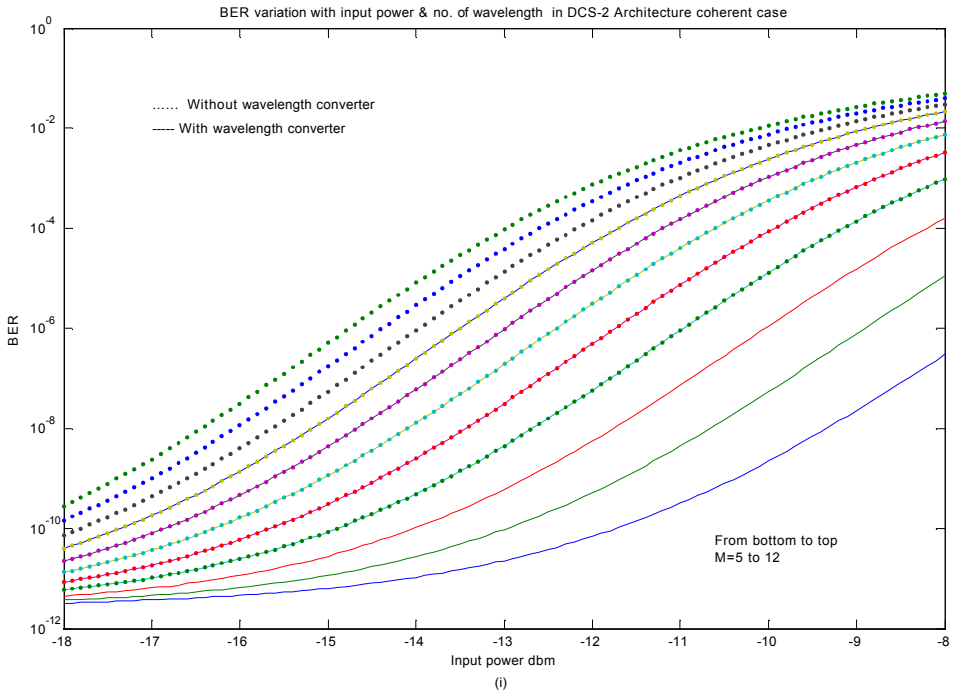

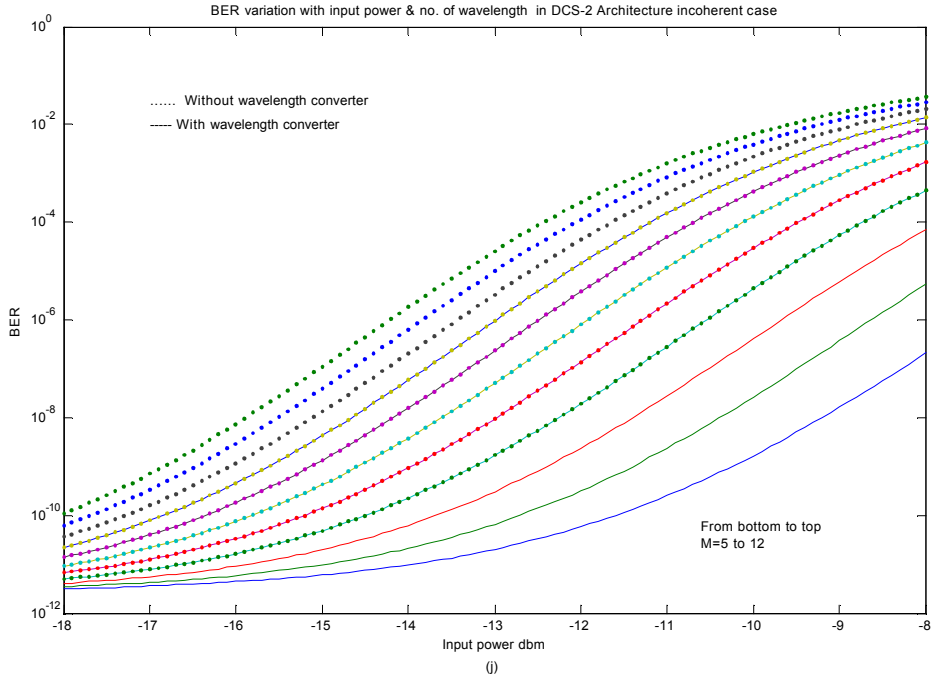

Fig. **4.11** Variation of BER with input power for different Number of wavelength per fiber M for DCS-2 architecture (a) Coherent case and (b) Incoherent case.(P_r = -19 dbm, V_n = 4, δ =-20 dbm, ε = -25 dbm and ε′= -25 dbm, N=8).

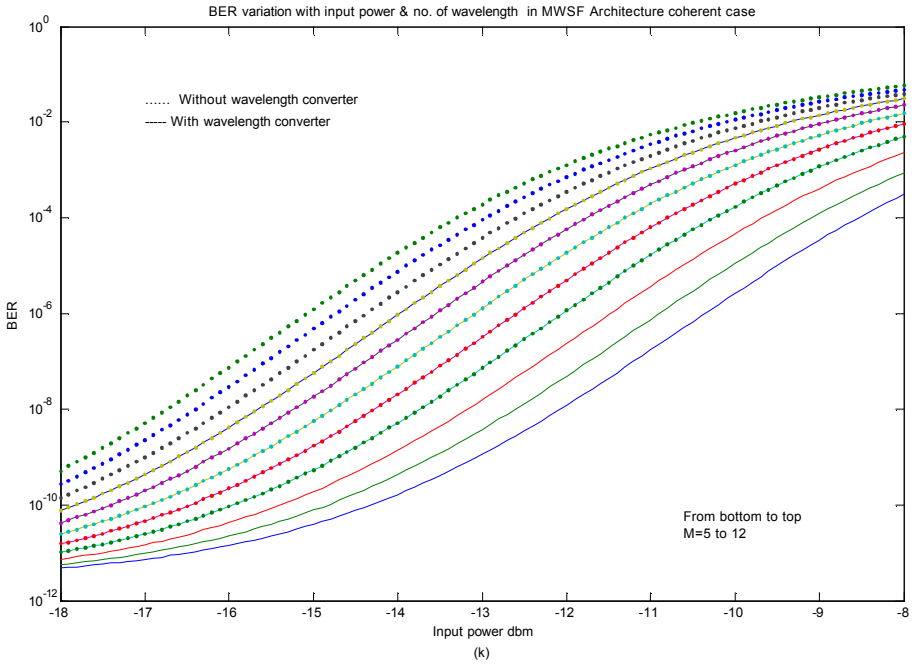

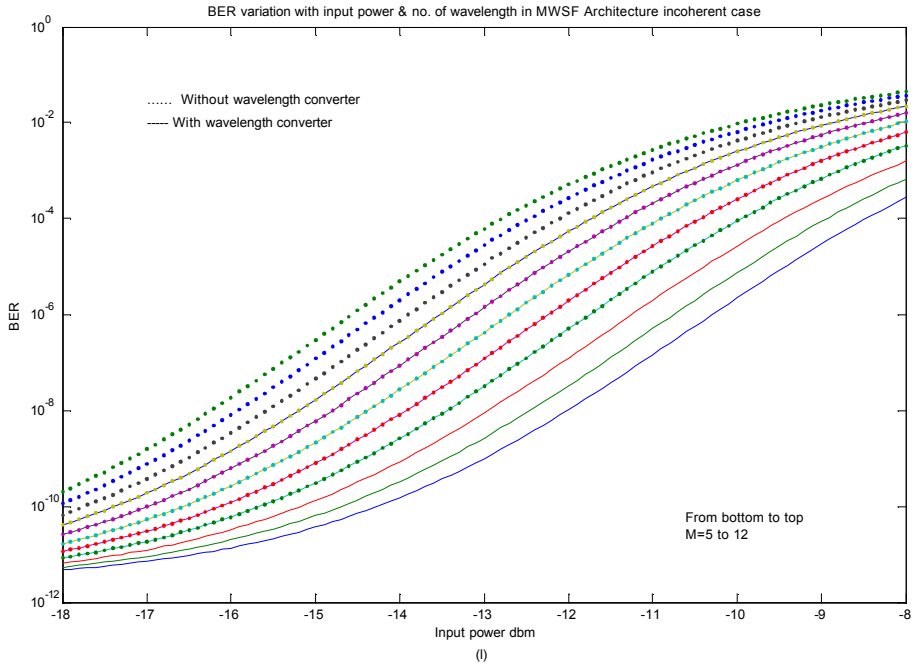

Fig. **4.12** Variation of BER with input power for different Number of wavelength per fiber M for MWSF architecture (a) Coherent case and (b) Incoherent case.(P_r = -19 dbm, V_n = 4, δ =-20 dbm, ε = -25 dbm and ε′= -25 dbm, N=8).

Fig. 4.7 to 4.12 show the variation of BER with input power and number of wavelength per fiber. In this case other parameters are as same as previous case. From the above figures we see that variation of BER at low input power for different number of wavelength per fiber M is low because thermal noise dominant crosstalk power at low input power. But at high input power this variation is high due to crosstalk power dominant the thermal noise at this point. At all input power and receive power BER increases with increasing the number of wavelength per fiber.

From the above two figures we observe that the signal suffers from more crosstalk as well as BER is high when there is no wavelength converter except share –per-node and DCS-1 architecture. This is because in these two cases a portion of the signals that have been converted by wavelength converters is present in the output but in other cases there is no such type of component.

4.4. Comparison of the effect of input power on Crosstalk and BER for different architectures with and without WC

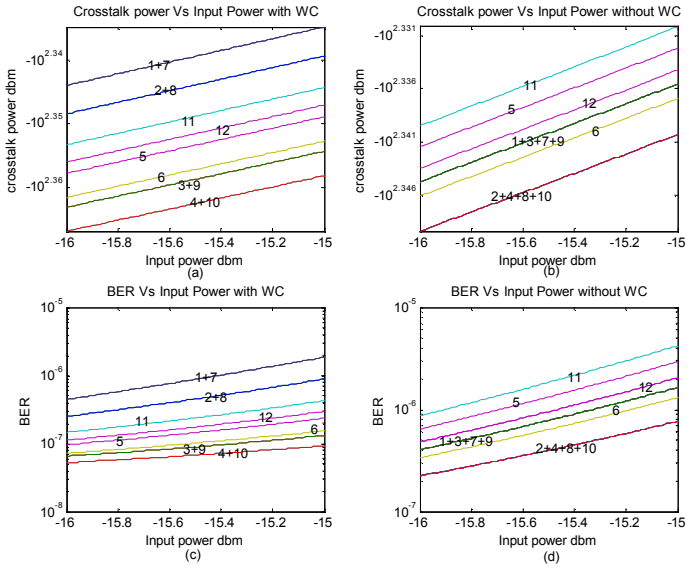

Fig. **4.13** Comparison of variation of (a) crosstalk power with WC (b) crosstalk power without WC (c) BER with wavelength converter (d) BER without wavelength converter with input power P_{in} for different architectures. (P_r = -27 dbm, N=8, M=8, V_n = 4 i.e V =32; δ =-20 dbm, ε = -25 dbm and ε′= -25 dbm).

Fig.-4.13 (a) and (b) shows variation of crosstalk power with input power with and without wavelength converter for different architectures. In all cases number of input wavelength per fiber M=8; number of input fiber N=8; number of wavelength converter per link V_n = 4 i.e. total number of wavelength converter =8×4 =32. This result also shows that crosstalk component is more when the interfering bit streams are well aligned with each other i.e. coherent case. Actually the coherent case gives an upper limit of the crosstalk while incoherent crosstalk gives a lower limit which can be obtained with a certain set of component parameters. The margin between upper and lower limit indicates the improvement which can be obtained by suppressing the beat term. Figure (c) and (d) shows that BER increases when the input power increases in both cases (with and without wavelength) but BER increases more rapidly in case of without wavelength converter. These figures also show that MWSF coherent case involves more crosstalk as well as BER without WC and Share per node coherent case and DCS-1 coherent cases involve more crosstalk as well as BER with WC than any other architectures.

4.5. Effect of number of input wavelength per fiber for different number of input fiber on Crosstalk with and without WC

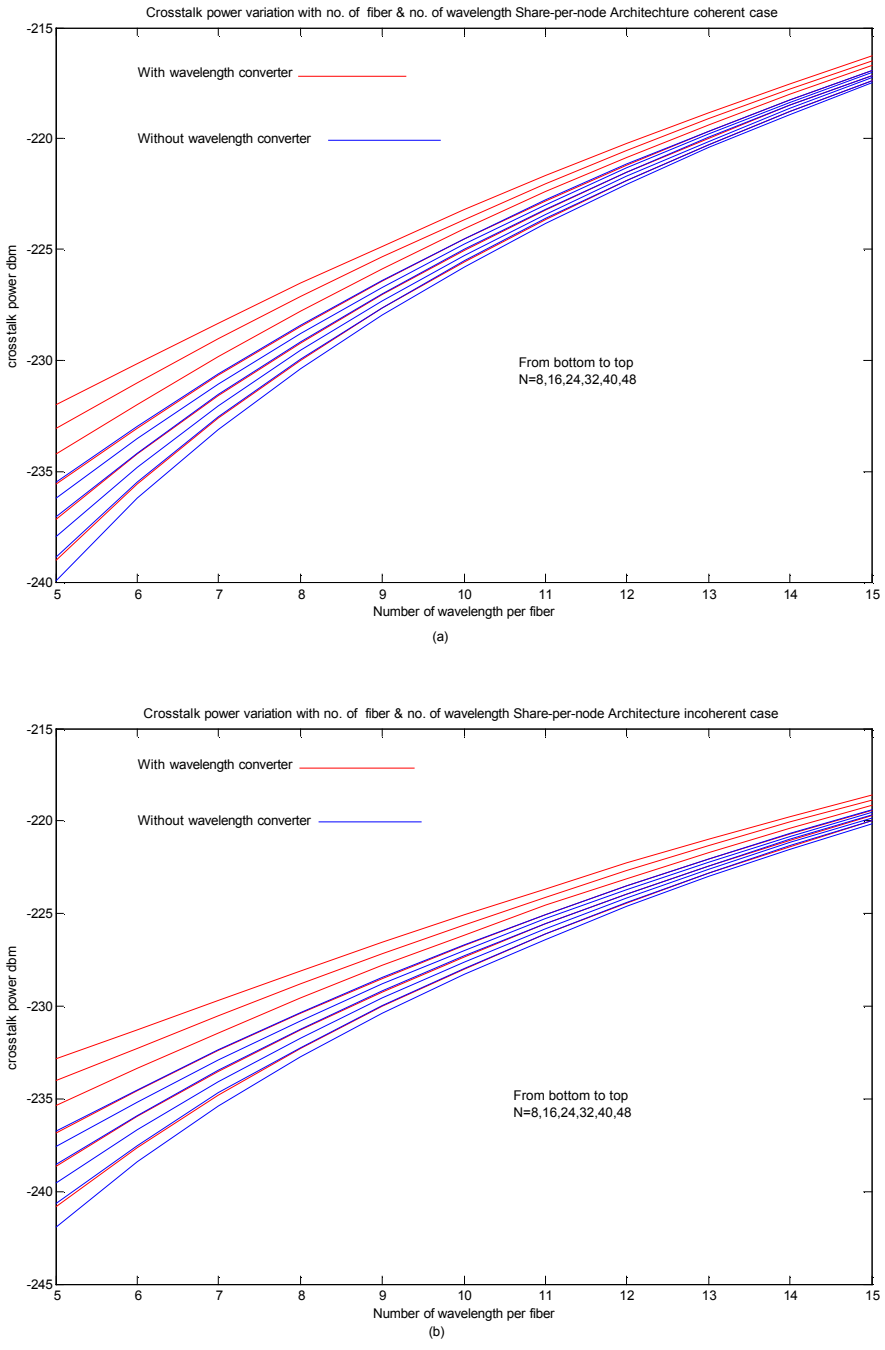

Fig. **4.14** Variation of crosstalk power with different number of input wavelength per fiber M for different Number of input fiber N for Share-per-node architecture (a) Coherent case and (b) Incoherent case.(P_{in} = -18 dbm, P_r = -19 dbm, V_n = 4, δ =-20 dbm, ε = -25 dbm and ε′= -25 dbm).

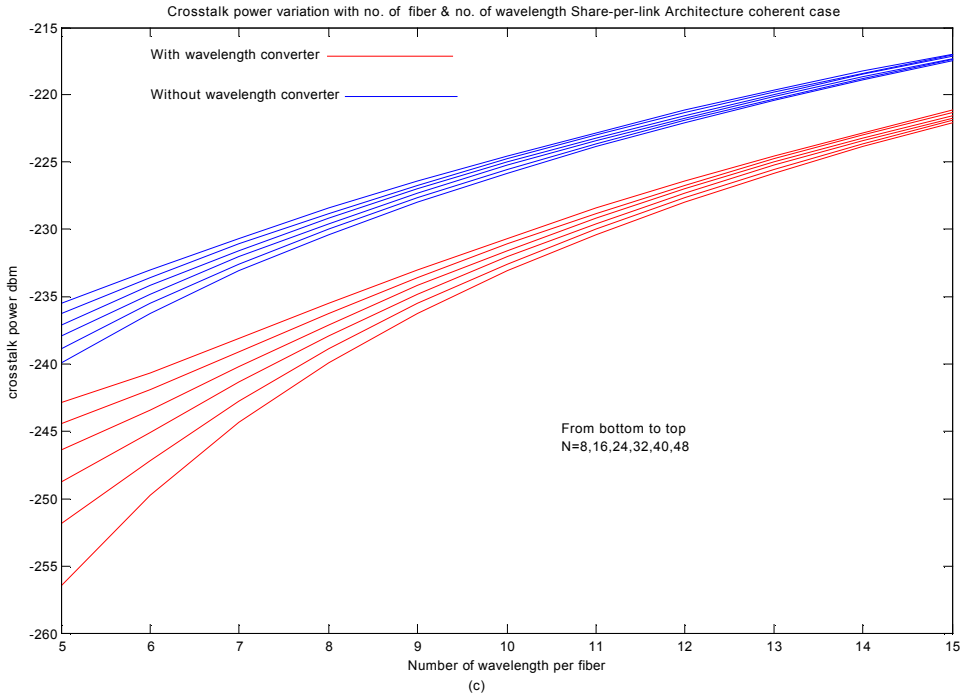

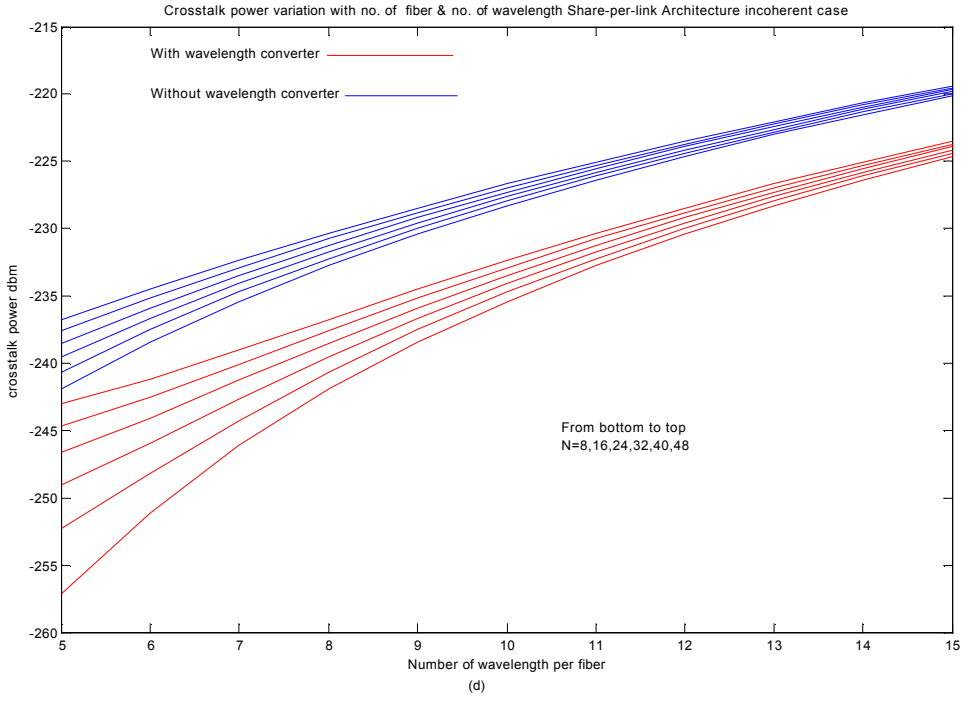

Fig. **4.15** Variation of crosstalk power with different number of input wavelength per fiber M for different Number of input fiber N for Share-per-link architecture (a) Coherent case and (b) Incoherent case.(P_{in} = -18 dbm, P_r = -19 dbm, V_n = 4, δ =-20 dbm, ε = -25 dbm and ε′= -25 dbm).

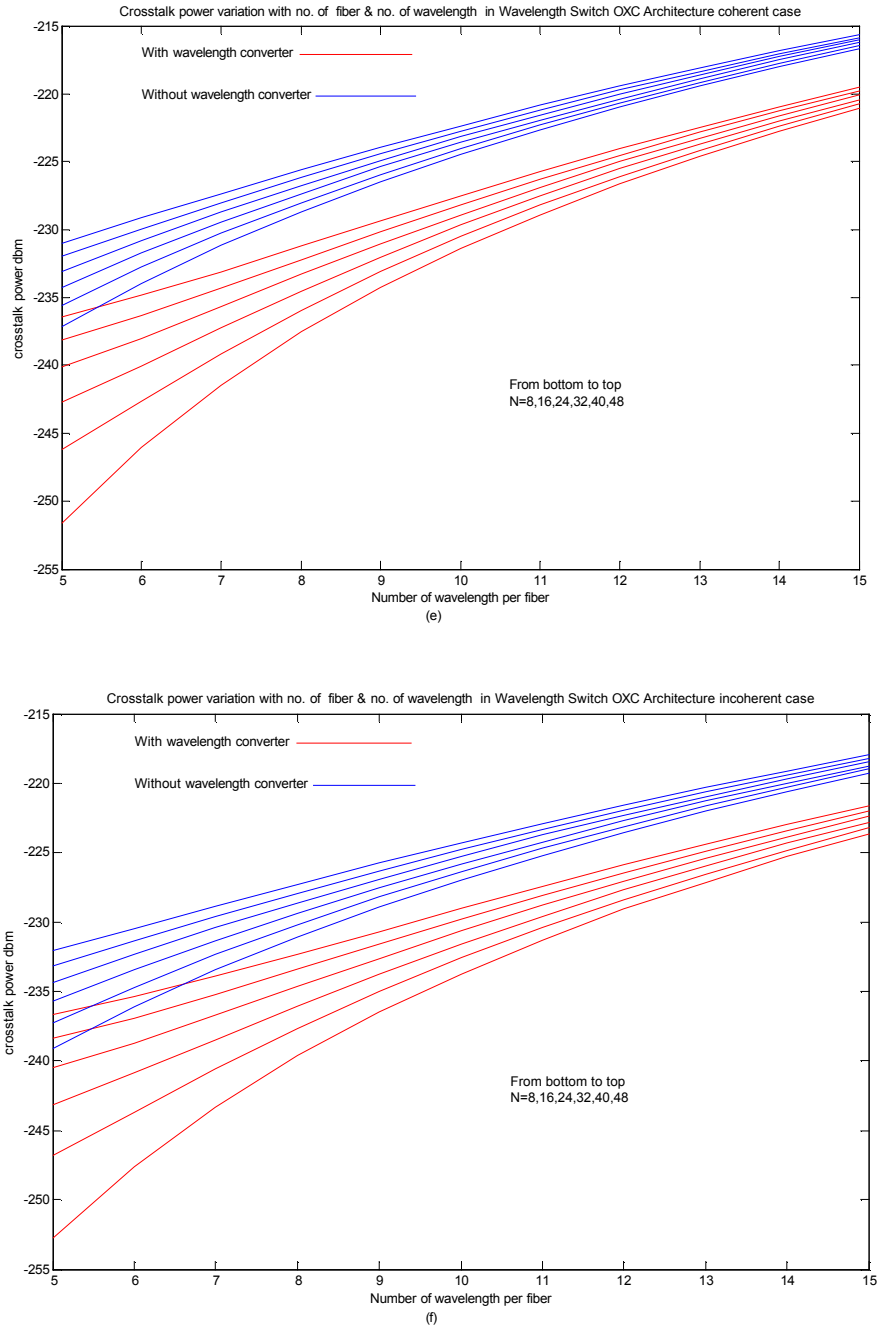

Fig. **4.16** Variation of crosstalk power with different number of input wavelength per fiber M for different Number of input fiber N for Wavelength switch OXC architecture (a) Coherent case and (b) Incoherent case.(P_{in} = -18 dbm, P_r = -19 dbm, V_n = 4, δ =-20 dbm, ε = -25 dbm and ε'= -25 dbm).

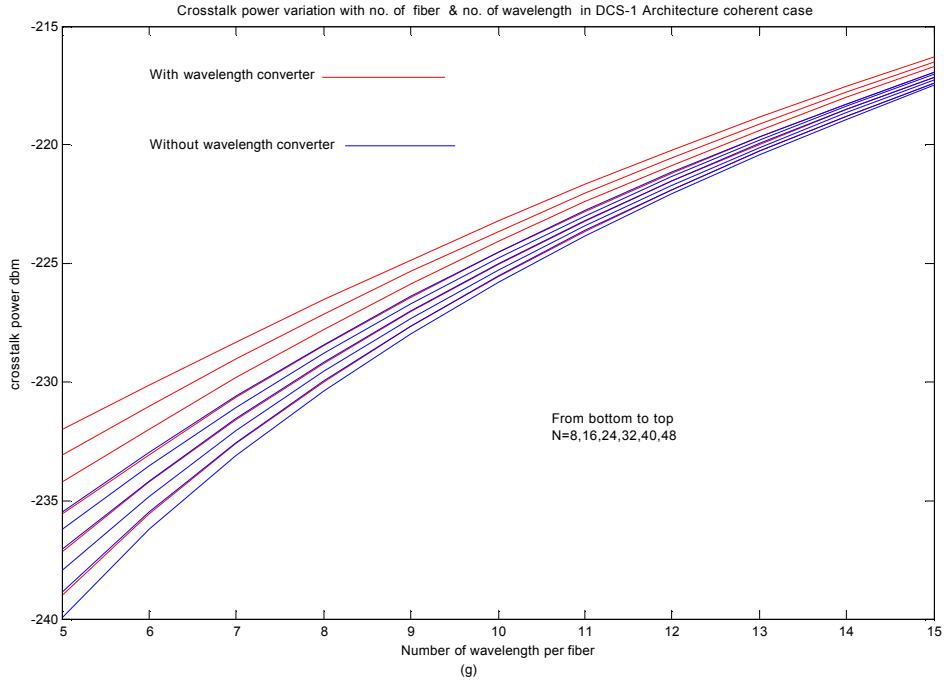

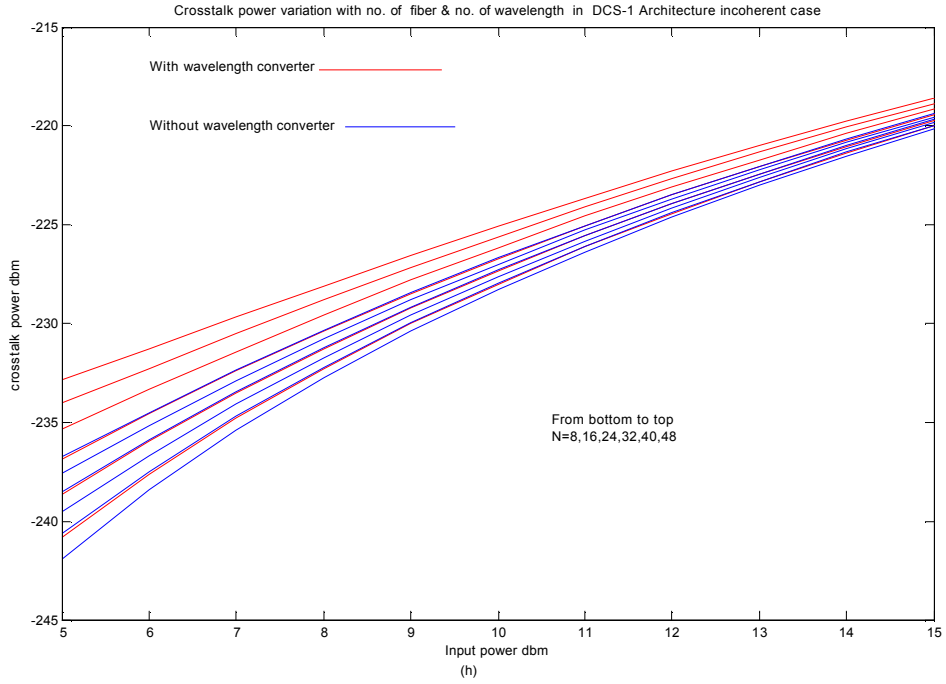

Fig. **4.17** Variation of crosstalk power with different number of input wavelength per fiber M for different Number of input fiber N for DCS-1 architecture (a) Coherent case and (b) Incoherent case.(P_{in} = -18 dbm, P_r = -19 dbm, V_n = 4, δ =-20 dbm,ε = -25 dbm and ε'= -25 dbm).

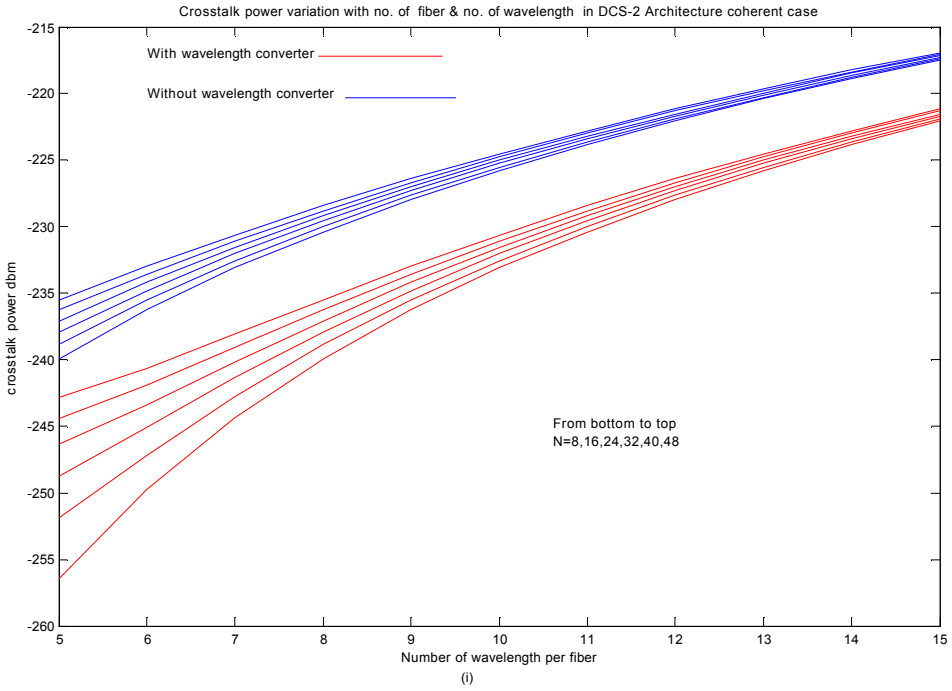

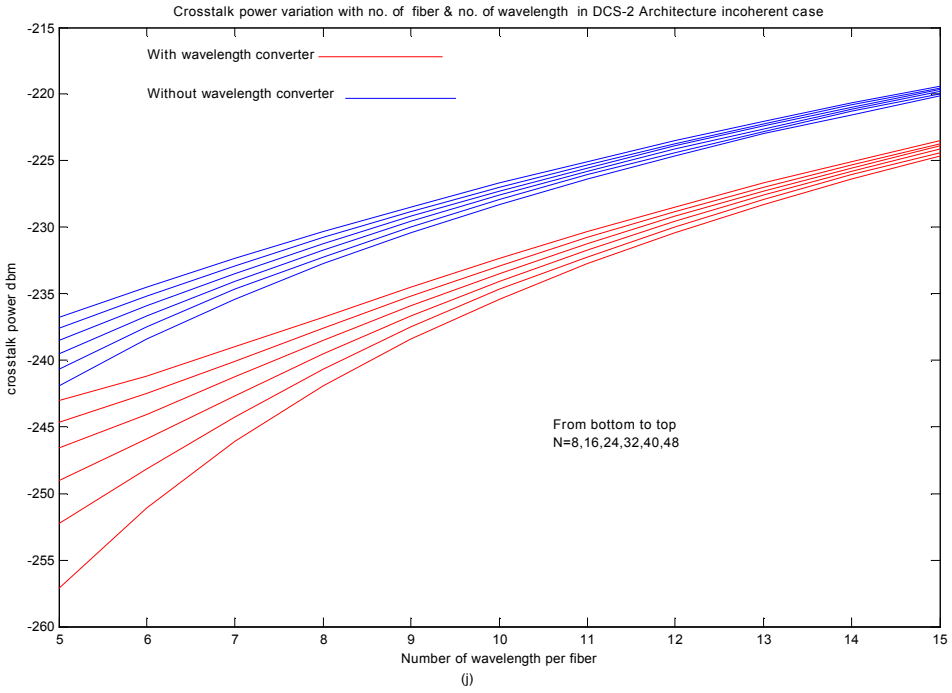

Fig. **4.18** Variation of crosstalk power with different number of input wavelength per fiber M for different Number of input fiber N for DCS-2 architecture (a) Coherent case and (b) Incoherent case.(P_{in} = -18 dbm, P_r = -19 dbm, V_n = 4, δ =-20 dbm,ε = -25 dbm and ε'= -25 dbm).

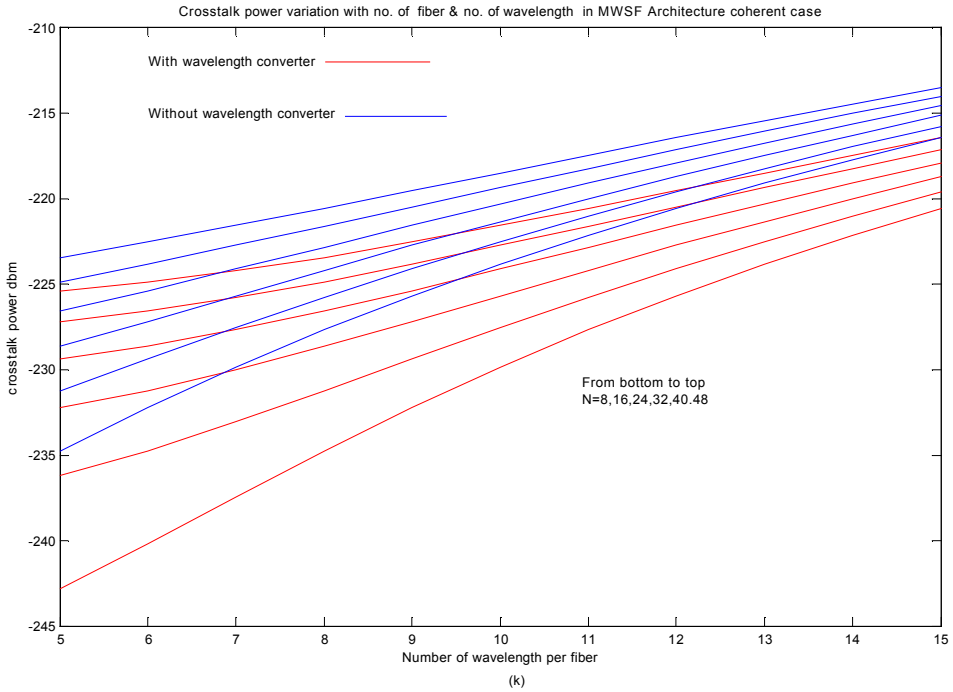

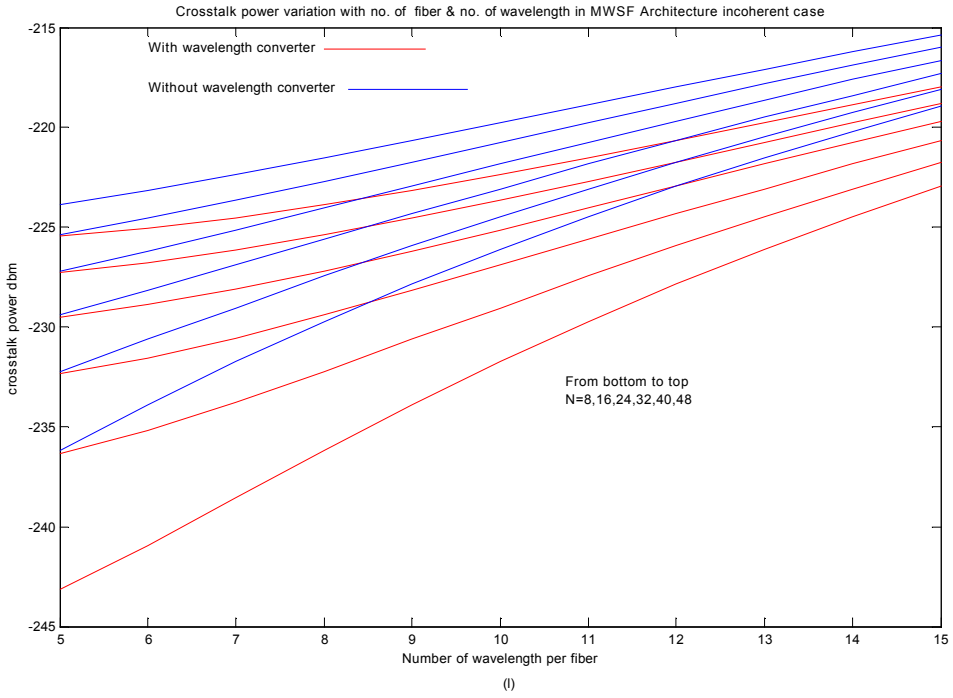

Fig. **4.19** Variation of crosstalk power with different number of input wavelength per fiber M for different Number of input fiber N for MWSF architecture (a) Coherent case and (b) Incoherent case.(P_{in} = -18 dbm, P_r = -19 dbm, V_n = 4, δ =-20 dbm,ε = -25 dbm and ε'= -25 dbm).

Fig.-4.13 to 4.19 show variation of crosstalk power with Number of wavelength per fiber M for different number of input fiber N. In the above figures received power is -18 dbm, input power is -10 dbm, number of wavelength converter per link is 4; optical power relative to the actual signal of the crosstalk contribution from the tunable filter/ Multiwavelength selective filter (MWSF), switch both first and second stage (incase of wavelength switch OXC) and second stage switch (incase of share-per-node architecture) are -25 dbm, -25 dbm and -30 dbm respectively. From the crosstalk power Vs number of input wavelength per fiber curves we see that crosstalk power increases with both number of wavelength per channel and number of fiber. The increase of crosstalk power at a fixed number of input fibers with number of wavelength per fiber is quadratic in nature but the increase of crosstalk power at a fixed number of wavelengths per fiber with number of input fiber is linear.

4.6. Effect of number of input wavelength per fiber for different number of input fiber on BER with and without WC

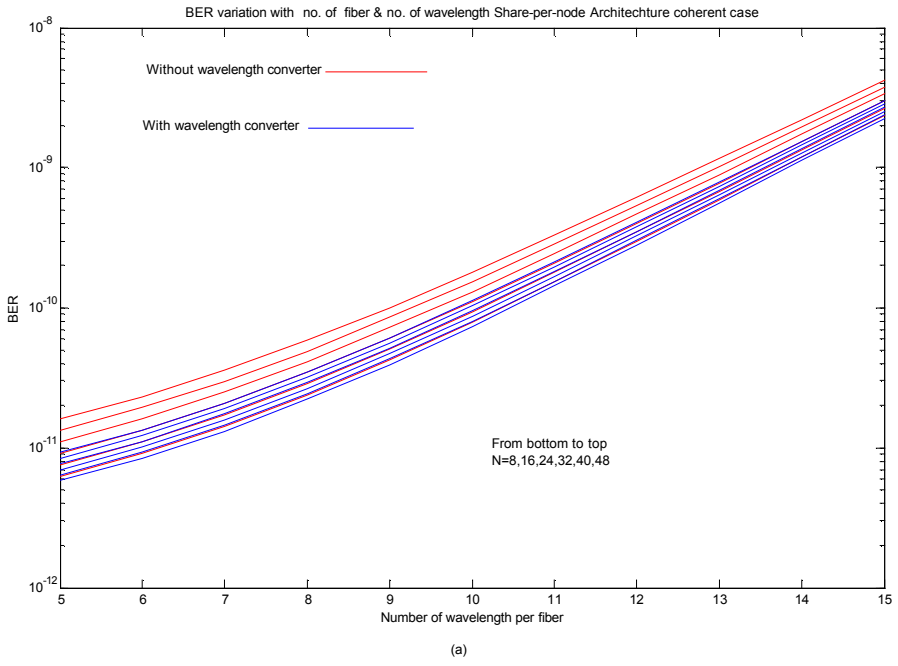

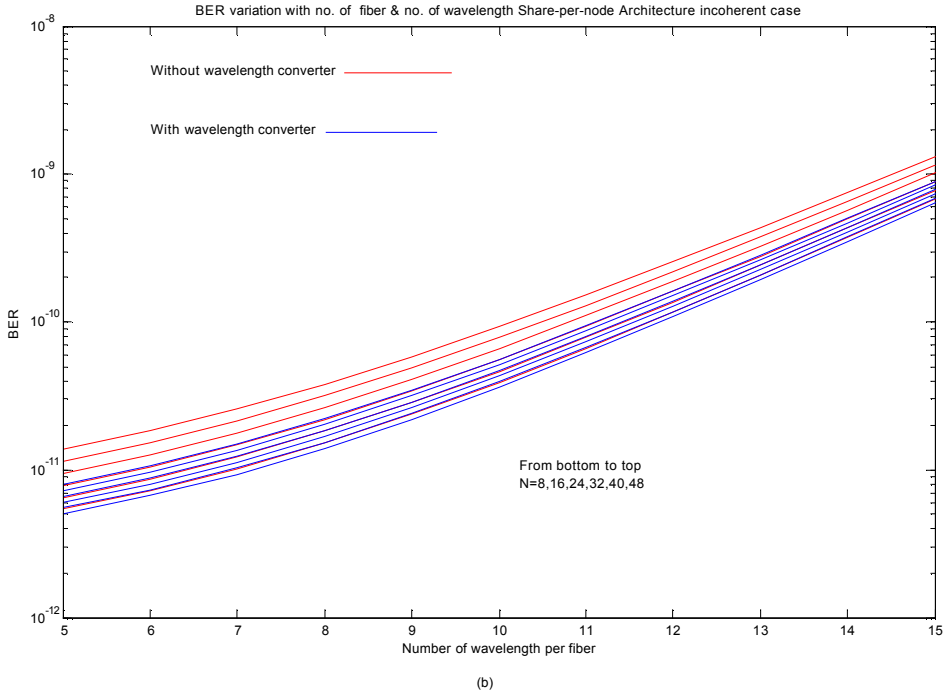

Fig. **4.20** Variation of BER with different number of input wavelength per fiber M for different Number of input fiber N for Share-per-node architecture (a) Coherent case and (b) Incoherent case.(P_{in} = -18 dbm, P_r = -19 dbm, V_n = 4, δ =-20 dbm,ε = -25 dbm and ε′= -25 dbm).

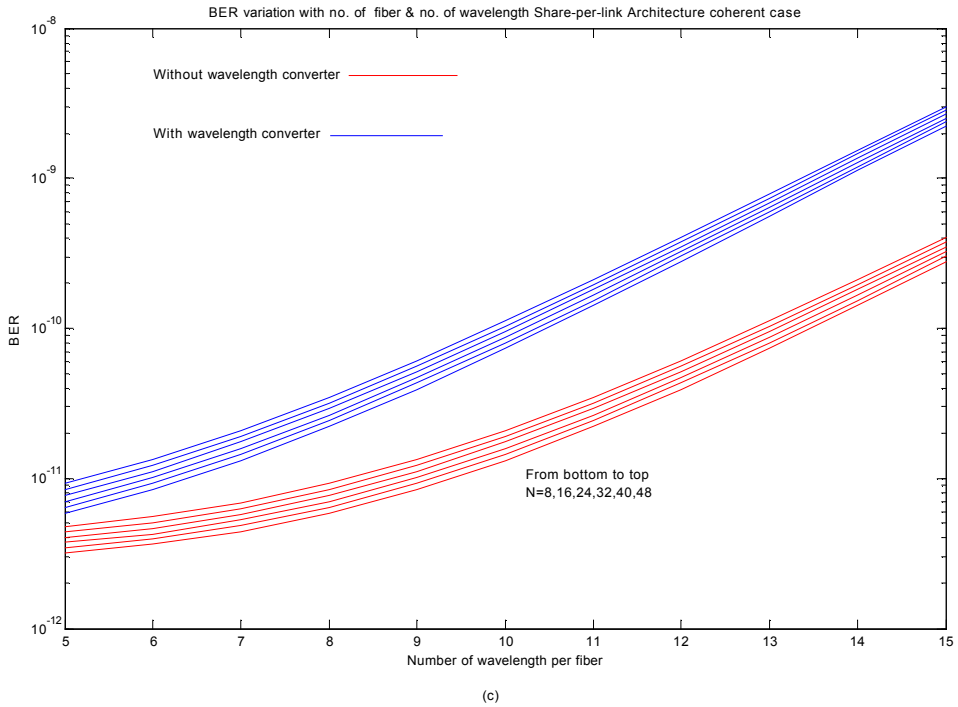

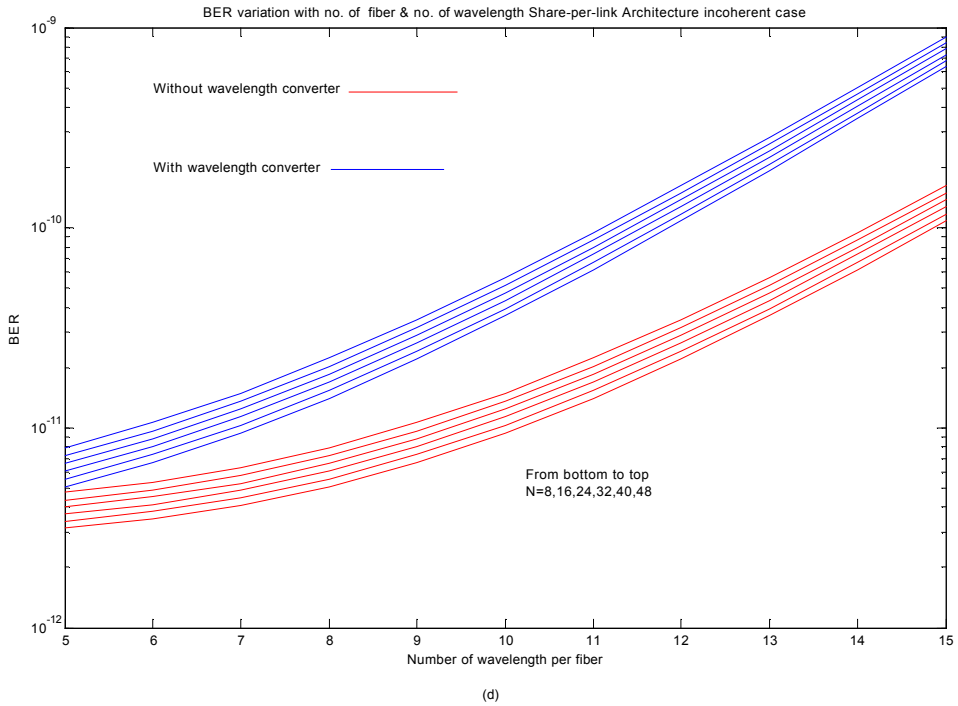

Fig. **4.21** Variation of BER with different number of input wavelength per fiber M for different Number of input fiber N for Share-per-link architecture (a) Coherent case and (b) Incoherent case.(P_{in} = -18 dbm, P_r = -19 dbm, V_n = 4; δ =-20 dbm,ε = -25 dbm and ε′= -25 dbm).

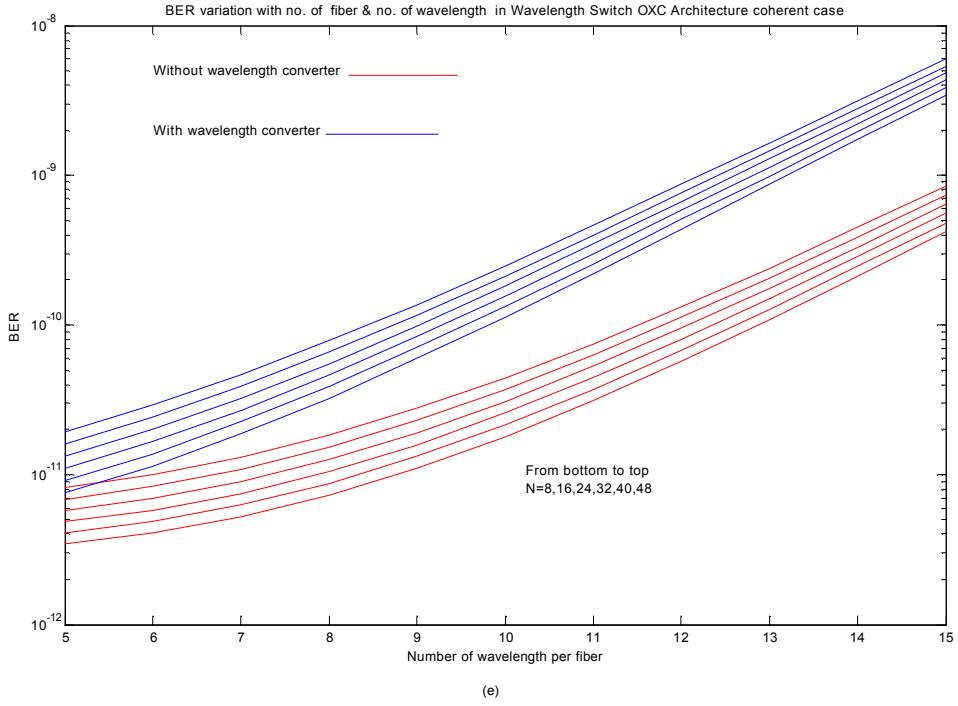

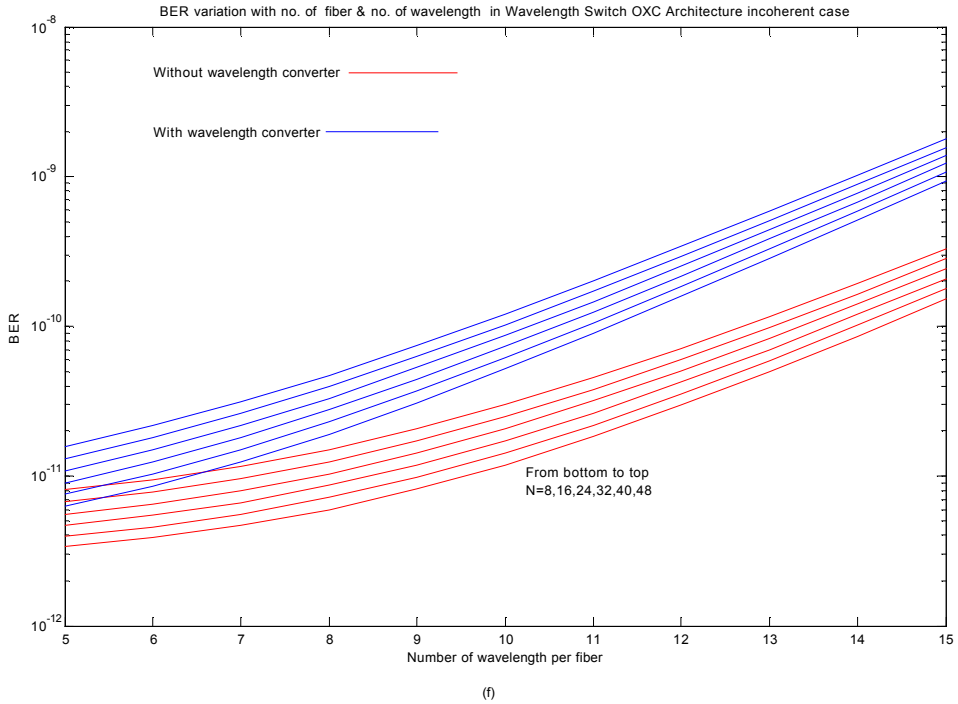

Fig. **4.22** Variation of BER with different number of input wavelength per fiber M for different Number of input fiber N for Wavelength switch OXC architecture (a) Coherent case and (b) Incoherent case.(P_{in} = -18 dbm, P_r = -19 dbm, V_n = 4, δ =-20 dbm, ε = -25 dbm and ε′= -25 dbm).

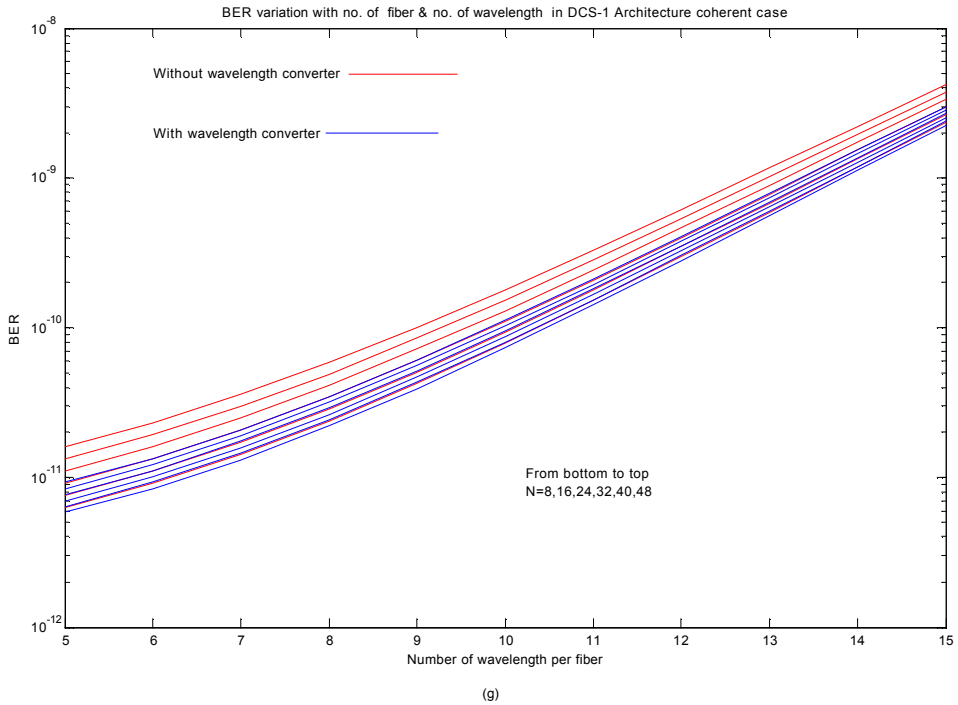

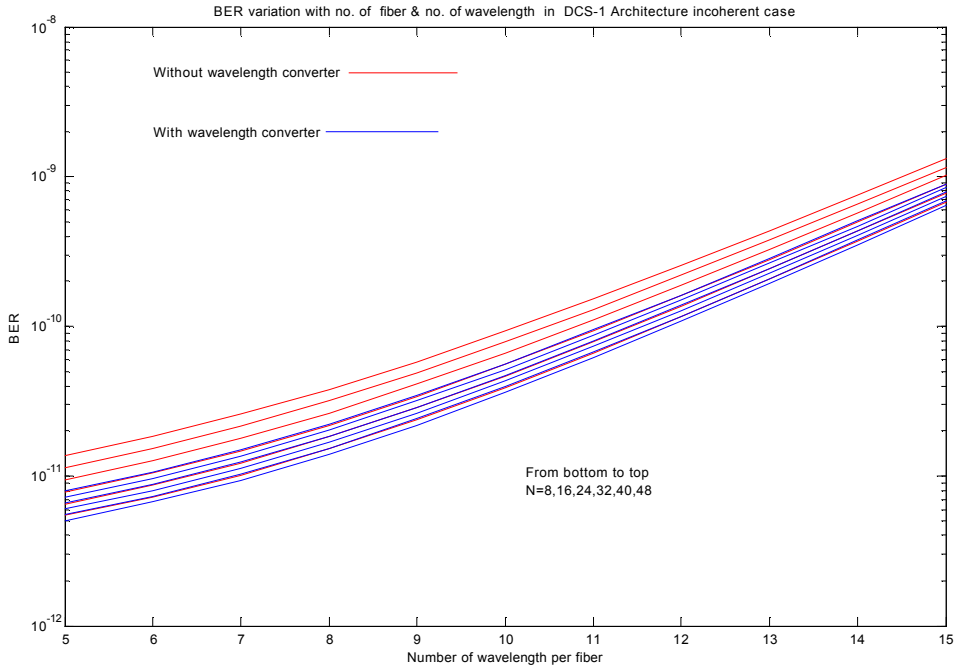

(h)

Fig. **4.23** Variation of BER with different number of input wavelength per fiber M for different Number of input fiber N for DCS-1 architecture (a) Coherent case and (b) Incoherent case.(P_{in} = -18 dbm, P_r = -19 dbm, V_n = 4, δ =-20 dbm, ε = -25 dbm and ε′= -25 dbm).

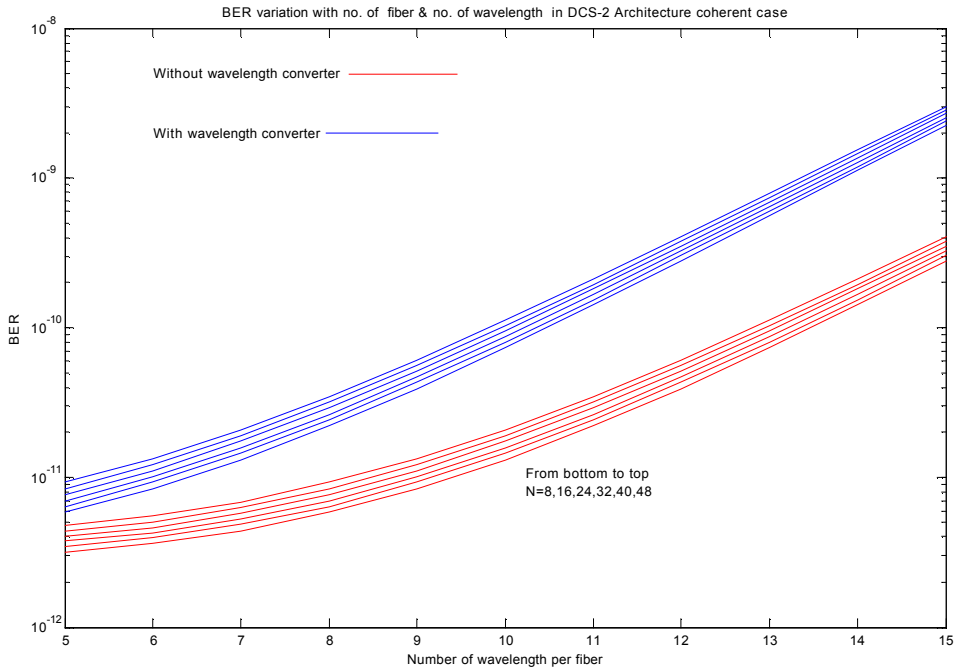

(i)

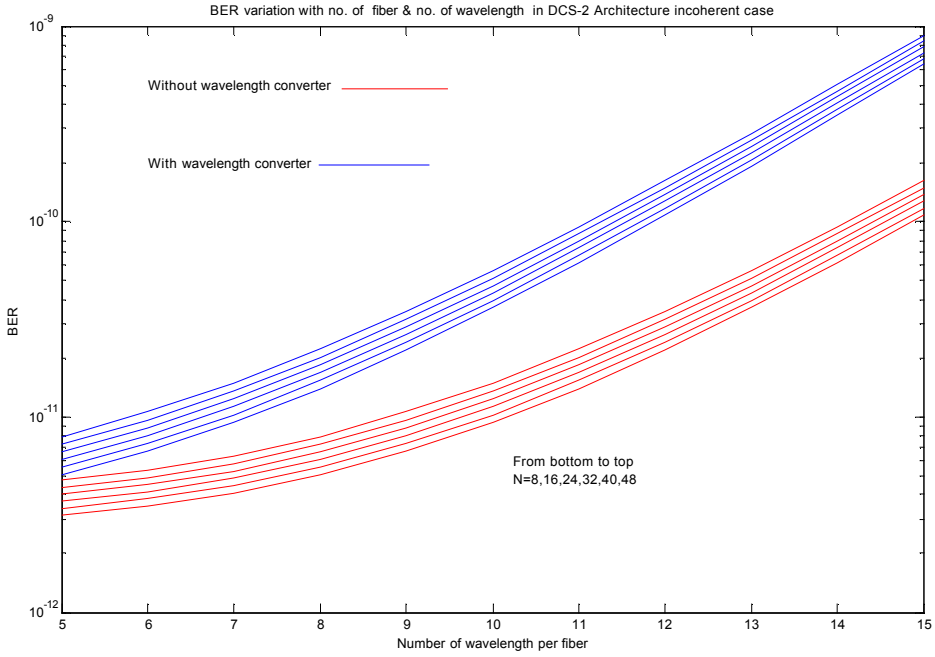

Fig. **4.24** Variation of BER with different number of input wavelength per fiber M for different Number of input fiber N for DCS-2 architecture (a) Coherent case and(b) Incoherent case.(P_{in} = -18 dbm, P_r = -19 dbm, V_n = 4, δ =-20 dbm, ε = -25 dbm and ε′= -25 dbm).

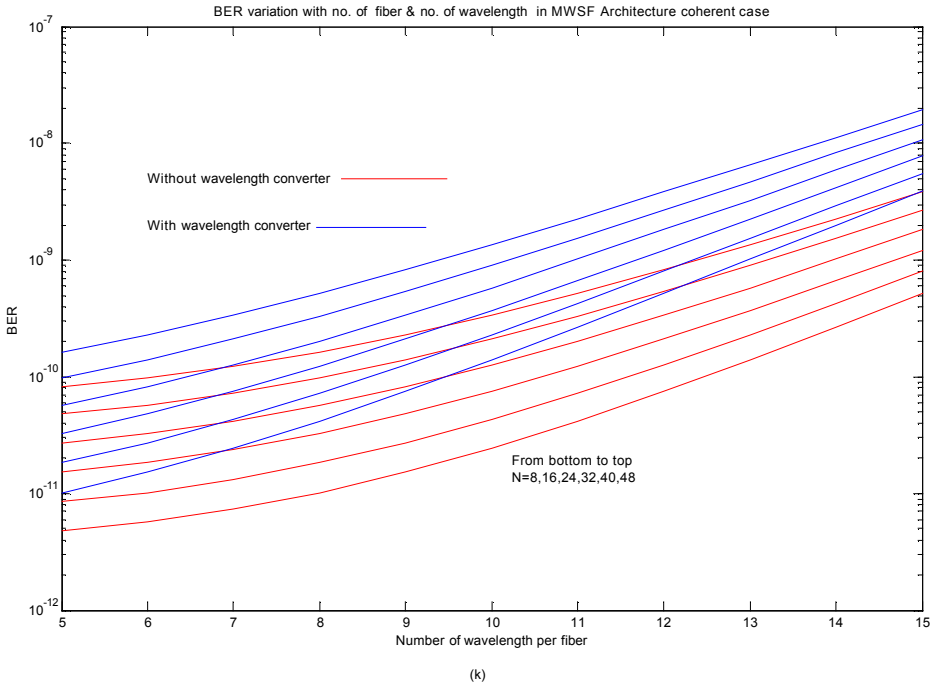

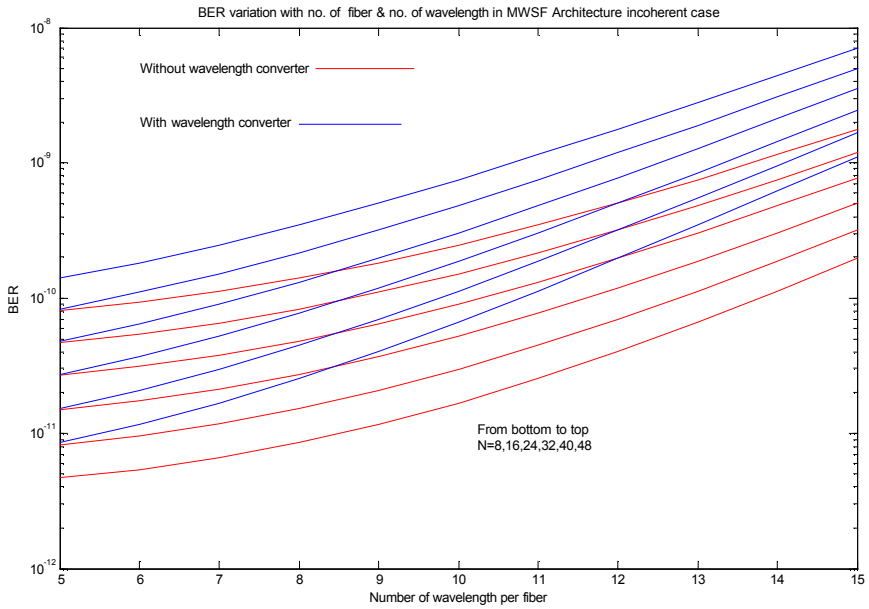

Fig. **4.25** Variation of BER with different number of input wavelength per fiber M for different Number of input fiber N for MWSF architecture (a) Coherent case and (b) Incoherent case.(P_{in} = -18 dbm, P_r = -19 dbm, V_n = 4, δ =-20 dbm, ε = -25 dbm and ε′= -25 dbm).

Fig. 4.20-4.25 show variation of BER with Number of wavelength per fiber for different number of input fiber. Other parameters are as like as previous figure. From the figure we see that when the receive power is high enough the BER Vs Number of wavelength per fiber curves diverse from each other as number of fiber N increases but at low receive power BER Vs Number of wavelength per fiber curves converse as N increases.

At low input power BER Vs Number of wavelength per fiber curves are equidistance from each other as N increases but at high input power they converse with increasing N.

At high receive power Variation of BER with number of fiber curves diverse from each other as number of wavelength per fiber is increased but at low receive power this curves become equidistance from each other. At all input power BER Vs N curves converse as increase of Number of wavelength per fiber M.

For a certain throughput (N multiplied with M) lowest crosstalk is obtained with large N and small M. At a result lower BER is obtained with large N and small M.

So if the total BER is to be kept constant than by increasing N and decreasing M we can increase the throughput.

4.7. Comparison of the effect of number of input wavelength per fiber on Crosstalk and BER for different architectures with and without WC

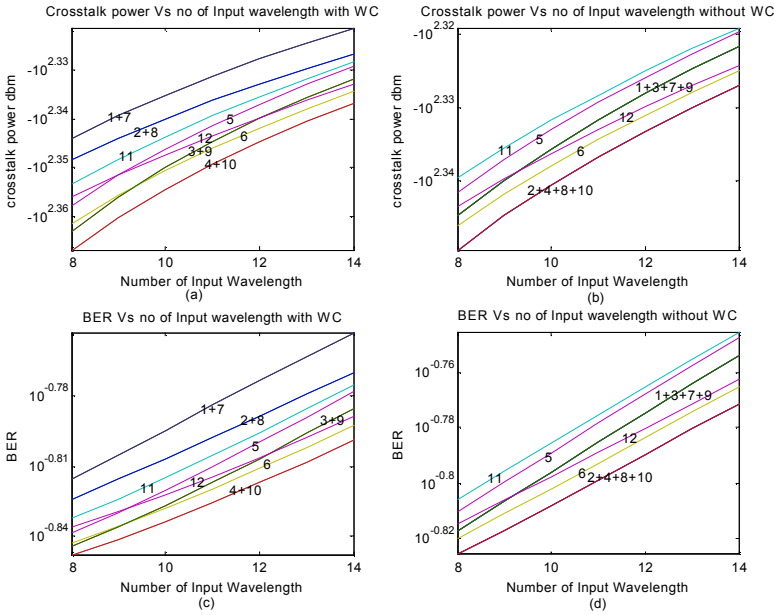

Fig. **4.26** Comparison of variation of (a) crosstalk power with WC (b) crosstalk power without WC (c) BER with WC (d) BER without wavelength converter with Number of input wavelength per fiber M for different architectures. (P_{in} = -16 dbm, P_r = -27 dbm, N=8, , V_n = 4 i.e V =32, δ =-20 dbm, ε = -25 dbm and ε′= -25 dbm).

Fig. -4.26 compares variation of crosstalk power and BER with number of input wavelength per fiber with and without wavelength converter for different architectures. In this case number of wavelength converter per link, V_n= 4; number of input fiber N= 8; input power P_{in} = -16 dbm, P_r = -27 dbm From the figure we see that both crosstalk power and BER increase as the number of input wavelength per fiber is increased in both with and without WC cases. From the figure we also see that when there is no wavelength converter MWSF coherent case architecture suffers from more crosstalk so the BER is higher than any other architecture. On the other hand when there are wavelength converters share-per-node and DCS-1 architectures suffer from more crosstalk than any other architecture so they involve more BER.

4.8. Comparison of the effect of number of input fiber on Crosstalk and BER for different architectures with and without WC

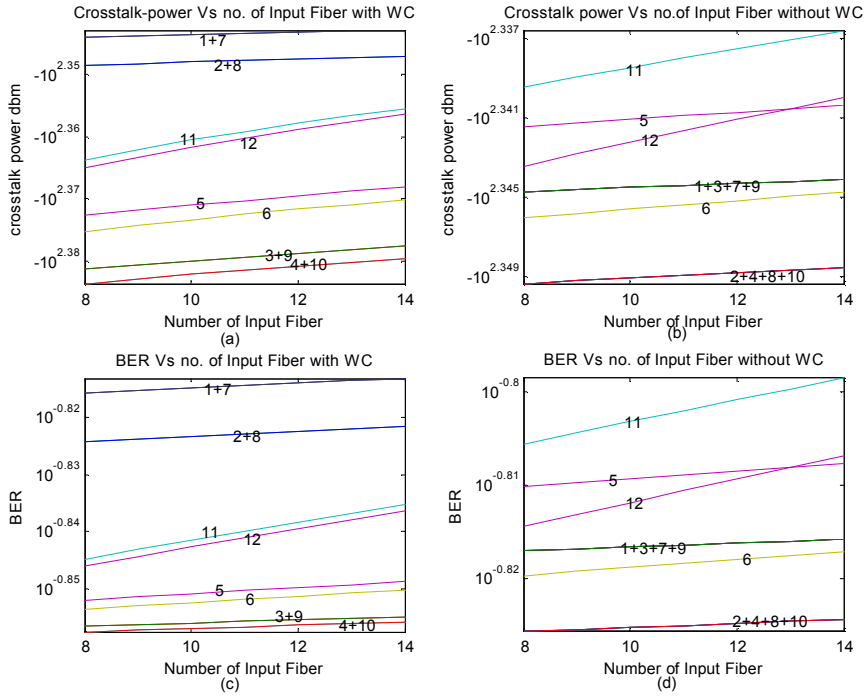

Fig. **4.27** Comparison of variation of (a) crosstalk power with WC (b) crosstalk power without WC (c) BER with WC (d) BER without wavelength converter with Number of input fiber N for different architectures. (P_{in} = -16 dbm, P_r = -27 dbm; M=8, V_n = 4, δ =-20 dbm, ε = -25 dbm and ε′= -25 dbm).

Fig. 4.27 shows variation of crosstalk power and BER with number of input fiber with and without wavelength converter. In this case number of wavelength converter per link, V_n= 6; number of input wavelength M= 8; input power P_{in} = -16 dbm, P_r = -27 dbm. From the figures we see that crosstalk power and BER increase as the number of input fiber is increased. Multiwavelength Selective Filters (MWSF) –OXC architecture posses higher rate of rise of crosstalk power and BER than any other architecture. The variation of crosstalk power and BER with Number of input fiber is smaller than that of with number of input wavelength per fiber.

.

4.9. Effect of input power on PP for different number of WC

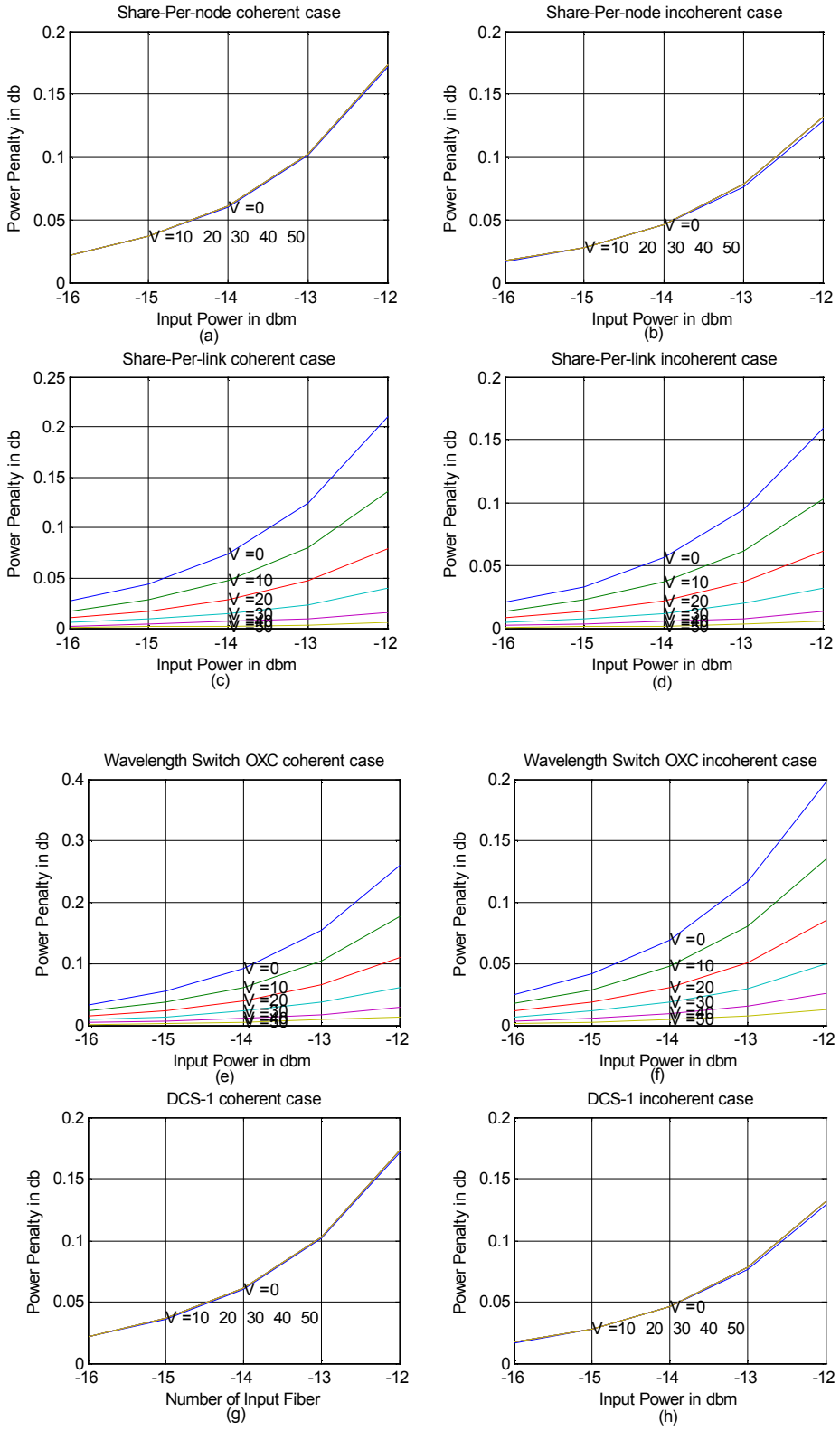

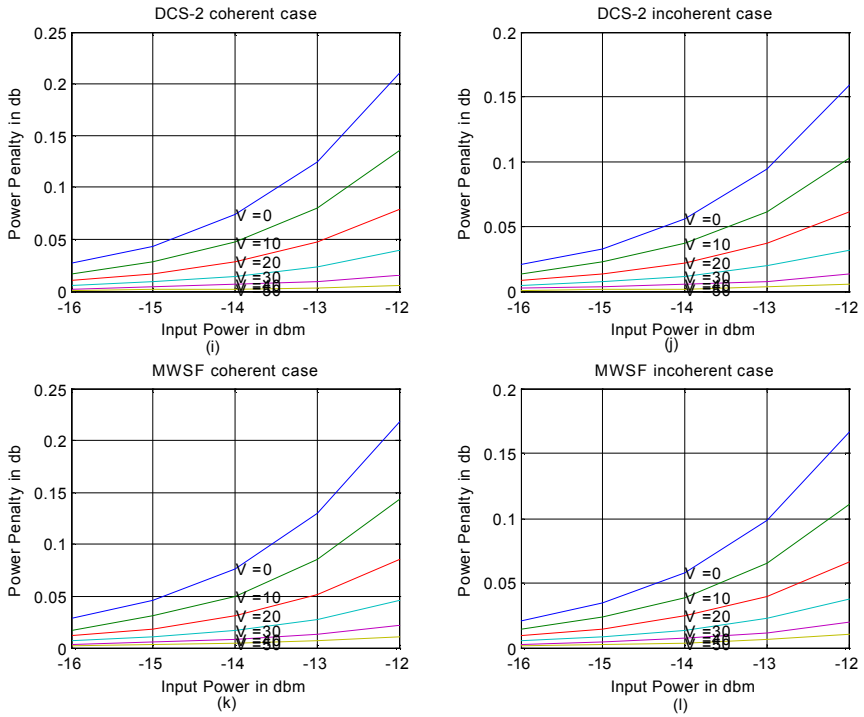

Fig. **4.28** Variation of power penalty with input power for different number of wavelength converters for all architecture at BER 10^{-12} (M=10, N=5, δ = -35 dbm, ε = -35 dbm and ε′= -40 dbm and V= total number of WC NX V_n).

Fig. 4.28 shows power penalty Vs input power characteristic for different number of wavelength converters at BER10^{-12}. From the figures we see that for a fixed number of wavelength converters if we increase the input power power penalty increase. But this increasing in power penalty can be reduced by increasing the number of wavelength converters in all case except in Share-per-node Architecture and DCS-1 architecture. In these two cases the signals those have been converted are also present in the output so PP increase with number of wavelength converter.

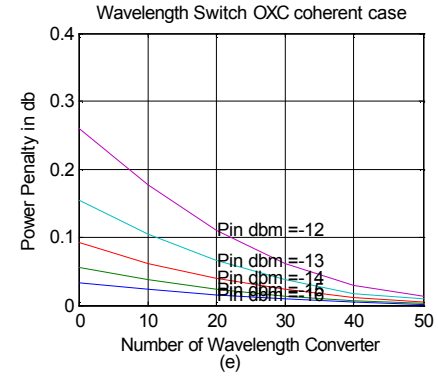
Wavelength Switch OXC coherent case
Power Penalty in db
Number of Wavelength Converter
Pin dbm =-12
Pin dbm =-13
Pin dbm =-14
Pin dbm =-15
Pin dbm =-16
(e)

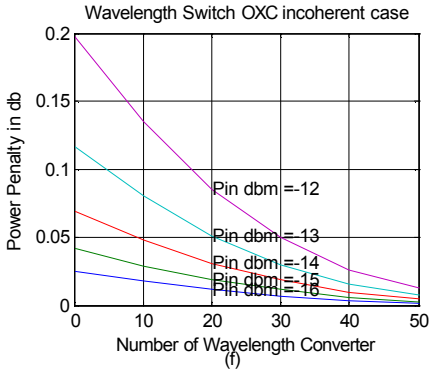
Wavelength Switch OXC incoherent case
Power Penalty in db
Number of Wavelength Converter
Pin dbm =-12
Pin dbm =-13
Pin dbm =-14
Pin dbm =-15
Pin dbm =-16
(f)

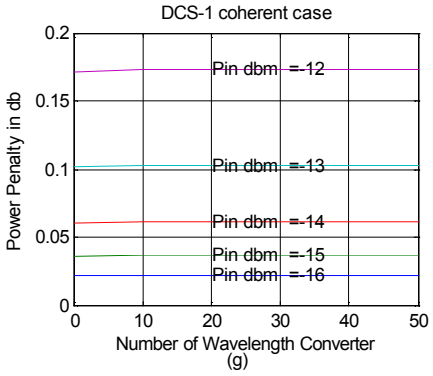
DCS-1 coherent case
Power Penalty in db
Number of Wavelength Converter
Pin dbm =-12
Pin dbm =-13
Pin dbm =-14
Pin dbm =-15
Pin dbm =-16
(g)

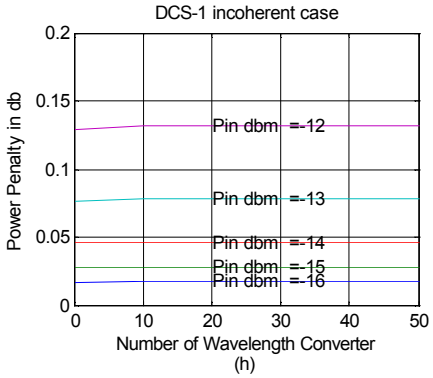
DCS-1 incoherent case
Power Penalty in db
Number of Wavelength Converter
Pin dbm =-12
Pin dbm =-13
Pin dbm =-14
Pin dbm =-15
Pin dbm =-16
(h)

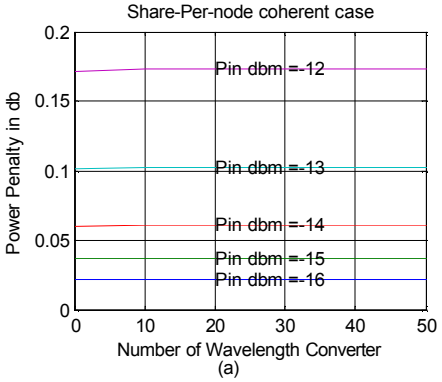
Share-Per-node coherent case
Power Penalty in db
Number of Wavelength Converter
Pin dbm =-12
Pin dbm =-13
Pin dbm =-14
Pin dbm =-15
Pin dbm =-16
(a)

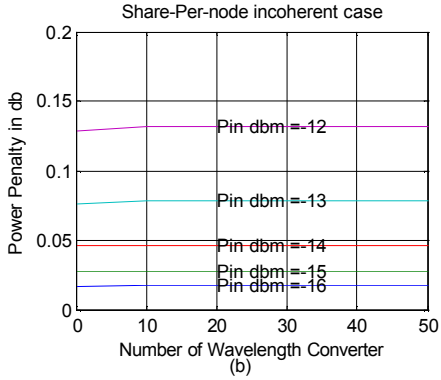
Share-Per-node incoherent case
Power Penalty in db
Number of Wavelength Converter
Pin dbm =-12
Pin dbm =-13
Pin dbm =-14
Pin dbm =-15
Pin dbm =-16
(b)

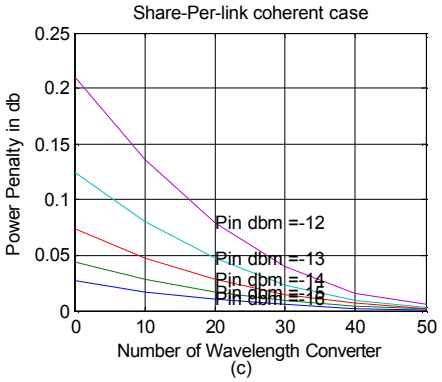
Share-Per-link coherent case
Power Penalty in db
Number of Wavelength Converter
Pin dbm =-12
Pin dbm =-13
Pin dbm =-14
Pin dbm =-15
Pin dbm =-16
(c)

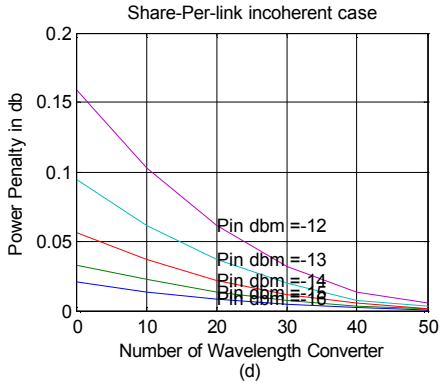
Share-Per-link incoherent case
Power Penalty in db
Number of Wavelength Converter
Pin dbm =-12
Pin dbm =-13
Pin dbm =-14
Pin dbm =-15
Pin dbm =-16
(d)

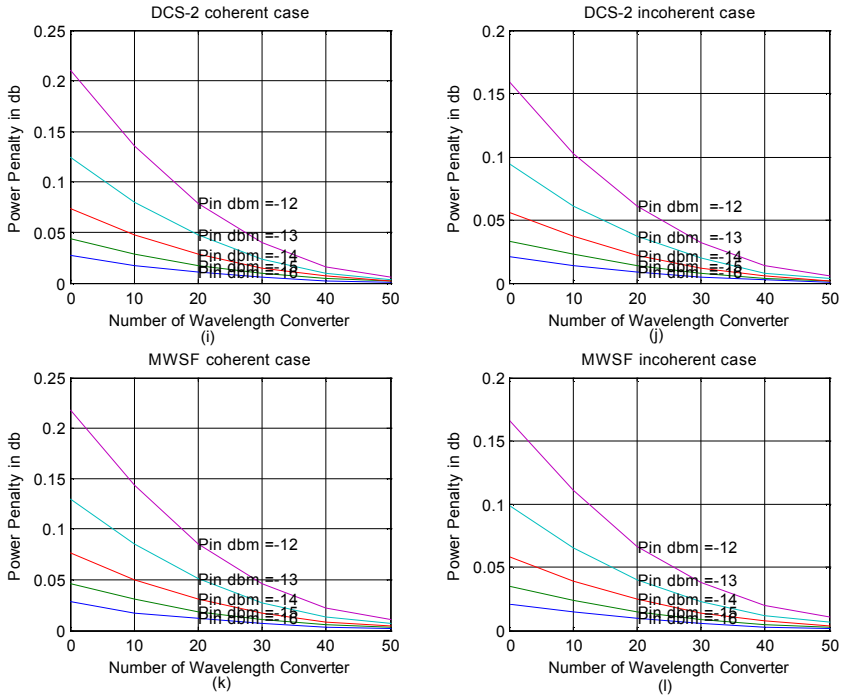

Fig. **4.29** Variation of power penalty with different number of wavelength converters for different input power for all architecture at BER10^{-12}. (M=10, N=5, δ = -35 dbm, ε = -35 dbm and ε'= -40 dbm, V= total number of WC NX V_n).

Fig. 4.29 show power penalty Vs number of wavelength converters characteristic for different input power at BER10^{-12}. From the figures we see that for a fixed input power if we increase the number of wavelength converters power penalty decreases in all case except in Share-per-node Architecture and DCS-1 architecture. In these two cases power penalty increases with increasing the number of wavelength converter and becomes fixed when the number of wavelength converter is equal N-1, where N is the number of input fiber. These results also agree with the previous results.

4.10. Effect of number of input wavelength per fiber on PP for different number of WC

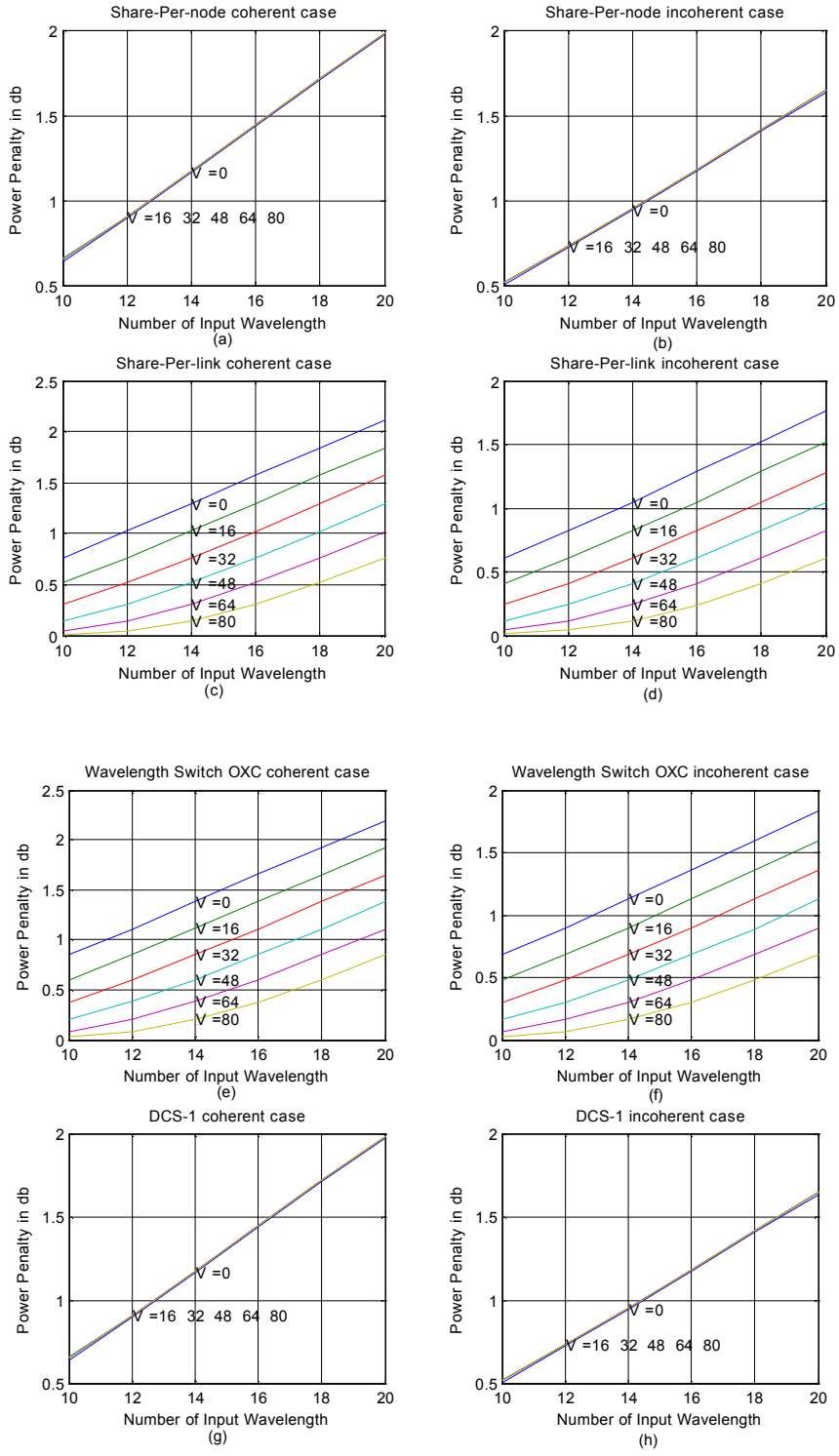

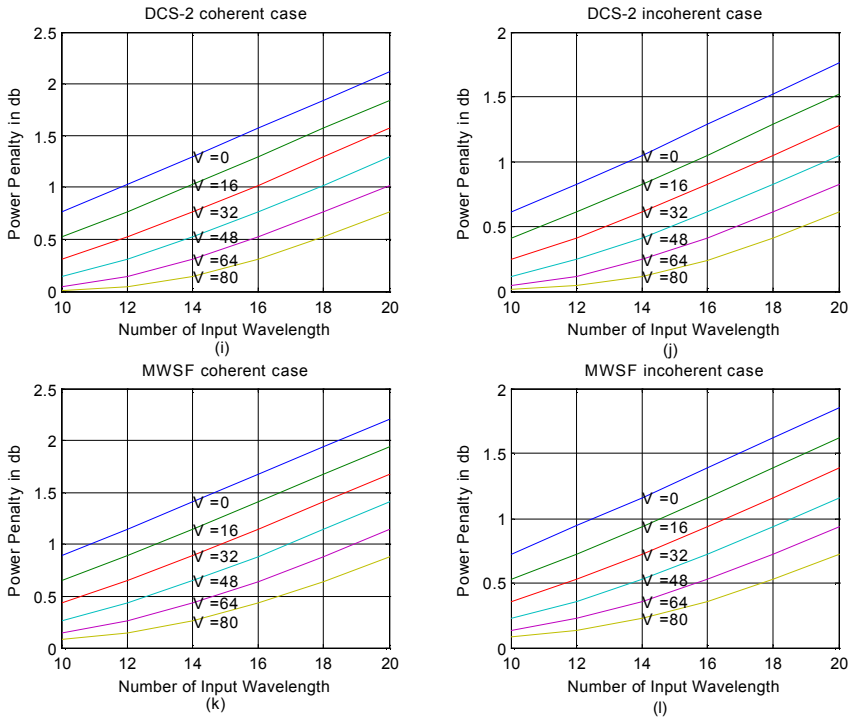

Fig. **4.30** Variation of power penalty with Number of input wavelength per fiber M for different number of wavelength converters for all architecture at BER 10^{-12} (P_{in} =-9 dbm, N=8, δ = -35 dbm, ε = -40 dbm and ε′= -40 dbm, V= total number of WC NX V_n).

Fig.4.30 shows power penalty Vs number of wavelength per fiber characteristic for different number of wavelength converters at BER10^{-12}. From the figures we see that for a fixed number of wavelength converters if we increase number of wavelength per fiber power penalty increase linearly. But this increase in power penalty can be reduced by increasing the number of wavelength converters in all case except in Share-per-node Architecture and DCS-1 architecture for the reason mention previously.

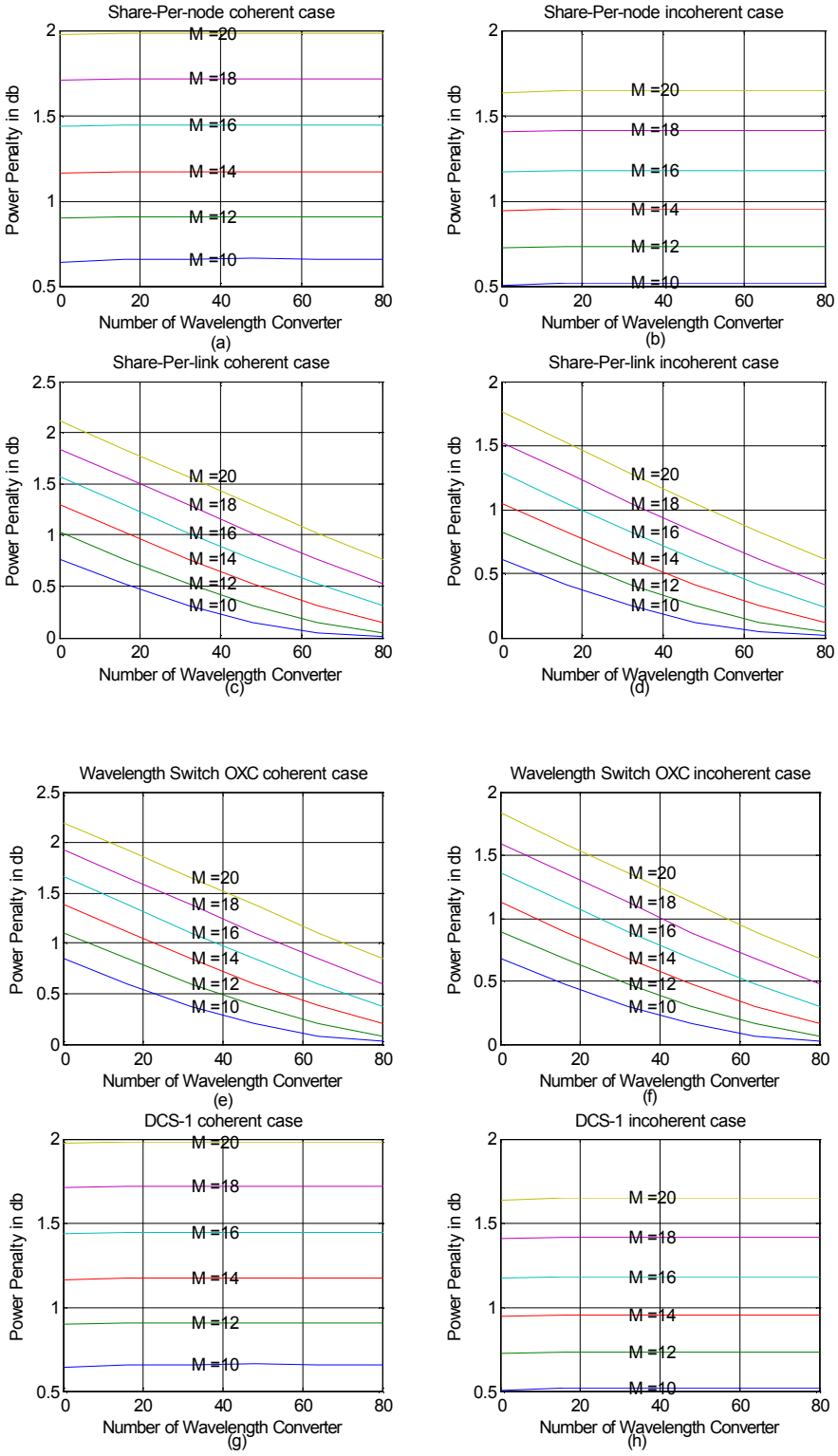
Share-Per-node coherent case
Power Penalty in db
Number of Wavelength Converter
M =20
M =18
M =16
M =14
M =12
M =10
(a)
Share-Per-node incoherent case
Power Penalty in db
Number of Wavelength Converter
M =20
M =18
M =16
M =14
M =12
M =10
(b)
Share-Per-link coherent case
Power Penalty in db
Number of Wavelength Converter
M =20
M =18
M =16
M =14
M =12
M =10
(c)
Share-Per-link incoherent case
Power Penalty in db
Number of Wavelength Converter
M =20
M =18
M =16
M =14
M =12
M =10
(d)
Wavelength Switch OXC coherent case
Power Penalty in db
Number of Wavelength Converter
M =20
M =18
M =16
M =14
M =12
M =10
(e)
Wavelength Switch OXC incoherent case
Power Penalty in db
Number of Wavelength Converter
M =20
M =18
M =16
M =14
M =12
M =10
(f)
DCS-1 coherent case
Power Penalty in db
Number of Wavelength Converter
M =20
M =18
M =16
M =14
M =12
M =10
(g)
DCS-1 incoherent case
Power Penalty in db
Number of Wavelength Converter
M =20
M =18
M =16
M =14
M =12
M =10
(h)

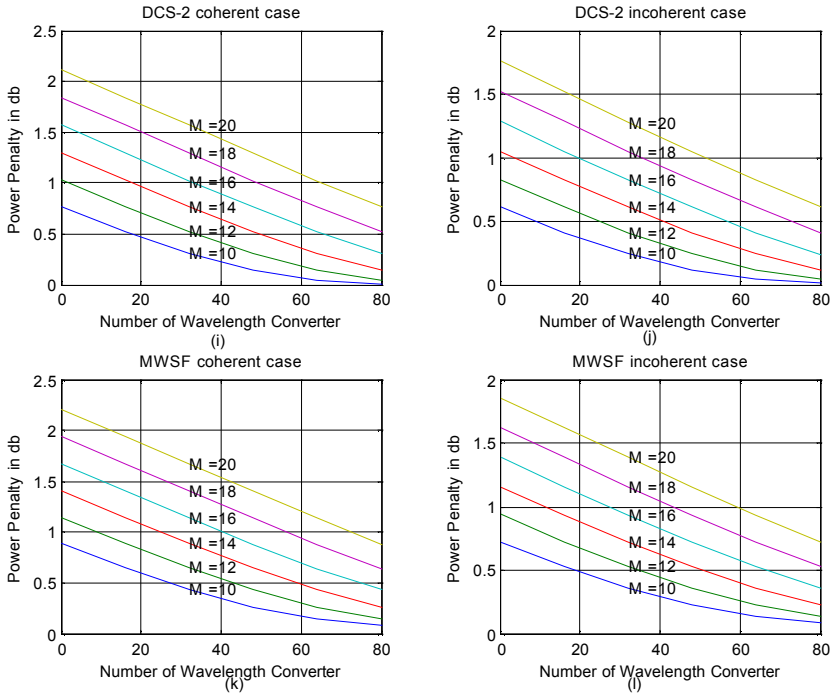

Fig. **4.31** Variation of power penalty with different number of wavelength converters for different Number of input wavelength per fiber M for for all architecture at BER10^{-12} (P_{in} =-9 dbm, N=8, δ = -35 dbm, ε = -40 dbm and ε′= -40 dbm, V= total number of WC NX V_n).

Fig. 4.31 shows power penalty Vs number of wavelength converters characteristic for different number of wavelength per fiber at BER10^{-12}. From the figures we see that for a fixed number of wavelength per fiber if we increase the number of wavelength converters Power penalty decreases in all case except in Share-per-node Architecture and DCS-1 architecture. In these two cases power penalty increase with increasing the number of wavelength converter and becomes fixed when the number of wavelength converter is equal N-1, where N is the number of input fiber. These results also agree with the previous results.

4.11. Effect of number of input fiber on PP for different number of WC

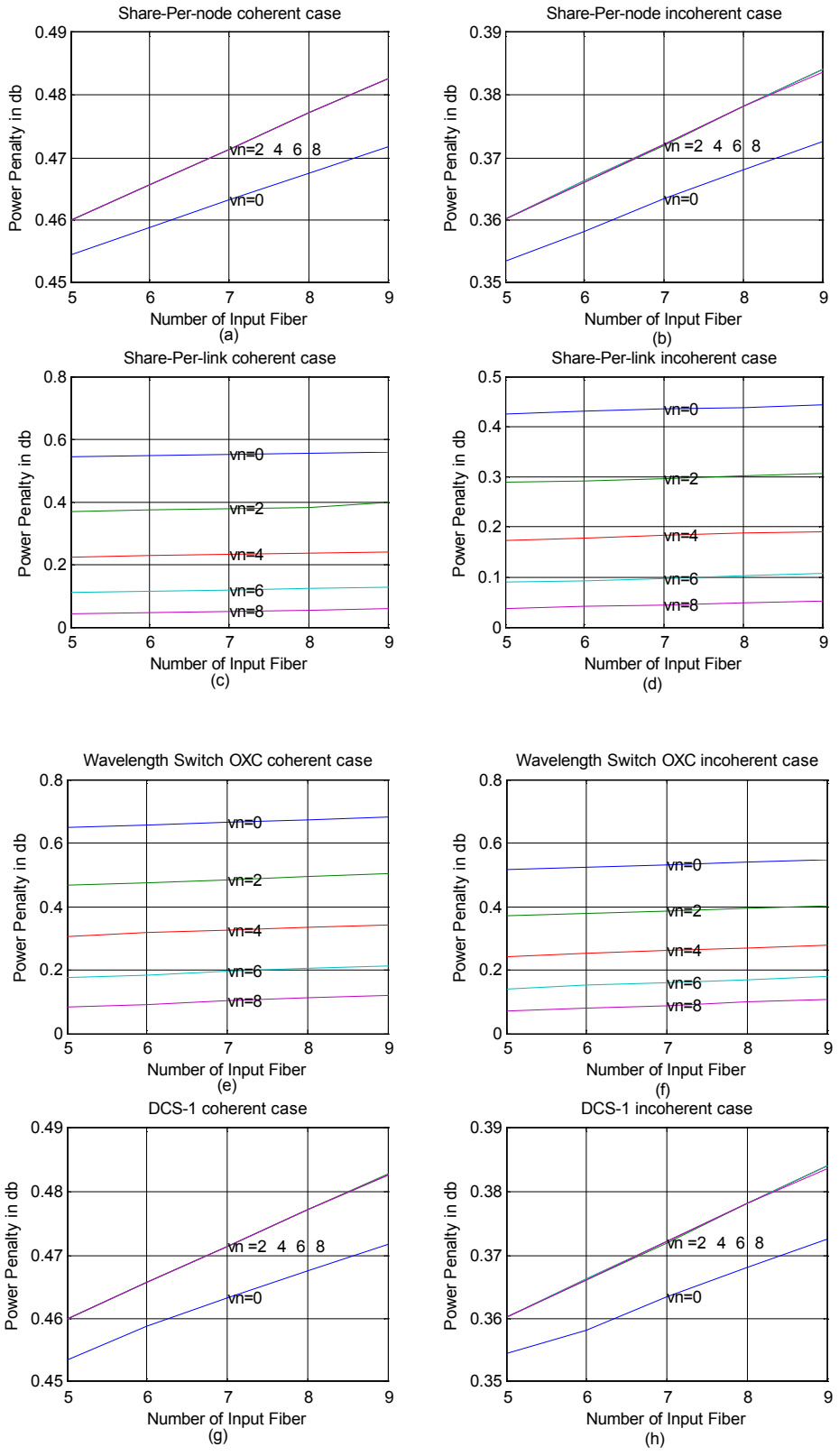

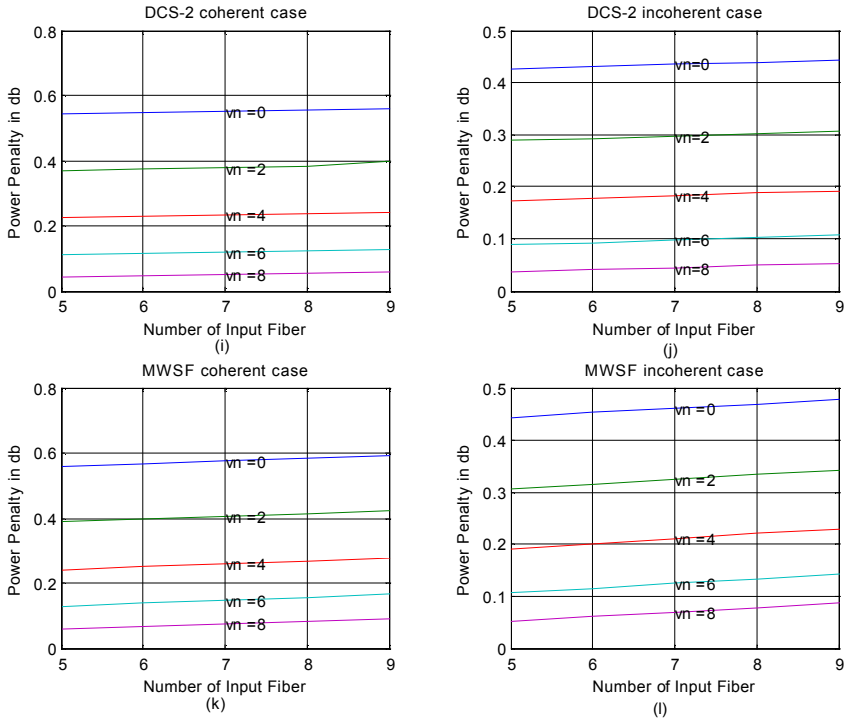

Fig. **4.32** Variation of power penalty with different Number of input fiber N for different number of wavelength converters for all architecture at BER10^{-12} (P_{in} = -9 dbm, N=8, δ = -35 dbm, ε = -40 dbm and ε′= -40 dbm, V= total number of WC NX V_n).

Fig.4.32 shows power penalty Vs number of input fiber characteristic for different number of wavelength converters at BER10^{-12}. From the figure we see that for a fixed number of wavelength converters if we increase number of input fiber power penalty increase at a low rate. But this increase in power penalty can be reduced by increasing the number of wavelength converters in all case except in Share-per-node Architecture and DCS-1 architecture for the reason mention previously.

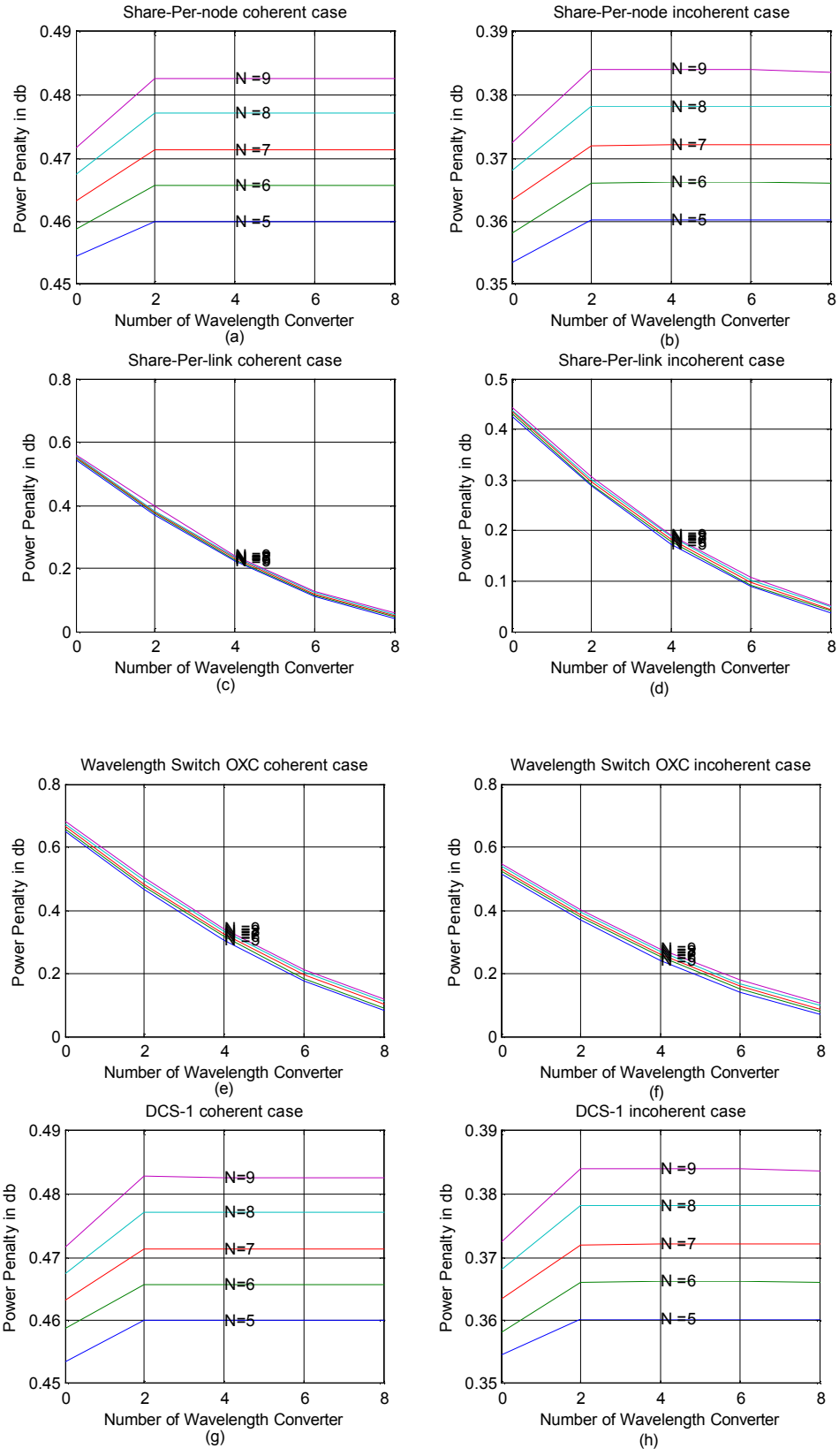
Share-Per-node coherent case
Power Penalty in db
Number of Wavelength Converter
(a)
N =9
N =8
N =7
N =6
N =5
Share-Per-node incoherent case
(b)
Share-Per-link coherent case
(c)
Share-Per-link incoherent case
(d)
Wavelength Switch OXC coherent case
(e)
Wavelength Switch OXC incoherent case
(f)
DCS-1 coherent case
N=9
N=8
N=7
N=6
N=5
(g)
DCS-1 incoherent case
(h)

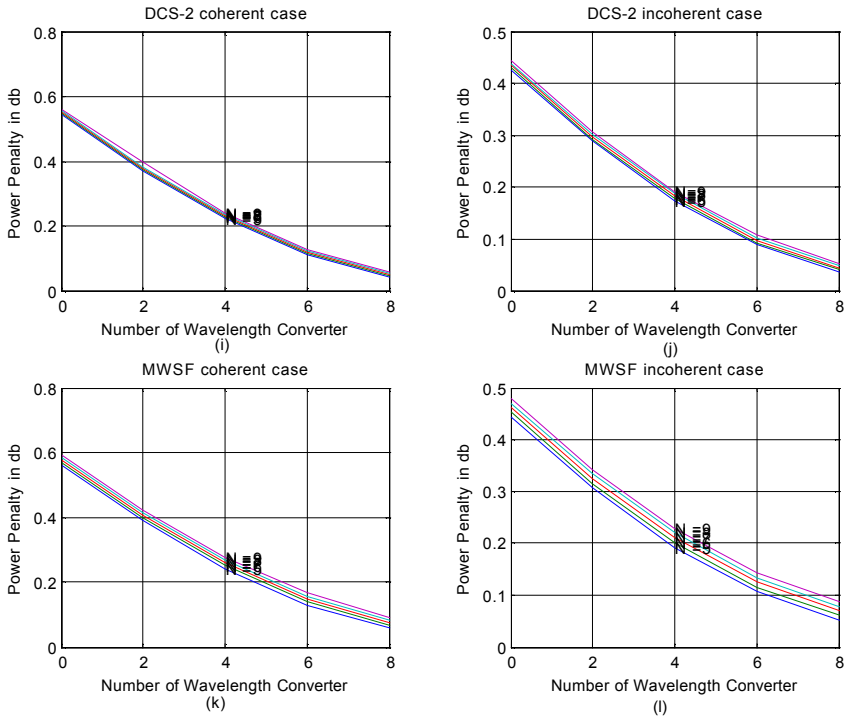

Fig. **4.33** Variation of power penalty with different Number of wavelength converters for different number of input fiber N for all architecture at BER10^{-12} (P_{in} = -9 dbm , N=8, δ = -35 dbm, ε = -40 dbm and ε′= -40 dbm , V= total number of WC NX V_n).

Fig. 4.33 shows power penalty Vs number of wavelength converters characteristic for different number of input fiber at BER10^{-12}. From the figures we see that for a fixed number of input fibers if we increase the number of wavelength converters power penalty will decrease in all case except in Share-per-node Architecture and DCS-1 architecture. In these two cases power penalty increases with increasing the number of wavelength converter and becomes fixed when the number of wavelength converter is equal N-1, where N is the number of input fiber. These results also agree with the previous results.

4.12. Comparison of the effect of number of input fiber, input wavelength per fiber and number of input fiber on PP for different architectures with limited number of WC

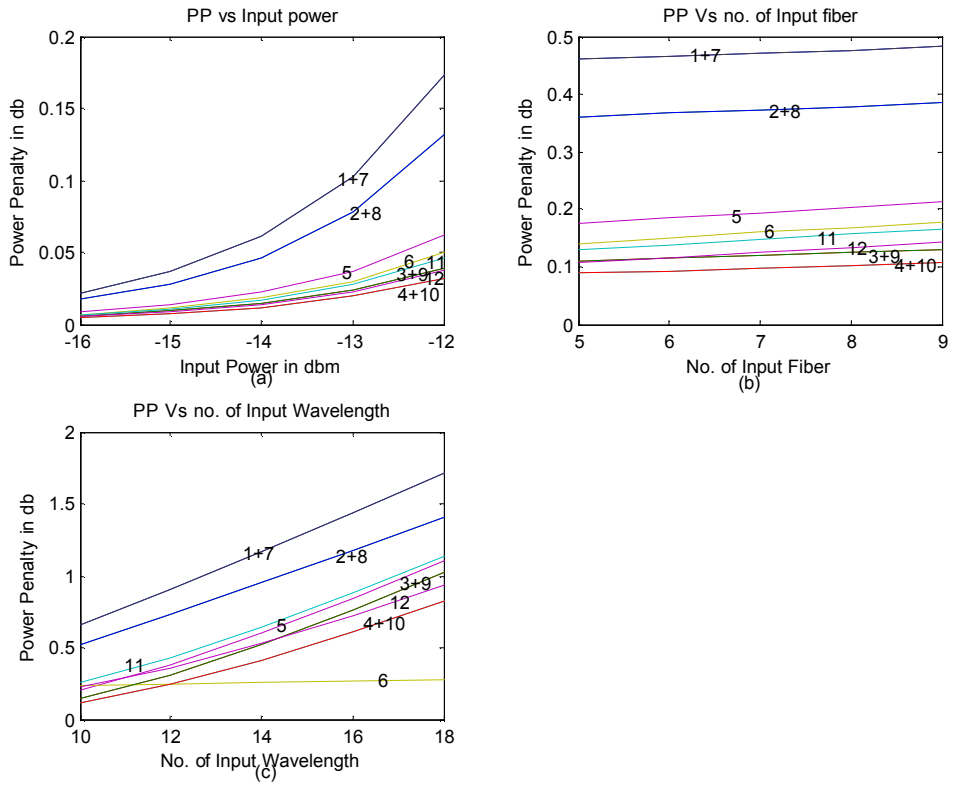

Fig. **4.34** Comparison of variation of PP with (a) input power (b) Number of input fiber(c) number of input wavelength per fiber for L-WIXC for all architecture at BER10^{-12}. (P_{in} = -9 dbm;δ = -35 dbm,ε = -40 dbm and ε′= -40 dbm).

Figure 4.34(a) shows the comparison of variation of power penalty with Input power, (b) shows the comparison of variation of power penalty with number of Input Fiber and (c) shows the comparison of variation of Power penalty with number of input wavelength per fiber with wavelength converter for different architecture. In all case number of wavelength converter per link, V_n=6.From these figure we see that power penalty increases as any of the parameters such as the number of input Wavelength per fiber or the number of input fiber or input power is increased keeping other parameters fixed. In all cases share-per-node and DCS-1 suffer from more power penalty and power penalty due to coherent crosstalk is much more than that of incoherent crosstalk.

CHAPTER-5
CONCLUSION AND FUTURE WORKS

5.1 Conclusions

In this research work crosstalk due to space switches, mux/demuxes, optical filters etc in a limited wavelength interchanging optical cross-connect for different architectures has been identified and analytical expressions for the crosstalk have been carried out for both coherent and incoherent cases. The effect of different system parameters such as input power, number of input wavelength per fiber and number of input fiber on system performance such as crosstalk, BER and PP has been investigated. A comparative picture of system performance for different architectures of limited wavelength interchanging cross-connect has been depicted. To find the expression we have considered that the signals traverse only one node, signals extinction ratio are infinite, the converted signal is free from the crosstalk carried with it before wavelength conversion and input output characteristic is assumed unity except propagation delay and phase change. We also avoid interferometric intensity noise (IIN),relative output noise (RON) and accumulated ASE noise. From figures 4.1 to 4.25 we see that both the crosstalk power and BER increase as anyone of the parameter such as input power, number of input wavelength per fiber or number of input fiber increases. From the above figures we also see that Share-per-node and DCS-1 architecture suffer from more crosstalk and BER when there are wavelength converters because in these two cases a portion of signals that have been converted by wavelength converters is present in the output signals. From the above figures we reveal that there is a distinct difference between the amount of crosstalk in coherent cases and incoherent cases. The difference between these two cases indicates the improvement which can be obtained by suppressing the beat term. Figures 4.20 to 4.25 indicate that if the total BER is to be kept constant then by increasing the number of input fibers and decreasing the number of wavelength per fiber we can increase the throughput. From the analysis we also see that Wavelength converter improved system performance in most case except share per node architecture and DCS-1 architecture for the reason mention previously. From Fig.

4.28 to Fig. 4.33 we see that power penalty increases if anyone of the parameter such as input power, number of wavelength per fiber or number of input fiber increases. But this increasing in power penalty can be reduced by increasing the number of wavelength converters in all case except in Share-per-node Architecture and DCS-1 architecture and becomes fixed when the number of wavelength converter is equal to N-1, when N is the number of input fiber. In all cases share-per-node and DCS-1 suffer from more power penalty and power penalty due to coherent crosstalk is much more than that of incoherent crosstalk.

5.2 Future Works

This thesis deals with the performance parameters when the signals traverse only one node. Further research work can be done to study the performance parameters when the signals traverse more nodes.

In this thesis work signal extinction ratio is considered to be infinite. But signal extinction ratio plays a significant role on the system performance. Therefore the role of system crosstalk on its performance can be studied by transmitting signals having finite extinction ratio.

In this research work it has been assumed that the converted signal is free from the crosstalk carried with it before wavelength conversion and the input-output characteristic is also assumed unity except propagation delay and phase change. But according to [10] the input-output characteristic of wavelength converter is not unity at all input power. So this research work can be extended to include the input-output characteristic of wavelength converter at all input power.

In WDM network with wavelength converter optical amplifier are used to compensate for transmission and splitting losses. However they encounter interferometric intensity noise (IIN), relative output noise (RON) and accumulated ASE noise. A research work can be done which will include all of above noise for limited wavelength interchanging cross-connect.

Reference

[1] Djafar K. Mynbaev and Lowell L. Scheiner, *Fiber-Optic Communication Technology,* Low Price Edition, pp. 21-22.

[2] Rajiv Ramaswami and Kumar N. Sivarajan, *Optical Networks*, South Asia Edition, pp. 3-4.

[3] Amaury Jourdan, Francesco Masetti, Matthieu Garnot, Guy Soulage, and Michel sotom, "Design and implementation of a fully reconfigurable all-optical crossconnect for high capacity multiwavelength transport network," *J. Lightwave Technol.*, vol. 14, pp. 1198-1206, No.6, June1996.

[4] Masafumi Koga, Atsushi Watanabe, Takeshi Kawai, Ken-ichi Sato, and Yasuji Ohmori, "Large-capacity optical path cross-connect system for WDM photonic transport network," *IEEE J. select. Areas in Commun.*, vol.16, pp. 1260-1269, No. 7, Sept. 1998.

[5] Byrav Ramamurthy, and Biswanath Mukherjee , "Wavelength conversion in WDM networking," *IEEE J. select. Areas in Commun.*, vol.16, pp. 1061-1073, No. 7, Sept.1998.

[6] Satoru Okamoto, Atsushi Watanabe, and Ken-ichi Sato, "Optical path cross-connect node architectures for photonic transport network," *J. Lightwave Technol.*,vol. 14, pp. 1410-1422, No.6, June1996.

[7] Kuo-Chun Lee and Victor O.K. Li, "A wavelength-convertible optical network," *J. Lightwave Technol.*, vol. 11, No. 5/6, pp. 962-970, May/June 1993.

[8] Eugenio Iannone and Roberto Sabella, "Optical path technology: A comparison among different cross-connect architectures", *J. Lightwave Technol.*, vol. 14, pp. 2184-2195, No.10, Oct. 1996.

[9] Teck Yoong Chai, Tee Hiang Cheng, Gangxiang shen, Sanjay K. Bose, Chao Lu, "Design and performance of optical cross connect architectures with converter sharing," *Opt. Net. Mag.* July/August 2002 pp.73-83.

[10] Tim Gyselings, Geert Morthier and Roel Baets, "Crosstalk analysis of multiwavelength optical cross connects," *J. Lightwave Technol.*, vol. 17, No. 8, pp.1273-1283, Aug. 1999.

[11] M.S. Islam, S.P.Majumder, Ngee Thiam Sim, "Performance limitations of optical cross connect without wavelength Converter due to crosstalk," *J. Opt. Commun*.,vol. 29, pp. 71-75, 2008.

[12] M.S. Islam and S.P.Majumder, "Bit error rate & cross talk performance in optical cross connect with wavelength converter," *J. Optical Networking*, vol. 6, No. 3, pp. 295-303, Mar. 2007.

[13] Tech Yoong chai and Tee Hiang Cheng , "In band crosstalk analysis of optical cross- connect Architectures," *J. Lightwave Technol*., vol. 23, No. 2, pp. 688-701, Feb. 2005.

[14] Shuto Yamamoto, Toshihide Yoshimatsu , Hidehiko Takara , Tetsuro Komukai , Yasuaki Hashizume , Hirokazu Kubota ,Heroji Masuda ,Masahiko Jinno ,Atsushi Takada , "Influence of intrachannel crosstalk with frequency dependence on signal degradation in optical switch network," *J. Lightwave Technol*., vol. 27, No.24, pp. 5716-5722, Dec. 2009.

[15] M. John D. Downie and A. Boh Raffin, "Analysis of signal distortion and Crosstalk penalties Induced by optical filters in optical Networks," *J. Lightwave Technol*., vol. 21, No.9, pp.1876-1886, Sept. 2003.

[16] V Saminandan, M Meenakshi, "Wavelength conversion and in-band crosstalk in WDM optical networks," *J.Optics* 38(3), pp 131-148, Optical Society of India, 2009.

[17] Tech Yoong chai,Tee Hiang Cheng, Sanjay K. Bose, Chao Lu and Gangiang Shen "Crosstalk analysis for limited-wavelength-interchanging cross connects," *IEEE Photon. Technol. Lett.*, vol. 14, No. 5, pp. 696-698, May 2002.

Appendix

Calculation of mean and variance of

$$J \approx \frac{1}{T}\int_{nT}^{(n+1)T} b_1^2(t)dt + \frac{2}{T}\sum_{j=1}^{X_1}\sqrt{\delta}\int_{nT}^{(n+1)T} b_1(t)b_1(t-\tau_{1j})dt\cos D_{1j}\cos v_{1j} +$$

$$\frac{2}{T}\sum_{i=2}^{N}\{\sum_{j=1}^{X_i}\sqrt{\delta}\int_{nT}^{(n+1)T} b_1(t)b_i(t-\tau_{ij})dt\cos[\varphi_1(t)-\varphi_i(t)+D_{ij}]\cos v_{ij} +$$

$$\sqrt{\varepsilon}\int_{nT}^{(n+1)T} b_1(t)b_i(t-\tau_{ix})dt\cos[\varphi_1(t)-\varphi_i(t)+D_{ix}]\cos v_{ix}\} +$$

$$\frac{2}{T}\sum_{i=2}^{K}\sqrt{\varepsilon'}\int_{nT}^{(n+1)T} b_1(t)b_1(t-\tau_i')dt\cos[\varphi_1(t)-\varphi'_i(t)+D'_i]\cos v'_i \qquad (A.1)$$

The case of interest is when $b_1(t) = 1$.

From (A.1), the second term may be expressed in the following more compact form:

$$\sum_j F_i q_i \qquad (A.2)$$

with $q_i = \frac{1}{T}\int_{nT}^{(n+1)T} b_1(t-\tau_{1j})dt$ and constants $F_i = 2\sqrt{\delta}\cos D_{1j}\cos v_{1j}$. Each coherent combination in the third and forth terms have the following general form :

$$\sum_j G_j r_j \cos[u + D_j] \qquad (A.3)$$

with random variables $r_j = \frac{1}{T}\int_{nT}^{(n+1)T} b(t-\tau_i)dt$ and constants G_j, while u is uniformly distributed over [0, 2π].

$$E\{\sum_j G_j r_j \cos[u + D_j]\}$$

$$= \sum_j G_j E\{r_j\}E\{\cos[u + D_j]\}$$

$$= 0 \qquad (A.4)$$

$$\text{var}\{\sum_j G_j r_j \cos[u + D_j]\}$$

$$= \text{var}\{\cos(u)\sum_j G_j r_j \cos D_j - \sin(u)\sum_j G_j r_j \sin D_j\}$$

$= E\{[A\cos(u) - B\sin(u)]^2\}$

$= E\{A^2\cos^2(u) - 2AB\sin(u).\cos(u) + B^2\sin^2(u)\}$

$= E\{A^2\}E\{\cos^2(u)\} - E\{AB\}E\{\sin(2u)\} + E\{B^2\}E\{\sin^2(u)\}$

$$= \frac{1}{2}E\{A^2\} + \frac{1}{2}E\{B^2\} \qquad \text{(A.5)}$$

Where $A = \sum_j G_j r_j \cos D_j$ and $= B = \sum_j G_j r_j \sin D_j$ are substituted. The actual distributions of q_j and r_j depend on the bit alignment, which is considered for two different cases, as follows.

1) $\tau_{ij}, \tau_{ix}, \tau'_i << T$: All $b(t-\tau)$ can be approximated as $b(t)$ so that $q_j = 1$ for all j, since $b_1(t-\tau_{1j})$ align with $b_1(t)$ and $r_1 = r_2 = r$ is a uniformly distributed random variables over [0, 1]. In this case, $E(r) = \frac{1}{2}$ and $E(r^2) = \frac{1}{3}$.

Var $[\sum_j F_i q_i] = 0$

$$E[A^2] = E[(\sum_j G_j \cos D_j r)^2]$$

$$= E(r^2)(\sum_j G_j \cos D_j)^2$$

$$= \frac{1}{3}(\sum_j G_j \cos D_j)^2 \qquad \text{(A.6)}$$

A similar result can be obtained for $E\{B^2\}$, which gives

var $\{\{\sum_j G_j r_j \cos[u + D_j]\}$

$$= \frac{1}{2}\ [E\{A^2\} + E\{B^2\}]$$

$$= \frac{1}{6}[(\sum_j G_j \cos D_j)^2 + (\sum_j G_j \sin D_j)^2] \qquad \text{(A.7)}$$

2) $\tau_{ij}, \tau_{ix}, \tau'_i > T$: All $b(t-\tau)$ become uncorrelated with each other and with the actual signal $b_1(t)$. $q_1, q_2, \ldots\ldots$ and r_1 , r_2 , ……. Are independent uniformly distributed random variables over [0, 1].

$$E[A^2] = E[(\sum_{j=1}^{X} G_j \cos D_j r_j)^2]$$

$$= \sum_{j=1}^{X} E\,(G_j{}^2 \cos^2 D_j r_j{}^2\ ) + [\sum_{j=1}^{X} E\,(G_j \cos D_j r_j\ )]^2 \ - \sum_{j=1}^{X} E^2(G_j\ \cos\ D_j r_j\ )$$

$$= \frac{1}{3}\sum_{j=1}^{X} G_j{}^2 \cos^2 D_j + \frac{1}{4}(\sum_{j=1}^{X} G_j \cos D_j)^2 - \frac{1}{4}\sum_{j=1}^{X} G_j{}^2 \cos^2 D_j$$

$$= \frac{1}{4}(\sum_{j=1}^{X} G_j \cos D_j)^2 + \frac{1}{12}\sum_{j=1}^{X} G_j{}^2 \cos^2 D_j \qquad \text{(A.8)}$$

Similarly ,

$$E[B^2] = \frac{1}{4}(\sum_{j=1}^{X} G_j \sin D_j)^2 + \frac{1}{12}\sum_{j=1}^{X} G_j{}^2 \sin^2 D_j$$

$$\text{var}\ \{\sum_{j} G_j r_j\ \cos\ [u + D_j]\}$$

$$= \frac{1}{2}E\{A^2\} + \frac{1}{2}E\{B^2\}$$

$$= \frac{1}{8}(\sum_{j=1}^{X} G_j \cos D_j)^2 + \frac{1}{8}(\sum_{j=1}^{X} G_j \sin D_j)^2 + + \frac{1}{24}\sum_{j=1}^{X} G_j{}^2 \qquad \text{(A.9)}$$

On the other hand ,

$$E[(\sum_{j=1}^{X} F_j q_j)^2] = \frac{1}{4}(\sum_{j=1}^{X} F_j)^2 + \frac{1}{12}\sum_{j=1} F_j{}^2 \qquad \text{(A.10)}$$

$$E[\sum_{j=1}^{X} F_j q_j] = \frac{1}{2}\sum_{j=1}^{X} F_j \qquad \text{(A.11)}$$

And

$$\text{Var}\ [\sum_{j=1}^{X} F_j q_j] = \frac{1}{4}(\sum_{j=1}^{X} F_j)^2 + \frac{1}{12}\sum_{j=1} F_j{}^2 - (\frac{1}{2}\sum_{j=1}^{X} F_j)^2$$

$$= \frac{1}{12}\sum_{j=1}^{X} F_j{}^2 \qquad \text{(A.12)}$$